

Direction des bibliothèques

AVIS

Ce document a été numérisé par la Division de la gestion des documents et des archives de l'Université de Montréal.

L'auteur a autorisé l'Université de Montréal à reproduire et diffuser, en totalité ou en partie, par quelque moyen que ce soit et sur quelque support que ce soit, et exclusivement à des fins non lucratives d'enseignement et de recherche, des copies de ce mémoire ou de cette thèse.

L'auteur et les coauteurs le cas échéant conservent la propriété du droit d'auteur et des droits moraux qui protègent ce document. Ni la thèse ou le mémoire, ni des extraits substantiels de ce document, ne doivent être imprimés ou autrement reproduits sans l'autorisation de l'auteur.

Afin de se conformer à la Loi canadienne sur la protection des renseignements personnels, quelques formulaires secondaires, coordonnées ou signatures intégrées au texte ont pu être enlevés de ce document. Bien que cela ait pu affecter la pagination, il n'y a aucun contenu manquant.

NOTICE

This document was digitized by the Records Management & Archives Division of Université de Montréal.

The author of this thesis or dissertation has granted a nonexclusive license allowing Université de Montréal to reproduce and publish the document, in part or in whole, and in any format, solely for noncommercial educational and research purposes.

The author and co-authors if applicable retain copyright ownership and moral rights in this document. Neither the whole thesis or dissertation, nor substantial extracts from it, may be printed or otherwise reproduced without the author's permission.

In compliance with the Canadian Privacy Act some supporting forms, contact information or signatures may have been removed from the document. While this may affect the document page count, it does not represent any loss of content from the document.

Université de Montréal

**Études des marqueurs physiologiques de la mémoire
visuelle à court terme : électrophysiologie,
magnétoencéphalographie et imagerie par résonance
magnétique fonctionnelle**

par

Nicolas Robitaille

Département de psychologie

Faculté des arts et sciences

Thèse présentée à la Faculté des études supérieures
en vue de l'obtention du grade de Ph. D.
en psychologie,
option neuropsychologie et cognition

Janvier 2009

© Robitaille, 2009



Université de Montréal
Faculté des études supérieures

Cette thèse intitulée :

Études des marqueurs physiologiques de la mémoire visuelle à court terme :
électrophysiologie, magnétoencéphalographie et imagerie par résonance magnétique
fonctionnelle

présentée par :
Nicolas Robitaille

a été évaluée par un jury composé des personnes suivantes :

Martin Arguin, président-rapporteur
Pierre Jolicoeur, directeur de recherche
Julien Doyon, membre du jury
John McDonald, examinateur externe

Résumé

La mémoire à court terme visuelle (MCTV) consiste en la capacité de maintenir disponible pour l'ensemble des processus cognitifs de l'information visuelle après sa disparition, pour une courte période de temps. Il a récemment été montré, à l'aide de différents marqueurs physiologiques de l'activité cérébrale, que les parties postérieures du cerveau, principalement le cortex pariétal, avaient un niveau d'activation qui était corrélé avec la quantité d'informations maintenues en mémoire. L'objectif de cette thèse est de mettre en lien ces différents marqueurs physiologiques afin de déterminer s'ils constituent des mesures parallèles d'un même phénomène neuronal.

La mesure électrophysiologique de la MCTV consiste en une mesure de la différence d'activation entre l'hémisphère controlatéral et l'hémisphère ipsilatéral à la présentation de stimuli à encoder en mémoire. La différence entre les deux hémisphères augmentait lorsque le nombre de stimuli présentés lors de l'encodage augmentait. Par contre, cette augmentation aboutissait à un plateau lorsque la capacité de la MCTV était atteinte. Lorsqu'une trop grande quantité d'informations est présentée aux participants, ceux-ci encodent seulement un sous-ensemble des stimuli, ce qui crée des activités cérébrales identiques pour toutes les conditions qui présentent un nombre de stimuli plus grand que la capacité de la MCTV. En imagerie par résonance magnétique fonctionnelle (IRMf), l'activité dans le sulcus intrapariétal et intraoccipital (IPS/IOS) montrait une augmentation lorsque le nombre de stimuli à être encodés en MCTV augmentait. Cette augmentation atteignait également un plateau lorsque la capacité de la MCTV avait été atteinte. Dans cette tâche, les stimuli étaient présentés de façon bilatérale, ce qui mena, de façon prévisible, à une activation bilatérale.

La première expérience a utilisé une nouvelle technique, la magnétoencéphalographie (MEG), pour mesurer l'activité cérébrale des participants lorsqu'ils effectuaient une tâche de MCTV latéralisée, similaire à ce qui avait été fait en électrophysiologie. Nous avons trouvé un équivalent magnétique du marqueur

électrophysiologique de la MCTV, qui montre une plus grande différence d'activation entre les hémisphères controlatéral et ipsilatéral aux stimuli encodés. Nous avons également trouvé, sur un ensemble différent de capteurs, une activation bilatérale qui ne montrait pas d'interactions avec le côté d'encodage. La présence de ces deux effets indique qu'un patron complexe d'activations cérébrales se produit durant cette tâche.

La deuxième expérience a utilisé la MEG ainsi que l'IRMf, enregistrés pour les mêmes participants en utilisant le même protocole de stimulation. Cette fois, quatre niveaux de charge ont été utilisés, afin d'utiliser la régression linéaire multiple pour isoler, en IRMf et en MEG, les activations qui montrent un plateau. La localisation de sources du signal MEG a indiqué qu'une grande partie du cortex pariétal et occipital, incluant l'IPS/IOS, a montré une augmentation de son activation suivant la charge en mémoire. De plus, la portion supérieure de l'IPS a montré une interaction entre la charge en mémoire et la position des stimuli à encoder, comme l'activation électrophysiologique. Les résultats IRMf pour l'IPS/IOS, par contre, ont montré une forte activation bilatérale, sans montrer une plus grande activation pour les stimuli controlatéraux. Le cortex occipital inférieur gauche, par contre, a montré un effet clairement latéralisé : l'activation augmente avec l'augmentation des charges, jusqu'à atteindre un plateau, mais seulement pour les stimuli controlatéraux. Parce que le cortex occipital inférieur droit montre la même activation pour les stimuli ipsilatéraux et controlatéraux, nous ne pouvons pas attribuer les activations MEG et électrophysiologiques à cette région cérébrale.

En conclusion, cette thèse montre qu'augmenter la charge en MCTV entraîne une augmentation bilatérale de l'activation en IRMf et en MEG, ainsi qu'une augmentation latéralisée en MEG et en électrophysiologie. Ces résultats indiquent qu'un patron d'activation complexe est en place dans le cortex occipital et pariétal suite à l'encodage de stimuli en provenance d'un seul hémichamp.

Mots-clés : mémoire visuelle à court terme, électrophysiologie, magnétoencéphalographie, imagerie par résonance magnétique fonctionnelle.

Abstract

Visual short-term memory (VSTM) is the capacity to keep visual information encoded from a stimulus in a readily available format for the various cognitive processes after the disappearance of that stimulus, for a brief period of time. Recently, evidence from various physiological markers of cerebral activity indicates that posterior areas of the brain, mainly in the parietal cortex, have a level of activation that correlates with the amount of information maintained in VSTM. The objective of this thesis is to link these various markers of VSTM, in order to determine if they correspond to a single set of underlying neuronal processes.

In electrophysiology, the main marker of VSTM is a difference across contralateral and ipsilateral cerebral hemispheres, relative to the spatial location of stimuli to be encoded. This difference increases while the number of stimuli presented for encoding increases. This increase, however, reaches a plateau when the capacity of VSTM is reached. When too much information is presented to the participant, they can only encode a portion of the display, which cause cerebral activity identical for every condition that presents a number of stimuli greater than the capacity of VSTM. In functional magnetic resonance imaging (fMRI), the activation in the intraparietal and intraoccipital sulci (IPS/IOS) usually increases when the numbers of stimuli to be encoded in VSTM is increased. This increase also reaches a plateau when the capacity of the VSTM is reached. Studies of VSTM using fMRI have typically presented the stimuli bilaterally, around the fixation point, which unsurprisingly lead to bilateral activations.

Our first experiment used magnetoencephalography (MEG), to monitor the brain activity of participants performing a lateralized VSTM task, similar to what was done in electrophysiology. We found a magnetic equivalent of the electrophysiological markers of VSTM, which showed a higher difference across the activation between the ipsilateral and contralateral hemisphere relative to the location of visual targets to be encoded. We also found, for a different subset of sensors, a bilateral activation that did not show an

interaction with the location of encoded stimuli. The presence of these two effects indicates that a complex pattern of cerebral activation is taking place during this task.

The second experiment used both MEG (with electroencephalography recorded simultaneously) and fMRI, recorded for the same subjects using the same stimulation protocol. We used four different mnemonic loads, which allowed us to use multiple linear regressions to isolate, both in fMRI and in MEG, the activation that increases for small loads and reaches a plateau for larger loads. Localization of sources in MEG indicated that IPS/IOS had an increase in activation with a plateau as load increased. Furthermore, the superior portion of the IPS also showed the interaction between the mnemonic load and the position of the stimuli to be encoded, just as for the electrophysiological activation. The fMRI results for IPS/IOS, however, showed a strong bilateral activation, without showing the higher activation for contralateral stimuli. The left inferior occipital cortex, however, did show a clear lateralized effect: activation increased with higher load, up to a plateau, but only for contralateral stimuli. Because the right inferior occipital cortex had the same activation for ipsilateral and contralateral stimuli, we cannot attribute the electrophysiological or MEG activations to this cerebral region.

In conclusion, this thesis showed that an increase in VSTM load causes bilateral increases of activation in both fMRI and MEG, while lateralized activity was visible only in MEG and electrophysiology. These results indicate that a complex pattern of activation across the parietal and occipital cortex is occurring after the encoding of stimuli from a single hemifield.

Keywords : visual short-term memory, electrophysiology, magnetoencephalography, functional magnetic resonance imaging.

Table des matières

Identification du jury	ii
Résumé	iii
Abstract	v
Liste des tableaux	ix
Liste des figures	x
Liste des sigles et abréviations	xi
Remerciements	xiii
Introduction	1
Mémoire à court terme	3
Débats actuels à propos de la mémoire à court terme visuelle (MVCT)	7
Introduction aux différents marqueurs physiologiques	8
Imagerie par résonance magnétique fonctionnelle	8
Électrophysiologie	9
Magnétoencéphalographie	10
Une note sur le niveau de base et la soustraction d'activation	11
Revue de la littérature sur la physiologie de la mémoire à court terme visuelle	13
Implication des aires frontales en mémoire à court terme visuelle	13
Liens entre la mémoire à court terme spatiale et la mémoire à court terme visuelle	14
Implication des aires postérieures en MCTV	16
Activation hémodynamique	16
Marqueur électrophysiologique : la SPCN	19
Méthodologie utilisée	21
Chapitre 2	23
Introduction	26
Methods	28
Results	32
Discussion	41
Conclusions	44
Chapitre 3	61
Abstract	63
Introduction	64
Results	67
Discussion	75
Conclusion	80
Methods	81
Conclusion	106

Article 1.....	106
Article 2.....	107
Discussion générale.....	111
Conclusion.....	113
Bibliographie.....	114
Annexe 1 : autre publication du candidat au cours de la thèse	
Annexe 2 : autorisation des co-auteurs	
Annexe 3 : Curriculum Vitae du candidat.....	

Liste des tableaux

Article 1:

Table 1 : Behavioral k values 54

Table 2 : Average amplitude of the magnetic field during the retention interval 55

Article 2:

Table 1 : Talairach coordinates of regions investigated 98

Liste des figures

Article 1:

Figure 1 : Experimental design	56
Figure 2 : Electrophysiological results.....	57
Figure 3 : Map of the magnetic activity	58
Figure 4 : Average and subtraction magnetic field maps.....	59
Figure 5 : Interaction between Load and Side: Map and waveforms.....	60
Figure 6 : Minimum-norm cortically constrained source localization.....	61

Article 2:

Figure 1 : Experimental design	99
Figure 2 : Behavioral and electrophysiological results	100
Figure 3 : Maps of the magnetic activity.....	101
Figure 4 : fMRI maps and activation	102
Figure 5 : BOLD activation in Inferior Occipital.....	103
Figure 6 : ER-SAM source localisation of the MEG signal.....	104
Figure 7 : BOLD and MEG activation in inferior IPS	105

Liste des sigles et abréviations

ANOVA : Analyse de Variance

IRMf, fMRI : Imagerie par résonance magnétique fonctionnelle

MEG : magnétoencéphalographie

EEG : électroencéphalographie

ERP : potentiels évoqués

MCT : mémoire à court terme

MCTV, VSTM : mémoire à court terme visuelle

IPS/IOS : cortex intrapariétal et intraoccipital

SPCN : Sustained posterior contralateral negativity

SPCM : sustained posterior contralateral magnetic activity

VO: Ventral occipital

IO: Inferior occipital

BOLD: Blood oxygenation-level dependent

SMT, TMS: stimulation magnétique transcrânienne

*« Le bon sens est la chose du monde la mieux
partagée. »*

René Descartes, *Le discours de la méthode*, 1637

Remerciements

Je tiens premièrement à remercier mon extraordinaire directeur de thèse, Pierre Jolicœur. Il est, comme tout le monde sait, un chercheur d'une compétence exceptionnelle, ce qui nous a permis d'explorer de nombreuses avenues de recherche avec succès. Pierre est avant tout le mentor idéal pour un étudiant gradué. Il consacre des heures à chacun de ses nombreux étudiants, nous apportant toujours le support nécessaire non seulement à la complétion de nos projets de recherche, mais également pour s'assurer du bon déroulement de nos études. Son calme olympien nous permet de toujours nous réfugier dans son bureau pour discuter de science en profondeur bien sûr, mais également pour faire face aux nombreuses difficultés que nous pouvons rencontrer dans nos études. Pierre est un homme d'une facture exceptionnelle et j'espère bien humblement réussir à approcher son niveau de compétence, de tolérance, de compréhension et de générosité. Pierre, merci pour tout.

J'aimerais également remercier mes collègues, ceux qui ont rendu cette aventure bien plus agréable. D'abord ceux qui sont là depuis le début. D'abord Benoît, la seule personne avec qui j'espère être en désaccord, juste pour le plaisir d'argumenter. Émilie et Catherine, qui me montrent toujours une façon différente de faire les choses. Il y a également les collègues des derniers moments, soient Christine et sa répartie implacable, Amy qu'il est si plaisant de taquiner, Stéphane à qui on ne permet pas d'oublier qu'il est français, François avec son sens de l'humour si subtil et tous ceux qui ne sont passés dans le laboratoire que l'espace d'un instant.

Je tiens également à remercier mes distants collaborateurs, soit Roberto et Paola, d'Italie, René et Jay, du Tennessee, ainsi que Douglas de Toronto. Bien qu'à l'époque je ne vous avais jamais rencontrés, vous avez tous pris le temps de m'offrir une aide inestimable pour les différents projets entrepris au cours de mon doctorat. Je tiens également à remercier la gang de la magnétoencéphalographie à Montréal, soit Christophe, Anne-Sophie, Stéphane et Jean-Marc. Ce fut un plaisir de découvrir cette technique en votre compagnie.

J'ai eu la chance de collaborer et d'avoir de nombreuses discussions avec Frédéric et Denis, professeurs au département, qui m'en ont appris beaucoup en m'enseignant, mais je les remercie spécialement pour les nombreuses discussions informelles qui m'ont appris beaucoup. Je tiens également à remercier Jean-Paul et Franco, qui m'ont donné ma première occasion de faire de la recherche et m'ont apporté la rigueur de pensée essentielle à ce métier.

Tous ces travaux n'auraient pas été possibles sans notre dévoué et toujours très agréable personnel de soutien, soit Manon, Nathalie et Mihaëla, nos techniciennes en électrophysiologie; Carolyn et Andrée à l'institut universitaire de gériatrie; Stéphane et Pia pour le support informatique. Vous êtes les piliers qui s'assurent que le potentiel de recherche demeure fort pour chaque nouvelle génération d'étudiants. Je remercie également nos nombreux assistants de recherche qui ont effectué une somme de travail impressionnante au cours de ces années.

Enfin, je remercie tous ces gens qui m'ont gardé une place dans le monde extérieur. C'est en équipe avec Julie que j'ai fait le grand saut vers les études supérieures. Je remercie Cynthia, qui trouve toujours les mots pour me remettre d'aplomb. Marie, qui me rappelle constamment qu'il existe un monde au-delà de la réflexion. Ma sœur Michèle, avec qui j'ai appris à découvrir le monde. Mon père qui n'a jamais cessé de croire une seule seconde en moi, et ma mère qui m'a transmis la capacité de prendre la vie du bon côté. Ceux qui restent à vos côtés même lorsque vous n'avez plus un seul sujet de conversation normal sont de véritables amis.

Chapitre 1 : Introduction

Position de la mémoire à court terme visuelle dans l'appareil cognitif

La mémoire consiste en la capacité de retenir de l'information une fois que celle-ci n'est plus accessible aux sens. L'être humain possédant bien évidemment cette faculté, il convient donc de dire que nous possédons au moins un système de mémoire. Un système de mémoire se caractérise par une capacité, une durée, un code, une procédure d'accès à l'information et des procédures d'encodage et de maintien de l'information. Dans cette section, nous allons revoir les différents systèmes de mémoire qui ont été identifiés chez l'humain, afin de délimiter celui qui sera l'objet d'intérêt, la mémoire à court terme visuelle.

Atkinson et Shiffrin (Atkinson & Shiffrin, 1968, 1971) ont proposé un modèle des différents systèmes de mémoire qui, encore aujourd'hui, est accepté dans sa forme générale. Ce modèle postule que l'information peut être encodée à trois niveaux différents, un système d'encodage sensoriel, un système de mémoire à court terme ainsi qu'un système de mémoire à long terme.

L'encodage sensoriel, ou le registre sensoriel, est un système de mémoire qui est l'extension directe des sens. Au niveau visuel, la capacité de la mémoire sensorielle (nommée iconique) est très grande (Sperling, 1960). Sa durée est très courte, environ 250 ms (Phillips, 1974; Sperling, 1960). L'information y est conservée sous sa forme originale (Phillips, 1974). Elle est habituellement considérée comme étant entièrement passive, c'est-à-dire qu'on ne peut influencer quelles informations y entrent, modifier son contenu ou encore influencer sa durée ou sa capacité. Dans cet esprit, on y réfère parfois par le terme de persistance sensorielle (Haber & Standing, 1969), qui laisse ainsi supposer qu'elle est principalement considérée comme étant une intégration temporelle au niveau perceptuel

plutôt qu'un système de mémoire proprement dit, donc qu'elle est un mécanisme perceptuel. L'information en mémoire sensorielle doit être encodée en mémoire à court terme afin d'être protégée contre la disparition. Il est possible de déterminer volontairement quelles informations vont être transférées en mémoire à court terme, ce qui suggère que son accès est volontaire.

La mémoire à long terme est la faculté de retenir de l'information pendant une longue période de temps, soit des heures, des jours, ou plus (Squire, Knowlton, & Musen, 1993; Squire & Zola, 1996; Tulving, 1972). Elle n'est pas divisée selon la modalité sensorielle. En effet, un seul élément en mémoire, par exemple le concept « chien », est utilisé lorsqu'on voit un chien, lorsqu'on entend un chien ou lorsque quelqu'un nous en fait la description. La mémoire à long terme se divise en mémoire déclarative et non déclarative. La mémoire déclarative, ou mémoire explicite, contient les faits et les événements. La recherche d'information dans la mémoire déclarative se fait de façon consciente et volontaire, par exemple essayer de se rappeler ce qu'on a mangé la veille. L'encodage en mémoire déclarative peut être volontaire (étudier pour un cours) ou involontaire (lors de traitement sémantique de l'information). La mémoire non déclarative, ou mémoire implicite, contient les apprentissages moteurs (ex. : la tâche de dessin en miroir), les phénomènes d'amorçage ainsi que l'apprentissage par conditionnement classique. Puisqu'elle est non déclarative, on y accède de façon inconsciente et son étude doit se faire de façon indirecte.

La mémoire à court terme sera décrite en détails dans la section suivante, mais dans sa conceptualisation initiale, la mémoire à court terme était originalement considérée comme un passage obligé de l'information pour entrer en mémoire à long terme (Atkinson & Shiffrin, 1968).

L'organisation sérielle de ces trois systèmes de mémoire a été contestée à certains niveaux. Un patient (K.F.), ayant une grave atteinte de sa mémoire à court terme suite à une lésion du cortex pariétal droit, arrivait néanmoins à encoder de nouvelles informations en mémoire à long terme (Shallice & Warrington, 1970). Par contre, une étude poussée d'un autre patient (P.V.), ayant également des troubles de mémoire à court terme et réussissant à encoder de nouvelles informations, a permis de déterminer que celui-ci rencontrait des difficultés à faire entrer de l'information en mémoire à long terme lorsque l'information ne pouvait pas être traitée au niveau visuel ou sémantique (des paires de mots dans une langue étrangère), donc qu'un traitement phonologique était nécessaire (Baddeley, 1988). Donc, l'étude réalisée avec ce dernier patient permet de déterminer que l'information devrait obligatoirement passer par la mémoire à court terme avant d'être encodée en mémoire à long terme, mais que ce passage peut s'effectuer par un traitement sémantique, phonologique ou visuel.

Mémoire à court terme

Les premiers travaux sur la mémoire à court terme (MCT), revue par Miller (Miller, 1956) ont permis de délimiter la capacité de la mémoire à court terme à environ sept éléments, plus ou moins deux. Un aspect important, identifié par Miller avec le terme anglais *chunk*, est le concept d'assemblage de l'information en petits groupes. Par exemple, les lettres « B » « M » « W » peuvent être assemblées dans le petit groupe « BMW », en référence à la marque de voiture. Ce petit groupe occuperait donc la place d'un seul élément en mémoire à court terme, tandis que les lettres « C » « F » « K », qui ne peuvent être assemblées (du moins par l'auteur de ces lignes), occuperaient la place de trois éléments en MCT. L'assemblage en petits groupes est une stratégie employée afin d'augmenter la totalité de l'information en mémoire. Il est important de ne pas confondre les *chunks* et les objets dans nos réflexions sur la mémoire à court terme. En effet, le processus de création des *chunks* consiste à assembler plusieurs éléments semblables (de la

même catégorie) de façon consécutive. Cela s'applique très facilement aux stimuli de nature verbale. Les objets, eux, sont des éléments qui peuvent être discriminés sur la base de plusieurs dimensions (par exemple, la couleur et la forme d'une figure géométrique). Miller a rapporté que les stimuli multidimensionnels sont mieux identifiés que chacune de leurs dimensions indépendantes, même lorsque ces différentes dimensions sont parfaitement corrélées. Par contre, ce gain de performance n'est pas parfaitement additif. Nous reviendrons plus en détails sur ces notions lorsque nous verrons le débat sur l'importance des objets en mémoire à court terme visuelle.

Le modèle dominant de la mémoire à court terme est celui initialement développé et continuellement remis à jour par Baddeley (Baddeley, 1986, 1992a, 1992b; Baddeley & Hitch, 1974; Repovs & Baddeley, 2006). Ce dernier préfère l'étiquette « mémoire de travail » pour son modèle, ce qui sous-tend un système actif plutôt qu'un bête accumulateur d'informations. Pour les fins du présent écrit, le terme « mémoire à court terme » sera conservé, puisqu'il introduit naturellement le terme « mémoire à court terme visuelle », qui sera abondamment utilisé. Le lecteur avisé notera qu'il y a un débat quant à l'équivalence de ces termes (Klapp, Marshburn, & Lester, 1983), mais celui-ci n'est pas l'objet de la présente introduction. L'objectif de Baddeley dans la création de son modèle est principalement de dissocier différents systèmes en unités indépendantes. Pour ce faire, deux types de résultats empiriques sont recherchés. Premièrement, l'existence d'un patient atteint d'une sévère difficulté pour un type de matériel précis en ayant des capacités préservées pour un autre type de matériel est utilisé comme preuve que des processus neuronaux différents sont utilisés dans chaque cas, ce qui implique pour le modèle une dissociation des systèmes de mémoire soutenant chaque matériel. Deuxièmement, l'absence d'interférence, lors de double tâche chez des sujets normaux, entre le maintien simultané de matériel de deux types permet également de dissocier les deux types de matériel. Baddeley divisera initialement la mémoire à court terme en trois éléments majeurs : un système de contrôle

(l'exécutif central) et deux systèmes esclaves, chaque système dédié à un type de matériel : la boucle phonologique et le calepin visuospatial.

L'exécuteur central est le système qui contrôle les autres sous-systèmes. Dans la version initiale du modèle, sa description était plutôt vague, une sorte d'homoncule provisoire (du propre aveu de Baddeley), en attente de résultats empiriques plus probants. Dans la version de 1986 de son modèle, il utilisa le modèle de Norman et Shallice (Norman & Shallice, 1986) comme remplacement au niveau de l'exécuteur central. Cette portion du modèle de Baddeley s'intéresse principalement aux relations entre l'appareil cognitif en général et les différents dépôts d'information en mémoire à court terme. En nommant ces dépôts d'informations « systèmes esclaves » de l'exécuteur central, il souligne premièrement que la mémoire à court terme est un système non passif puisque ses éléments interagissent, et deuxièmement qu'il est très difficile d'étudier la mémoire à court terme sans que le système « maître » ne soit impliqué. En effet, si l'exécuteur central est impliqué dans les processus d'entrée et de sortie en mémoire à court terme, on ne pourra éviter de le solliciter lors d'une tâche expérimentale. Nous verrons plus tard des travaux (Klaver, Talsma, Wijers, Heinze, & Mulder, 1999; Todd & Marois, 2004; Vogel & Machizawa, 2004), qui utilisent des marqueurs physiologiques de la mémoire à court terme visuelle afin de l'étudier au cours de son utilisation. Cela permet donc de suivre l'activité en mémoire à court terme visuelle de façon plus indépendante vis-à-vis de l'exécuteur central.

Les systèmes esclaves, la boucle phonologique et le calepin visuospatial ainsi que le tampon épisodique qui sera ajouté par la suite (Baddeley, 2000), sont considérés comme étant indépendants les uns des autres. La boucle phonologique est le sous-système qui a reçu le plus d'attention des chercheurs. Elle est constituée d'un magasin phonologique, qui peut accumuler de l'information acoustique ou verbale pour une à deux secondes, et d'une boucle articulatoire, qui consiste en la répétition sub-vocale du matériel à retenir.

Bien entendu, Baddeley nous fournit également une description fort utile et bien intégrée à son modèle du calepin visuospatial. Par contre, rapporter cette description ici ne serait pas approprié, et ce pour plusieurs raisons. D'abord, bien que la contribution de ce modèle à notre compréhension de l'appareil cognitif humain est indéniable et gigantesque, l'objectif de cette thèse n'est pas de valider ou d'invalider ce modèle. Ensuite, l'adoption stricte d'un modèle théorique par l'auteur de ces lignes irait nécessairement influencer le contenu des écrits qui seront présentés dans la prochaine section, ce qui n'est pas souhaitable. De plus, certains travaux-clés pour la présente thèse n'ont toujours pas été intégrés au modèle. Enfin, le modèle de la mémoire de travail de Baddeley est en réalité un modèle du système cognitif humain, dans lequel le maintien de l'information de façon provisoire occupe une place centrale.

Les travaux qui ont été rapportés dans la présente section nous permettent de situer la mémoire à court terme visuelle (MCTV). Bien que toute conclusion soit amenée à être remise en cause, les quelques éléments suivants seront considérés comme établis, dans le contexte des présents travaux. La MCTV est un système d'emmagasinement de l'information visuelle de courte durée (quelques secondes) et de faible capacité (quelques items tout au plus). L'information y est encodée de façon plus complexe qu'en mémoire iconique, sans toutefois rejoindre la complexité sémantique de la mémoire à long terme. Il est possible d'y accéder de façon consciente et de manipuler l'information qui s'y trouve. Elle se situe de façon sérielle entre la mémoire iconique et la mémoire à long terme, ce qui lui permet de recevoir de l'information de la part de ces deux systèmes. Elle existe en parallèle avec d'autres systèmes de mémoire à court terme, notamment verbale.

Débats actuels à propos de la mémoire à court terme visuelle (MVCT)

Parmi les caractéristiques d'un système de mémoire, soit la durée, le code, l'encodage, le maintien et l'accès à l'information, les débats actuels pour la MCTV se situent principalement au niveau du code mnésique et des substrats neuronaux du maintien de l'information.

Au cœur du débat sur le code mnésique utilisé en MCTV se trouve la notion d'objet visuel. En effet, la capacité de la MCTV est d'environ 3 items. Si ces items sont des objets unidimensionnels, tel que des cercles de différentes couleurs, alors la capacité de la MCTV est d'environ 3 couleurs. Pareillement, si ces items sont définis par leurs formes mais toujours de la même couleur, la capacité de la MCTV est d'environ 3 formes. Par contre, si ces objets sont multidimensionnels, tel que des objets définis par une forme et une couleur, la capacité de la mémoire est encore d'environ 3 items, (Luck & Vogel, 1997; Vogel, Woodman, & Luck, 2001). Dans le cas présent, cela signifie que le participant a encodé six caractéristiques (3 couleurs et 3 formes). Ces résultats serviront de base aux modèles à ressources fixes et discrètes (« fixed slot model »). Ces modèles postulent que la MCTV encode un petit nombre d'objets, mais que ceux-ci sont entièrement représentés en mémoire, tandis que les autres objets n'auraient reçu aucune ressource et n'auraient aucune représentation en mémoire (Zhang & Luck, 2008). Ces modèles s'opposent à ceux des ressources partagées, qui stipulent que certains objets plus complexes requièrent plus de ressources, ce qui expliquerait pourquoi la capacité de la MCTV varie en fonction de la complexité des objets (Alvarez & Cavanagh, 2004).

La présente thèse va porter sur les substrats neuronaux du maintien de l'information. Au niveau méthodologique, les expériences présentées ici s'inspirent de la tradition ayant

mené au « fixed slot model », car nous présentons des objets simples (des disques de couleurs) sans jamais en varier la nature ou la complexité. En effet, puisque les régions cérébrales sensorielles situées en première ligne du traitement de l'information ne sont pas les mêmes lorsque la nature des stimuli est changée, une différente activation cérébrale est toujours attendu. Il devient donc difficile de conclure que les différences observées dans l'activité cérébrale survenant au niveau des processus plus tardifs comme la mémoire ne sont pas uniquement dû à ces différences initiales. Par contre, advenant une falsification du « fixed slot model », nos résultats ne seraient en rien invalidés. En effet, notre principale manipulation (augmenter le nombre d'items présentés) prédit une plus grande utilisation de ressources pour les modèles à ressources partagés et une utilisation de plusieurs « slot » pour le « fixed slot model ». Une plus grande activité neuronale est prévue pour une région cérébrale supportant l'un ou l'autre de ces deux processus.

Introduction aux différents marqueurs physiologiques

Dans cette section, les différents marqueurs physiologiques utilisés dans la littérature et dans cette thèse sont présentés, en prenant soin d'expliquer leurs avantages et limites, ainsi que les ajustements au paradigmes expérimentaux qui ont été nécessaires à leurs utilisations.

Imagerie par résonance magnétique fonctionnelle

L'imagerie par résonance magnétique fonctionnelle (Kwong et al., 1992; Ogawa et al., 1992) consiste à enregistrer les variations de concentration en oxygène du flux sanguin dans les tissus vivants, que l'on appelle le signal BOLD (*Blood-Oxygen-Level Dependant*). Puisque les neurones ne possèdent aucune réserve d'oxygène interne, ils consomment rapidement celui disponible dans leur environnement immédiat. Cela entraîne alors une

augmentation du flux sanguin local (la réponse hémodynamique), mesurable par le scanner d'imagerie par résonance magnétique. La réponse hémodynamique est lente, son maximum est atteint environ 6 secondes après un événement. Cette méthode possède donc une très faible résolution temporelle (quelques secondes), mais une excellente résolution spatiale (quelques millimètres). Elle permet de plus d'observer simultanément l'ensemble des parties du cerveau avec une qualité de signal équivalente d'une région à l'autre.

Dans le contexte d'études en sciences cognitives, une attention particulière doit être portée aux intervalles inter-essais ainsi qu'à l'ordre de présentation des différents essais ou stimuli (Dale, 1997). Étant donnée la durée de la réponse BOLD (+- 20 sec), l'étude doit présenter chaque essai suffisamment longtemps les uns après les autres pour s'assurer qu'il n'y a pas de contamination d'un essai à l'autre (*slow event-related*). Heureusement, la réponse BOLD s'additionne de façon linéaire s'ils sont présentés au plus vite au rythme d'un par seconde (Burock, Buckner, Woldorff, Rosen, & Dale, 1998), ce qui permet de présenter les stimuli rapidement (au maximum d'un par seconde, *fast event-related*) si on s'assure que l'ordre des essais est aléatoire ou contrebalancé. Il est ensuite possible de retrouver la réponse BOLD pour chaque type d'essais en effectuant une moyenne reliée aux événements ou par analyse de déconvolution (Serences, 2004).

Électrophysiologie

L'électrophysiologie consiste à enregistrer l'activité électrique produite par les neurones, principalement au niveau cortical (voir Luck, 2006; Picton et al., 2000), pour une introduction). Elle sera enregistrée ici à la surface du cuir chevelu, mais il est possible de l'enregistrer sur la surface corticale. Son équivalent magnétique (la magnétoencéphalographie, MEG, voir (Hämäläinen, Hari, Ilmoniemi, Knuutila, & Lounasmaa, 1993) consiste à l'enregistrement de l'activité magnétique émise par les

neurones. Ces signaux physiologiques possèdent une résolution temporelle de l'ordre de la milliseconde. Par contre, l'identification de la position des sources cérébrales ayant mené à la génération de l'activité électrique et magnétique enregistrée à l'extérieur de la boîte crânienne est un problème insoluble. Le signal électrique, lorsqu'il se propage aux travers des différents tissus, entraîne des courants secondaires (qui créent de surcroît une activité magnétique secondaire) et se diffuse dans plusieurs directions, ce qui résulte en des activités électriques très étendues lorsque mesurées à l'extérieur du crâne. De plus, pour chaque patron de sources cérébrales postulé comme étant responsable de l'activation trouvée au niveau des capteurs, il est possible de trouver une infinité d'autres patrons qui créeront une activité identique. Cela pose un problème de sous-détermination, puisqu'il y a beaucoup plus de générateurs à identifier que de capteurs. Afin de contourner ce problème, il faut contraindre les sources via des a priori, tels que prédéterminer le nombre de sources et contraindre leurs positions à l'aide d'informations anatomiques.

Les potentiels évoqués (PE) sont la forme la plus répandue d'utilisation de l'électrophysiologie en sciences cognitives. Ils s'observent en présentant plusieurs fois un stimulus ou une condition expérimentale. Le signal électrique enregistré aux capteurs est ensuite une moyenne reliée aux événements et est calculé pour chaque condition. Cette approche permet d'identifier des composantes des PE. Une composante des PE a une topographie, un patron d'apparition temporelle ainsi qu'un contexte expérimental précis nécessaire à son apparition.

Magnétoencéphalographie

La magnétoencéphalographie constitue la contrepartie de l'électroencéphalographie. En effet, un courant électrique entraîne toujours la création d'un champ magnétique qui l'entoure. Ce champ magnétique peut être enregistré à l'extérieur de la boîte crânienne, de

façon non invasive. À plusieurs niveaux, la MEG et l'EEG sont similaires. Les deux méthodes consistent à capturer l'activité électrique cérébrale en continu, à un rythme de plusieurs centaines de mesures par seconde. Des potentiels évoqués peuvent être calculés et les activités oscillatoires quantifiées.

Les principales différences entre la MEG et l'EEG se situent au niveau de l'analyse de sources. Premièrement, un courant électrique crée un champ magnétique qui lui est perpendiculaire. Cela implique donc qu'un générateur électrique orienté perpendiculairement à la surface du crâne créera une activité électrique directement au dessus de lui sur le crâne, mais par contre son champ magnétique sera parallèle à la surface du crâne, ce qui le rendra difficile à détecter. Inversement, un générateur orienté parallèlement à la surface du crâne sera très facilement visible en MEG, mais sera difficile à observer en EEG. Par contre, l'amplitude d'un signal magnétique diminue avec le carré de la distance, ce qui rend presque impossible l'enregistrement de nombreuses structures logées profondément à l'intérieur de la boîte crânienne. Ensuite, un grand avantage de la MEG est que le signal magnétique n'est pas influencé par les tissus qu'il traverse, ce qui amène des activations plus focales, donc des localisations plus précises. Cette plus grande précision requiert également une mesure précise de la position de la tête par rapport aux capteurs.

Une note sur le niveau de base et la soustraction d'activation

Une notion critique lors de l'utilisation de signaux physiologiques est la recherche d'un niveau de base. Les signaux physiologiques ne sont jamais nuls, le cerveau, même au repos, produit une activité structurée (Bellec et al., 2006; Chen, Feng, Zhao, Yin, & Wang, 2008). De plus, un bruit de fond est habituellement présent dans l'environnement et dans le matériel d'enregistrement. Différentes méthodes ont été développées pour chaque outil de

recherche afin d'aider à isoler l'activité cérébrale d'intérêt. Un niveau de base peut avoir deux objectifs : servir à quantifier l'amplitude de l'activité cérébrale par la création d'une mesure normalisée ou bien être soustrait à une autre activité cérébrale. La soustraction peut également être utilisée pour comparer deux signaux d'intérêt.

Une mesure normalisée, que ce soit un index, un ratio ou même un score z , nécessite un niveau de base reflétant une absence de modulation de l'activation, d'un bruit de fond en quelque sorte. L'augmentation des valeurs dans la ligne de base aura pour effet de diminuer l'amplitude des valeurs trouvées pour la condition active. Dans un cas de figure extrême où la ligne de base consiste en un signal de plus grande amplitude que le signal actif, le signal actif sera d'amplitude minime et donc invisible. Par exemple, lors du calcul d'un score Z pour l'activité oscillatoire, la moyenne et l'écart-type sont obtenus pour l'activité durant la ligne de base et ensuite utilisés pour transformer en score Z le signal d'intérêt. Pour l'IRMf, la valeur obtenue initialement dans un voxel pour une séquence d'acquisition est parfois normalisée afin d'obtenir une valeur moyenne prédéterminée, dans mon cas pour le chapitre 3 en divisant la valeur à chaque échantillon temporel par la moyenne, pour ensuite multiplier par 100.

La soustraction d'activité d'une ligne de base consiste simplement en la soustraction du signal lors de deux états cérébraux, un étant considéré comme reflétant une condition inintéressante. C'est la procédure habituelle avec des potentiels évoqués en EEG et MEG, l'activité précédant l'apparition du stimulus d'intérêt est soustraite à l'ensemble de la fenêtre d'analyse. En IRMf, la ligne de base peut consister en une condition contrôle pour laquelle le patron temporel d'activation est extrait et ensuite soustrait de l'activation d'intérêt. La soustraction entre deux activations d'intérêt est identique, sauf que le choix de la direction de la soustraction est arbitraire. Dans cette thèse, j'ai choisi de toujours

soustraire l'activation à droite de l'activation à gauche, par souci de simplicité. La soustraction permet donc d'isoler la partie du signal qui varie en fonction des conditions.

La logique de la soustraction peut être reformulée en terme de régresseur dans une régression linéaire multiple. Une soustraction simple entre deux valeurs se traduit en un régresseur $[-0.5 \ 0.5]$. La méthode des moindres carrés sera utilisée pour identifier le béta associé à ce régresseur. Dans une régression linéaire, le béta consiste en la valeur par laquelle chaque régresseur est multiplié pour obtenir les valeurs prédites par le model. Le béta (en absence de colinéarité avec les autres régresseurs) aura la même valeur que le résultat de la soustraction. Par extension, il est possible d'utiliser un contraste plus complexe, comme le nombre de stimuli encodés en mémoire.

Donc, le traitement du signal sera très différent pour chaque marqueur physiologique, mais ces différences sont dictées par la nature du signal mesuré et permettent, dans le cas présent, de mettre en lien ces différents signaux.

Revue de la littérature sur la physiologie de la mémoire à court terme visuelle

Dans cette section, les travaux sur la physiologie de la mémoire à court terme visuelle seront revus.

Implication des aires frontales en mémoire à court terme visuelle

Les premiers indices de l'implication des lobes frontaux dans les processus de mémoire à court terme viennent d'études de patients cérébrolésés (Petrides, 1995; Petrides,

2000). Des études d'imagerie cérébrale (Cohen, Perlstein, Braver, Nystrom, & et al., 1997; Courtney, Ungerleider, Keil, & Haxby, 1997) sont venues préciser l'importance d'une structure du lobe préfrontal, le cortex dorso-latéral (DLPFC, *Dorso-Lateral PreFrontal Cortex*). Cette structure a été associée à la mémoire à court terme spatiale (Mottaghy, Gangitano, Sparing, Krause, & Pascual-Leone, 2002; Nyffeler et al., 2004; Nyffeler et al., 2002) à la mémoire épisodique (Epstein, 2002; Rami et al., 2003), à la mémoire à court terme visuelle (Mottaghy et al., 2002), à la mémoire à court terme verbale (Mottaghy et al., 2003; Mull & Seyal, 2001) et même à une tâche de sélection aléatoire, modifiée pour qu'elle ne requière pas la mémoire de travail (Hadland, Rushworth, Passingham, Jahanshahi, & Rothwell, 2001). De plus, certaines évidences (Kelley et al., 1998; Wagner et al., 1998) associent le cortex préfrontal droit à la mémoire spatiale et visuelle, tandis que le cortex préfrontal gauche serait associé à la mémoire verbale. Petrides (1995) propose que le cortex préfrontal ventral serait responsable du maintien et de la comparaison des items en mémoire de travail, tandis que le cortex préfrontal dorsal serait impliqué lorsque les opérations sont plus complexes et difficiles, comme pour la surveillance et la manipulation d'information.

Liens entre la mémoire à court terme spatiale et la mémoire à court terme visuelle

Les lecteurs concernés auront anticipé une confusion possible entre la mémoire à court terme visuelle et la mémoire à court terme spatiale. En effet, la position des stimuli dans l'espace est une des dimensions retenues lors d'une tâche de MCTV. Une erreur lors de l'exécution de cette tâche peut donc s'expliquer par une difficulté d'encodage, de maintien ou de récupération de la position des stimuli dans l'espace. Bien que la mémoire à court terme spatiale s'étudie habituellement dans le contexte de mouvement oculaire retardé, ce qui implique des processus oculomoteurs supplémentaires, il est utile de garder ces résultats à l'esprit lors de l'étude de la mémoire à court terme visuelle.

Une carte rétinotopique de localisation spatiale retenue en mémoire à court terme a été identifiée au niveau du IPS (Serenio, Pitzalis, & Martinez, 2001). Cette carte se partageait dans chaque hémisphère; chacun représentant l'hémichamp visuel controlatéral. Muri et ses collègues (Muri et al., 2000; Muri, Vermersch, Rivaud, Gaymard, & Pierrot-Deseilligny, 1996) ont fait l'étude très complète de l'effet de la stimulation magnétique transcrânienne (SMT) sur le cortex postérieur pariétal (PPC, une région qui englobe l'IPS/IOS) sur une tâche de saccade oculaire retardée. Par contre, ils ont utilisé un appareil de SMT ayant un effet diffus, ce qui rend difficile l'identification précise des structures stimulées. Ils ont déterminé que la SMT du PPC lors de l'exécution d'un mouvement oculaire réduisait la précision de ce dernier (résultat répliqué par (Kapoula, Isotalo, Muri, Bucci, & Rivaud-Pechoux, 2001) dans des expériences sans composantes mnémoniques), peu importe la direction du mouvement ou l'hémisphère impliqué. Cela indique donc que cette structure est impliquée dans la tâche, même en absence de mémorisation. Ils ont également montré que la SMT du PPC droit réduisait la précision de la production d'un mouvement oculaire retardé, mais seulement si appliquée immédiatement (260 ms) après l'apparition de la cible. La SMT du PPC durant la période de maintien n'a eu aucun effet. Le résultat de Muri et al., (1996, 2000) sur l'implication du PPC droit dans l'encodage d'information spatiale a été reproduit (Kessels, D'Alfonso, Postman et de Haan, 2000) dans une tâche de détection de changement (spatiale); de même que par Smyrnis, Theleritis, Evdokimidis, Muri et Karandreas (2003), dans une tâche de production de mouvement manuel retardé (à l'aide d'un *joystick*). Donc, le cortex pariétal est impliqué dans l'encodage des positions spatiales. Par contre, puisque l'application de la SMT durant la période de maintien n'a aucun effet sur la performance mais qu'une carte rétinotopique des positions spatiales maintenues en mémoire a été observé, il semble qu'un autre processus neuronal soit à l'œuvre qui empêche l'information maintenue dans le PPC d'être vulnérable à la SMT.

Implication des aires postérieures en MCTV

Activation hémodynamique

Todd et Marois (2004) ont identifié, à l'aide d'imagerie par résonance magnétique fonctionnelle (IRMf), une région (le sulcus intrapariétal/intraoccipital, IPS/IOS; bilatéral) dont l'activité variait en fonction du nombre d'items présents en MCTV. La procédure (inspirée de la tâche de détection de changements de Luck et Vogel, 1997) consistait à présenter des disques de différentes couleurs (de 1 à 8 disques) pour une brève période de temps. Après une attente de 1200 ms, un disque était présenté et le participant devait indiquer si le disque était de la même couleur que celui présenté précédemment au même endroit. Le nombre d'items effectivement retenus en mémoire était calculé par la formule de Cowan (2001). La région IPS/IOS augmentait son activité BOLD lorsque le nombre d'items présents en mémoire augmentait et ce, jusqu'à ce que la capacité de la MCTV soit atteinte.

Des efforts ont été faits pour essayer de diviser l'IPS en IPS supérieur et IPS inférieur (Xu, 2007; Xu & Chun, 2006; Xu & Chun, 2007). Chaque volontaire de leurs expériences a également participé à deux pré-expériences servant à identifier l'IPS supérieur et l'IPS inférieur (Xu & Chun, 2007). Afin d'isoler l'IPS supérieur, une tâche semblable à celle de Todd et Marois (2004) était utilisée. L'IPS inférieur était identifié en comparant la réponse hémodynamique aux stimuli visuels utilisés dans la tâche de mémoire à la réponse hémodynamique à des plages de bruit visuel. Dans les cartes d'activation qui en résultent, la portion pariétale était attribuée au IPS inférieur, tandis que la portion occipitale était considérée comme faisant partie du complexe latéral occipital (LOC), une région cérébrale impliquée dans la reconnaissance d'objet (Grill-Spector, Kourtzi, & Kanwisher, 2001; Kanwisher, Chun, McDermott, & Ledden, 1996; Kanwisher, Woods,

Iacoboni, & Mazziotta, 1997). Cette seconde manipulation est par contre imparfaite. L'aire LOC est située sur la surface latérale du cortex occipital, mais il est difficile de l'identifier de façon uniquement anatomique. La procédure habituelle pour isoler LOC consiste à comparer la réponse hémodynamique des objets à des stimuli contrôles soigneusement choisis afin qu'ils soient constitués des mêmes éléments. Par exemple, les stimuli contrôles d'une image d'un objet dessiné à l'aide de lignes sont ces mêmes lignes éparpillées en tous sens (Kanwisher et al., 1996). Heureusement, dans le cas de l'IPS inférieur, les coordonnées obtenues correspondent à l'anatomie du cortex pariétal. Une fois l'IPS divisé, par contre, des différences intéressantes ont été trouvées.

La réponse BOLD de l'IPS supérieur augmente en fonction du nombre d'items encodés en MCTV, qu'ils soient définis par leur couleur, leur forme ou la conjonction des deux (Song & Jiang, 2006), ou bien encore qu'ils soient définis par leur couleur, leur forme, la direction d'un mouvement à l'intérieur de l'objet ou la conjonction de ces trois caractéristiques (Kawasaki, Watanabe, Okuda, Sakagami, & Aihara, 2008). Pour ces deux expériences, la performance des sujets pour la conjonction était égale ou inférieure à la performance du cas le plus difficile, amenant une dissociation entre la réponse BOLD dans l'IPS supérieur (qui augmente avec le nombre d'item présentés, jusqu'à atteindre un plateau après quatre items) et la performance comportementale (qui plafonne à deux items dans le cas des conjonctions). Afin de dissocier l'effet du nombre de caractéristiques de l'effet du nombre d'objets, Xu (2007) a utilisé des objets composés d'une caractéristique facile à mémoriser (la couleur), qui entraîne une bonne performance, et une caractéristique difficile à mémoriser (la forme), qui entraîne plus d'erreurs. La réponse BOLD augmente en fonction du nombre de caractéristiques, même si celles-ci appartiennent à des objets non entièrement encodés en mémoire car la caractéristique difficile n'était pas retenue (Xu, 2007). De plus, présenter ces deux caractéristiques sur deux objets distincts ou sur un seul, (en les juxtaposant) entraîne la même réponse. Lorsque des objets dont la forme est simple ou complexe sont encodés, la réponse BOLD dans l'IPS supérieur suit le même patron que la

performance comportementale (Xu & Chun, 2006). Lorsque les objets sont groupés et que cette manipulation améliore la capacité de la MCTV, la réponse BOLD augmente également (Xu & Chun, 2007).

L'IPS inférieur, par contre, présente une réponse BOLD directement proportionnelle au nombre d'items présentés (Xu, 2007) ou au nombre de groupes (Xu & Chun, 2007). En utilisant une période de rétention étendue (8300 ms), la réponse hémodynamique de l'IPS inférieur augmente de deux à quatre items complexes, alors que la capacité des participants et la réponse de l'IPS supérieur n'augmentent pas dans ce cas (Xu & Chun, 2006). Lorsque les objets sont présentés en série au point de fixation, la réponse de l'IPS inférieur est équivalente pour les charges 1 à 4, tandis que lorsqu'elle sont présentés en série à différentes positions excentriques, la réponse BOLD est proportionnelle au nombre d'items présentés (Xu & Chun, 2006). Bien que cette dernière démonstration ait mené Xu et Chun à affirmer que l'IPS inférieur maintenait en mémoire l'emplacement de chaque objet, l'excentricité est un facteur qui a été confondu avec l'utilisation de différentes positions de ces objets. Les observations concordent avec l'hypothèse stipulant que l'IPS inférieur est responsable du maintien de la mémoire des positions spatiales, mais cela reste à démontrer.

Il est à noter que bien que Todd et Marois (2004) aient mis ensemble les activations de ce qui deviendra plus tard plusieurs sous-régions cérébrales, les coordonnées Talairach qu'ils ont rapportées correspondent à la portion supérieure de l'IPS. De plus, bien que non testé directement, il est évident à l'œil que l'activation dans l'IPS supérieur est de plus grande amplitude que celle de l'IPS inférieur (Xu, 2007; Xu & Chun, 2006; Xu & Chun, 2007), donc l'activité jointe de ces deux régions reflète possiblement en plus grande partie celle de l'IPS supérieur.

Une augmentation de la réponse hémodynamique en fonction du nombre d'objets encodés en mémoire pour le complexe latéral occipital (LOC) a été observée (Xu & Chun, 2006; Xu & Chun, 2007). Par contre, ces résultats n'ont pas été répliqués (Song & Jiang, 2006). De plus, cette région n'a pas été identifiée par Todd et Marois (2004), bien qu'ils n'aient imposé aucun a priori au niveau des régions cérébrales. Puisque LOC est certainement une région impliquée dans le traitement de stimuli visuels (Grill-Spector et al., 2001; Kanwisher et al., 1997; Kourtzi & Kanwisher, 2000), il serait plausible de considérer qu'elle participe principalement aux premières étapes du traitement requis par la tâche, soit l'encodage. Par contre, en utilisant une période de rétention étendue (8300 ms), il existe une dissociation soutenue entre les charges 1 et 2 (pour des objets complexes, la capacité des participants est de 2 objets) durant la période de rétention, ce qui suggère que ce sont plus que les processus d'encodage en mémoire qui sont observés dans LOC.

Marqueur électrophysiologique : la SPCN

Klaver, Talsma, Wijer, Heinze et Mulder (2001) ont identifié une composante des potentiels évoqués visuels (PEV) dans les aires postérieures du cerveau, dont l'amplitude variait en fonction de l'endroit de présentation des stimuli. Cette composante consistait en une plus grande négativité dans l'hémisphère controlatéral aux stimuli à retenir. Par contre, leur tâche impliquait la mémorisation de stimuli visuels complexes générés aléatoirement. Ils n'ont pas fait varier la charge mnésique et ils ont inclus une condition où deux figures complexes étaient à retenir, une de chaque côté du champ visuel. Dans cette condition, la performance était diminuée (augmentation de 100 ms du temps de réaction, baisse de 15% du taux de succès). Pour la première seconde suivant l'apparition des stimuli, l'activité dans chaque hémisphère était identique à l'activité lorsqu'un seul item était présenté dans l'hémichamp controlatéral, indiquant que l'item a été maintenu en mémoire dans cet hémisphère. Par contre, après une seconde, l'activité est revenue au même niveau que

lorsqu'il n'y avait pas d'item à mémoriser dans l'hémichamp controlatéral, possiblement reflétant l'incapacité du participant à retenir l'ensemble de l'information.

Vogel et Machizawa (2004) ont décrit une composante des PEV dont l'amplitude variait de la même façon que la réponse BOLD du IPS/IOS décrite par Todd et Marois (2004). Cette composante, qu'ils ont nommée la CDA pour *Contralateral Delayed Activity*, mais que notre groupe nomme SPCN pour *Sustained Posterior Contralateral Negativity*, consiste en une plus grande négativité dans l'hémisphère controlatéral à l'hémichamp visuel où des items à mémoriser ont été présentés. Dans ces expériences, des stimuli contrôle étaient toujours présentés dans l'autre hémichamp visuel, afin de pouvoir utiliser l'hémisphère ipsilatéral comme contrôle. La procédure était très semblable à celle de Todd et Marois (2004), sauf qu'au début de chaque essai, une flèche indiquait aux participants de quel côté de l'écran (gauche ou droit) ils devraient faire la tâche. Cette composante était présente tant que les items étaient présents en mémoire. De plus, Vogel et Machizawa (2004) ont observé une corrélation entre la capacité de la MCTV observée pour chaque participant et le nombre d'items présentés pour lequel la composante atteignait son amplitude maximale. Ils ont donc obtenu une mesure électrophysiologique des différences individuelles en MCTV.

La capacité des individus à sélectionner les items visuels présents à l'écran pour être encodés en MCTV, capacité reflétée par l'observation de la SPCN, était également prédite par la capacité de la MCTV (Vogel, McCollough, & Machizawa, 2005). Ils ont également montré que la SPCN s'obtient avec différents types de stimuli, qu'elle ne dépend pas de l'étendue spatiale des stimuli à encoder et que les essais où le sujet produit la mauvaise réponse ont en moyenne une SPCN de plus faible amplitude (McCollough, Machizawa, & Vogel, 2007).

La SPCN a été utilisée dans plusieurs travaux afin de suivre l'évolution de la quantité d'informations en mémoire à court terme visuelle. La SPCN observée à la deuxième cible d'une tâche de vacillement de l'attention (Jolicoeur, 1999; Raymond, Shapiro, & Arnell, 1992) était de plus faible amplitude (Jolicoeur, Sessa, Dell'Acqua, & Robitaille, 2006; Robitaille, Jolicoeur, Dell'Acqua, & Sessa, 2007) ou même abolie (Dell'Acqua, Sessa, Jolicoeur, & Robitaille, 2006; Jolicoeur, Sessa, Dell'Acqua, & Robitaille, 2006). D'ailleurs, des stimuli entraînant une SPCN dans une tâche de discrimination n'entraînent pas de SPCN dans une tâche de détection (Mazza, Turatto, Umiltà, & Eimer, 2007).

Méthodologie utilisée

L'objectif est d'observer les différents marqueurs de l'activité cérébrale durant la rétention d'items en mémoire à court terme visuelle. En se basant sur le principe de la convergence d'évidences, nous allons tenter de clarifier le rôle du cortex pariétal en mémoire à court terme visuelle. Nous allons créer des protocoles inspirés de ceux utilisés par Vogel et Machizawa (2004) et Todd et Marois (2004) en les adaptant pour faire des enregistrements en magnétoencéphalographie (MEG) comprenant l'enregistrement simultané de l'EEG et des enregistrements en imagerie par résonance magnétique fonctionnelle (fMRI).

Le premier objectif de cette thèse est d'identifier une contrepartie magnétique de la SPCN. Le second objectif est de vérifier si le signal BOLD montrera une latéralisation de son activité qui suivra le nombre d'items encodés en MCTV, donc de trouver une contrepartie de la SPCN dans le signal BOLD. Le but général est de déterminer si la SPCN et l'activation BOLD dans IPS/IOS sont le résultat de l'activité des mêmes générateurs neuronaux.

Le chapitre deux présentera une étude en MEG qui a permis d'identifier un équivalent magnétique de la SPCN. Le chapitre trois présente une étude en MEG et IRMf qui étudie plus en détails l'équivalent magnétique de la SPCN et cherche les effets de latéralisation dans le signal BOLD.

Chapitre 2: Article 1

ARTICLE 1

Nicolas Robitaille, Stephan Grimault et Pierre Jolicœur (sous presse, *Psychophysiology*)

Bilateral parietal and contralateral responses during maintenance of unilaterally-encoded objects in visual short-term memory: Evidence from magnetoencephalography.

Running title: VSTM and MEG

Bilateral parietal and contralateral responses during maintenance of unilaterally-encoded objects in visual short-term memory: Evidence from magnetoencephalography.

Nicolas Robitaille¹, Stephan Grimault^{1,2}, and Pierre Jolicœur¹

¹Centre de recherche en neuropsychologie et cognition, Département de psychologie,
Université de Montréal, Montréal, Québec, Canada.

²Centre national de la recherche scientifique, France.

Corresponding author :
Robitaille, Nicolas
Département de Psychologie
Pavillon Marie-Victorin
90, avenue Vincent d'Indy
Montréal, Québec
H2V 2S9
Tel.: 514 343-6111 #2631

E-Mail: 

Abstract

A component of the event-related magnetic field (ERMF) response was observed in magnetoencephalographic signals recorded during the maintenance of information in visual short-term memory (VSTM). This *sustained posterior contralateral magnetic* (SPCM) field is likely the magnetic equivalent of the *sustained posterior contralateral negativity* (SPCN) found in electrophysiology. MEG data showed, at the sensor level, a bilateral activation over the parietal cortex that increased in amplitude for higher memory load. Other sensors, also over the parietal cortex, showed an activation pattern similar to the SPCN with higher activation for the hemisphere contralateral to the visual field from which visual information was encoded. These two activation patterns suggest that the SPCN and SPCM are generated by a network of cortical sources that includes bilateral parietal loci, likely IPS/IOS, and contralateral parietal sources.

Keywords: magnetoencephalography (MEG), visual short-term memory (VSTM), intra-parietal/intra-occipital cortex (IPS/IOS), sustained posterior contralateral negativity (SPCN), sustained posterior contralateral magnetic field (SPCM).

Introduction

We used magnetoencephalography (MEG) to study how the human brain stores and retains low-level visual information over short periods of time. Posterior areas of the brain have been identified as participating to the maintenance of information in visual short-term memory (VSTM). Lateralized visual stimuli, to be encoded and maintained for a brief period of time (1500 ms), lead to sustained neural activity over the posterior regions of the cerebral hemisphere contralateral to the stimuli to be encoded (Klaver, Talsma, Wijers, Heinze, & Mulder, 1999). Vogel and Machizawa (2004) replicated and extended these results by observing an increase of the amplitude of the memory-related ERP component as the number of items to be remembered (memory set size) was increased. Interestingly, the increase in the amplitude of the component generally reaches a maximum at the subject's maximal VSTM capacity (calculated using Cowan's K formula, Cowan, 2001), leading to a correlation between changes in the amplitude of the component and estimated capacity on a subject-by-subject level. We will refer to this ERP waveform as the SPCN, for sustained posterior contralateral negativity. The SPCN was shown to be a useful index of encoding and maintenance in VSTM in several experiments examining attention and memory (i.e., Brisson & Jolicoeur 2007a, 2007b, 2007c; Dell'Acqua, Sessa, Jolicoeur, & Robitaille, 2006; Jolicoeur, Brisson, & Robitaille, 2008; Jolicoeur, Sessa, Dell'Acqua, & Robitaille, 2006a, 2006b; Robitaille, Jolicoeur, Dell'Acqua, Sessa, 2007; Robitaille & Jolicoeur, 2006).

Using functional magnetic resonance imaging (fMRI), Todd and Marois (2004) isolated a parietal area (intra-parietal sulcus and intra-occipital sulcus, IPS/IOS) involved in the maintenance of information in VSTM, which has a number of similarities with the SPCN. The stimulation protocol was similar to the one used by Vogel and Machizawa (2004) and included a manipulation of memory set size. The blood oxygenation level-dependent (BOLD) response increased as the number of items to be memorized increased, and it reached a maximum and levelled off at the capacity of VSTM. Furthermore, as for

the SPCN, individual differences in VSTM storage capacity could be predicted from the BOLD response in IPS/IOS (Todd & Marois, 2005). A retinotopic map of spatial locations to be remembered for short intervals (three seconds) was also found in the IPS (Serenó, Pitzalis, & Martínez, 2001). Other cortical areas have also been found to have an implication in short-term memory (Cohen, Perlstein, Braver, Nystrom, & et al., 1997; Courtney, Petit, Maisog, Ungerleider, & Haxby, 1998; Courtney, Ungerleider, Keil, & Haxby, 1997; Curtis & D'Esposito, 2003; Linden et al., 2003; Postle, Berger, & D'Esposito, 1999; Rowe, Toni, Josephs, Frackowiak, & Passingham, 2000). However, Todd and Marois pioneered the use of a regression analysis that allowed them to isolate cerebral regions with activation patterns that mirrored the number of items that could be maintained in VSTM (most particularly a BOLD response that increased with number of items to be remembered and that levelled off at the estimated maximum capacity of VSTM). This methodological advance, which is now used by other researchers to isolate brain regions engaged specifically in representing information in VSTM (e.g., Xu & Chun, 2006) lead them to conclude that IPS/IOS is the principal locus of maintenance of information in VSTM.

Taken together, the results of Vogel and Machizawa (2004) and Todd and Marois (2004) raise the straightforward issue of whether the IPS/IOS area isolated based on the BOLD response is responsible for the SPCN observed in the human electrophysiology of VSTM. This hypothesis implies that the left and right IPS/IOS areas should be more active (or even only active) for the maintenance of information encoded from the respective contralateral hemifield. More precisely, validating this hypothesis requires finding that a higher contralateral-ipsilateral difference is observed for higher VSTM loads than for lower VSTM loads. The goal of the current study was to test this hypothesis using MEG. We capitalized on the higher spatial resolution of MEG, relative to electroencephalography (EEG), to find the cortical areas involved in the neural representation of objects held in VSTM.

Methods

Subjects

Twenty-seven subjects were recorded using MEG. Four were rejected because of high environmental magnetic noise during recordings. Three were rejected because of breathing artefacts in the signals. Four were rejected because they had too many rejected trials following the eye blinks and eye movement rejection procedures. The remaining 16 subjects (eleven female) were between 19 and 24 years old, average 22. They reported no neurological problems, normal or corrected-to-normal vision, and normal color vision. We obtained informed consent from each subject prior to the experiment.

Procedure

The stimuli were presented on a back-projection translucent screen located 75 cm in front of the subject. The stimulation protocol is illustrated in Figure 1. The subject initiated each trial by pressing any of the buttons on a 4-button response pad linked to an interface outside the magnetically-shielded room. A fixation cross appeared and remained alone on the screen for a duration randomly selected between 300 and 1000 ms. Two arrowheads then appeared, for 400 ms. After the offset of the arrowheads, the fixation cross was displayed for a duration randomly selected between 400 and 1100 ms. Then, the stimuli to be encoded were displayed for 200 ms. Two or four colored disks (diameter of 1.4° of visual angle) were presented on each side. The colors of the disks were randomly selected from 8 colors. The colors on a given side were always different, but a color could be present on both sides of fixation. The locations of the colored disks were randomly selected from a 3 X 4 imaginary grid located on each side of the display (the total display size was 14.9° in width and 7.2° in height). The fixation cross was present on the screen for

the following 1200 ms (the retention interval). Then, the test display appeared and remained on the screen until the subject's response. The test display consisted of one disk on each side of fixation, each disk was presented at the location of one of the disks in the initial display at the same hemifield. The task was to indicate if the disk on the side indicated by the initial arrows was in the same color as the disk presented initially at that location. They had to press one button (with the right index finger) if the disk was in the same color (50% of the trials) and another button (with the right middle finger) if the disk was in another color (50% of the trials). When the color was different, it was randomly selected across the seven remaining colors. The test disk on the side not indicated by the arrow was manipulated using the same rules as for the relevant side. Each trial ended with a fixation symbol at the centre of the display. This symbol also provided feedback for the previous response (+ if the response was correct or – if the response was incorrect).

INSERT FIGURE 1 ABOUT HERE

Each subject was tested in twelve blocks of 64 trials each, for a total of 768 trials. Each condition (encode left vs. right X memory set size [2 vs. 4]) was presented equally often, in random order, in each block of testing. The experiment began with a block of 64 practice trials that was performed outside the magnetically shielded room, during which the experimenter ensured that subjects understood the task and was able to perform above chance level.

The amount of information maintained in VSTM was assessed using Cowan's k' formula (Cowan, 2001) on the behavioural results: (proportion of hits – proportion of false alarms) * the number of item presented. This formula is useful because it corrects for possible biases in the propensity to respond 'same' or 'different' (see also Pashler, 1988).

EEG and MEG recording

A CTF-VSM whole-head 275-sensor MEG system in a magnetically shielded room was used for the recording. Data were first filtered with a 60 Hz low-pass filter; prior to being digitalized at 240 Hz. Together with the 275 sensors, 29 reference channels were recorded, allowing the computation of a third order gradiometer noise reduction. Bad MEG channels (3 or 4, depending on the subject) were excluded from the recording. EEG (PO7, PO8, right mastoid) was also recorded with reference to the left mastoid, and later algebraically re-referenced to the average of the mastoids. Bipolar EOG (electrodes placed at the left and right canthi for horizontal EOG and above and below the left eyes for vertical EOG) was recorded in order to monitor eye blinks and eye movements.

The MEG analysis was done using CTF software, EEGLAB (Delorme & Makeig, 2004), Fieldtrip (F. C. Donders Centre for Cognitive Neuroimaging: <http://www.ru.nl/fcdonders/fieldtrip/>), and custom programs. The data were inspected visually in order to remove trials containing eye blinks, eye movements, or other artefacts in the electric or magnetic signals. Trials with and without a correct response were included in the analyses.¹ Data sets from subjects with at least 100 trials per condition were kept for

¹ Trials with a correct and incorrect response were included because an error in this task can arise at several stages of processing, and importantly because we expect errors even when subjects are performing the task as well as they can. Consider accuracy in the Load 4 condition. The subject could have successfully encoded part of the display (e.g., 3 out of the 4 disks). If the test disk corresponded to one of the encoded disks, the subject will make a correct response. If, on the other hand, the test disk probed one of the disk that was not encoded, the subject will have no information in memory and this will result in an

further analysis. The signals were filtered with a second order Butterworth low-pass filter (cut-off of 35 Hz for the MEG and of 10 Hz for the EEG).

Cortically-constrained source localization of the MEG signals during the retention period was performed for the 5 subjects for whom we had an anatomical MRI. Minimum-norm estimation of the current (Hämäläinen & Ilmoniemi, 1994) over the cortical surface was performed (with Brainstorm, <http://neuroimage.usc.edu/brainstorm/> and the MEG/EEG toolbox, <http://cogimage.dsi.cnrs.fr/logiciels/index.htm/> for BrainVisa, <http://brainvisa.info/>). One map was calculated for every time point and all maps covering the time window of interest were subsequently averaged. The group averages were performed by converting the surface-based representations of the minimum norm solutions to a volumetric representation and then projecting them to a common Talairach space. Given that minimum-norm estimates often have a positive value for one side of a given sulcus and a negative value for the other side, and that the sulci do not always align closely

error on many trials (incorrect guess). Note, however, that the same number of disks was in VSTM in both of these trials and that we would expect brain measures of VSTM activity to be the same in the two cases. Thus, for errors of this type, which will be more frequent at Load 4 than at Load 2, we wish to include both correct and error trials in the analysis of EEG and MEG activity during the retention interval. Finally, the inclusion of trials with errors resulting from a general failure to encode any information from the initial display can only lead to an attenuation of the SPCN and of differences in SPCN amplitude across load conditions. Thus, their inclusion in the analysis could not have produced the observed load effects.

across subjects, we computed the absolute values of estimated currents prior to averaging across subjects. A spatial filter (10 mm FWHM) was applied before averaging using SPM <http://www.fil.ion.ucl.ac.uk/spm/>. The group averages were then projected onto a brain template (Collin's N27 brain from the Montreal Neurological Institute) using SUMA and AFNI (Cox, 1996) for visualization purposes.

Results

Behaviour

Subjects encoded more stimuli in the load-4 condition ($k = 1.92$) than in the load-2 condition ($k = 1.54$), $F(1, 15) = 7.38$, $MSE = .2902$, $p < .015$. The position (left vs. right visual field) of the stimuli, however, had no effect ($F < 1$) on k , and the interaction between load and side was not significant ($F < 1$), see Table 1 for the values. For the trials where the test color changed, we observed that using a test color present in the encoding display lead to lower accuracy (76%) than using another color (88%), $F(1,15) = 37.88$, $MSE = .2902$, $p < .00002$. This factor had no interaction with the numbers of items, $F < 1$.

INSERT TABLE 1 ABOUT HERE

EEG

The EEG was segmented starting 200 ms prior to the onset of the memory array and ending 1400 ms after the onset of the memory array, and baseline corrected based on the mean voltage during the 200 ms pre-stimulus period, separately for the four conditions in

the experiment. We then averaged the EEG for all artefact-free segments separately for electrodes PO7 (left-posterior) and PO8 (right-posterior). Four subjects had to be excluded from the EEG analysis because at least one of the EEG electrodes did not keep a noise-free signal thorough the recording. The grand average waveforms for each condition are shown in Figure 2A. A clear separation of the waveforms is visible for the retention period. For both electrodes, the load-4 contralateral waveforms (i.e., load-4 Right for PO7 and load-4 Left for PO8) were more negative than the others, and the load-2 ipsilateral waveforms were more positive than the others, replicating the expected pattern of results for the SPCN.

INSERT FIGURE 2 ABOUT HERE

Figure 2B shows the SPCN calculated independently for each electrode (PO7 and PO8) by subtracting the ipsilateral waveforms from the contralateral waveforms. The mean voltage in a window of 400–1400 ms relative to the onset of the memory array for each condition (Load X Side) was submitted to a 2 (load-2 vs. load-4) X 2 (left vs. right) ANOVA, independently for each electrode. For PO8, as expected from previous research, the amplitude of the SPCN was higher for load-4 trials than for load-2 trials, $F(1, 11) = 5.87$, $MSE = .6108$, $p < .033$. This means that there was a greater side effect (a greater difference between activity for left trials than for right trials) at load-4 than at load-2. For PO7, however, this was not the case, $F(1, 11) = .01$, $MSE = .4333$, $p > .9$. Thus, we did replicate the load-related modulation of the SPCN, but only for the right electrode.

MEG

First, we computed the event-related magnetic field (ERMF) averaging over all conditions. In Figure 3 a map of the sensor distribution of mean magnetic field strengths

based on the grand average waveforms during the retention interval (400–1400 ms) is shown. The ERMF for each condition for each sensor was also computed. Figure 3 also shows selected grand average ERMFs for each condition at sensors chosen to be at the magnetic extrema in the global field map. It is interesting to note that each extremum had an equivalent one located roughly symmetrically on the other side of the midline, but in the opposite polarity. We will consider here the amplitude of the magnetic fields at each of the six major extrema in the grand average field map, and subject these means to ANOVAs that consider memory load and encoding side as within-subject factors. Note that we use the term amplitude here to refer to deviation from the mean. So for a negative-going waveform, a higher amplitude refers to lower values (more negative values).

INSERT FIGURE 3 ABOUT HERE

A higher mean absolute amplitude was found for load-4 trials than for load-2 trials at the two occipito-parietal extrema (MLO24²: $F(1, 15) = 4.75$, $MSE = 838.4$, $p < .045$ and MRO242: $F(1, 15) = 10.65$, $MSE = 840.86$, $p < .006$). A higher mean absolute amplitude was also found when the stimuli were on the contralateral side: right stimuli for MLO24, $F(1, 15) = 24.54$, $MSE = 271.05$, $p < .0002$, and left stimuli for MRO24, $F(1, 15) = 11.28$, $MSE = 381.41$, $p < .006$. However, this effect was identical for load-2 and load-4 trials, as indicated by the absence of a significant interaction between Load and Side (both $p > .1$). In others words, signals at these extrema showed an additive pattern: evoked-responses increased in absolute amplitude when observers maintained stimuli encoded from the

² CTF system sensors label. The second letter (R, L or Z) refer to the overlaid cerebral hemisphere (right, left or just above the midline). The third letter (F, C, O, P, T) refer to the overlaid cerebral lobe (Frontal, Centro-frontal, Temporal, Parietal or Occipital).

contralateral hemifield, but the effect was of equivalent magnitude for load-2 and load-4 trials. The degree of lateralization of the activity was identical across loads, which means that calculating the SPCM from these sensors leads to waveforms of equal amplitude in both load conditions. Thus the activity at these sensors could not reflect the generators of the SPCN found in the ERP literature (e.g., Jolicœur et al., 2006a, 2008; Klaver et al., 1999; Vogel & Machizawa, 2004).

The two temporal extrema exhibited an opposite modulation by load. The right temporal sensor (MRT222) showed a decrease in absolute amplitude at load-4 relative to load-2, for the first half of the retention period (400–900 ms), $F(1, 15) = 5.99$, $MSE = 821.15$, $p < .027$, which was not influenced by the position of the stimuli (both main effect of side and interaction, $p > .15$). The left temporal sensor (MLT222) had a marginally significant decrease of absolute amplitude at load-4 relative to load-2 conditions, $F(1, 15) = 3.43$, $MSE = 1110.07$, $p < .08$, for the first half of the retention period (400–900 ms). It also had a higher amplitude for trials with encoding from the ipsilateral side, $F(1, 15) = 6.14$, $MSE = 446.38$, $p < .026$. No effects were found for the second part of the retention period (900–1400 ms; $p > 0.3$ in every case).

The activity during the retention period for the two central extrema (MLC312 and MRC312), were not influenced by any of the experimental conditions ($p > .11$ in every case).

The foregoing analyses revealed that signals at sensors at the extrema of magnetic field strengths shown in Figure 3 could not reflect the magnetic equivalent of the SPCN. Occipito-parietal extrema had clear effects of memory load and side, but no interaction between these two factors (needed to produce the SPCN).

To examine in detail the influence of memory load and stimulus side during the memory retention interval, topographical difference maps of magnetic field strengths were calculated. The maps are shown in Figure 4, for all possible combinations of Load and Side. The top row contains maps averaged across the load conditions, and the bottom row contains maps from which the load-2 condition was subtracted from the load-4 condition. The left column contains maps averaged across the side conditions, and the right column contains maps from which the right condition was subtracted from the left condition.

INSERT FIGURE 4 ABOUT HERE

These maps allow us to visualise the effects of the conditions on the previously identified magnetic extrema. The two central extrema were visible in every map in the central rectangle (Figure 4E), which contains the topographical maps for the four conditions, but are absent from all the subtraction maps (right column and bottom row), confirming that activity measured at these sensors was identical across conditions. The two temporal extrema are visible in the load-4 – load-2 maps (Figure 4G), but they changed polarity, implying a decrease in activity as load increased. Indeed, statistical analyses reported earlier showed that these extrema were more active at load-2 than at load-4. These extrema are absent from the left minus right maps (right column), confirming that stimulus position did not affect activity at these locations. The two parieto-occipital extrema, however, are visible in the left minus right difference maps. In the average for left trials (Figure 4B, left map), the right parieto-occipital extremum is more active (more positive: red) than in the average for right trials (Figure 4B, right map), so the left – right subtraction leaves a red extremum on the right. The left extremum, however, is of inverted polarity (the left parieto-occipital extremum is negative: blue), but also exhibits an inverted effect (it is higher for the right than the left conditions), so the left – right subtraction also gives rise

to a red extremum in the difference map. These results allow us to see the distribution of activity across all sensors showing an effect of side (greater activity for stimuli encoded on the contralateral side).

The interaction between Load and Side can also be seen in the map shown in Figure 4I (bottom right of the figure). This map was computed as the difference of the effect of side at load-2 (Figure 4F, top) and at load-4 (Figure 4F, bottom); or as a difference of the effect of load for the encode-left (Figure 4H, left) and the effect of load for the encode-right (Figure 4H, right) conditions. The interaction map (Figure 4I) shows that there is a structured field pattern reflecting the interaction of Load and Side, and in particular an extremum over left parietal cortex, and a weaker one over central occipital regions.

The double-subtraction, interaction, map was rescaled and replotted in Figure 5 to ease visualization of its structure. Twenty sensors had a significant interaction of Load and Side ($p < .05$) for the retention period. These sensors are shown in white in Figure 5 where it can be seen that they clustered into two groups, a left cluster of 13 sensors and a right cluster of 7 sensors, overlapping the magnetic field extrema identified in this map. The grand average activity waveforms for each condition for the left cluster are shown in Figure 5 (top). The mean magnetic field strength in the time window of 400–1400 ms computed for each condition and subject was submitted to an ANOVA that considered Load and Side as within-subjects factors. We found a significant Load X Side interaction, $F(1, 15) = 8.67$, $MSE = 1333.52$, $p < .01$, and the pattern of activations suggests that the extremum at sensors over left parietal cortex could reflect the magnetic counterpart of the SPcN. It is clear that there was a significant load effect for stimuli encoded from the right, $F(1, 15) = 11.47$, $MSE = 3600.05$, $p < .005$, but no effect for stimuli encoded from the left, $F(1, 15) = .75$, $MSE = 3478.5$, $p > .39$. The second cluster was near the midline but included more right than left sensors. The mean activity for these sensors during the

retention interval also produced a significant Load X Side interaction, $F(1, 15) = 7.27$, $MSE = 343.04$, $p < .02$. Further analysis did not indicate load effects for stimuli encoded from the left or right (both $p > .25$), but indicated that the load-4 Left waveform was of higher amplitude than the average of the three others $F(1, 15) = 8.8$, $MSE = 2148.448$, $p < .01$. These two clusters thus have activation patterns that are consistent with the expected pattern of the magnetic equivalent of the SPCN component of the ERP. We will refer to this pattern in the MEG results as the SPCM (sustained posterior contralateral magnetic) response.³

Ipsilateral activation

We compared the magnitude of the ipsilateral activation in MEG and EEG to the magnitude of the SPCM and SPCN. The magnitude of the load effect (difference between load 2 and load 4) for the ipsilateral stimuli at MLO24 and MRO24 sensors was of 16.96

³ It could be argued that the statistical criteria we used to identify the sensors showing an interaction were not sufficiently strict. Indeed, a statistical threshold of .05 could lead to 14 false positive sensors out of 270 tested, which is only slightly lower than the 20 we found. However, several considerations convinced us that this was not the case here. First, the location of the twenty sensors had a clear spatial structure (they were all adjacent to others sensors showing the interaction), which should not be the case if these were random false positives. Second, the summed activity of each cluster was coherent and led to significant interactions in further statistical tests. Third, their activations during the retention period followed our hypotheses concerning the relative amplitude of load effects at ipsilateral and contralateral sensors. Indeed, all the sensors showing a significant interaction term in the ANOVA were selected, without specifying the pattern giving rise to that interaction. The clusters identified showed a larger effect of memory load when subjects encoded stimuli from the contralateral visual field than from the ipsilateral field, which provides strong confirmation that these results are not accidental.

fT). This value is close to the magnitude of the SPCM differences between the SPCM at load 2 and the SPCM at load 4 for the interaction-significant cluster (mean effect of 18.47 fT). Indeed, no statistical differences were found between these two measures, $t(15) = .206, p > .83$. Conversely, for the SPCN, (Figure 2), the magnitude of the load effect for the ipsilateral stimuli (.378 μV), was not significantly different from the amplitude of the SPCN (.371 μV), $t(11) = .026, p > .98$, with PO7 and PO8 electrodes combined. The ipsilateral load effect, which is subtracted-out in the SPCN and SPCM calculation, can have an amplitude equivalent to the SPCN and SPCM themselves, and therefore it seems important also to consider these effects in future research.

INSERT FIGURE 5 ABOUT HERE

Minimal-Norm estimation of the current density

The cortical sources of the Load effect were localized using a minimum norm estimation of the current density (Hämäläinen & Ilmoniemi, 1994) for each of the 5 subjects for whom we had an anatomical MRI. To determine if subjects in this subset of our sample were representative of the whole sample, the previously described ANOVAs were re-calculated using only these five subjects. Although the average values were different across groups they generally exhibited the same patterns of effects (load, side), and the significant differences observed earlier with the larger sample were still significant or marginally significant for most of them. See Table 2 for the means of both samples.

Insert Table 2 about here

The effect of load for the encode-left condition (Figure 6A; the same data as Figure 4H, left) was localized within the left and the right parietal and occipital cortex. For the encode-right conditions (Figure 6B; the same conditions as for Figure 4H, right), the

localization was mainly within the left parietal and occipital cortex, although some activity is visible within the right parietal cortex. Together, these results show that both hemispheres had higher activation for higher loads although the left hemisphere had greater activity overall. The difference between the two previous sets of measures is shown in Figure 6C. The activation was less extended (although a threshold of 0.5 nA is used instead of 1 nA previously) and of lower magnitude, but showed roughly the same localization pattern. The more interesting results from these analyses were the inversion of the effect for the left and the right hemisphere. Indeed, the negative differences for the left hemisphere indicated higher activation for the load-4 – load-2 Right map (i.e., contralateral load effect) than for the load-4 – load-2 Left map (i.e., ipsilateral load effect). Conversely, the positive differences for the right hemisphere indicated a higher activation for the contralateral (load-4 – load-2 Left) map than for the ipsilateral map. These results converged with what was seen with Figure 5, namely an increase in activation when more stimuli were encoded from the contralateral hemifield.

The exact location of the different maximal activation varied across conditions. There was occipital activation for the left hemisphere when the stimuli were encoded from the left hemifield (Figure 6a) which was not present when the stimuli were encoded from the right hemifield (Figure 6b). There was also activation in the post-central gyrus for this source localization solution which was not present for the corresponding encode-right condition.

INSERT FIGURE 6 ABOUT HERE

Discussion

We recorded EEG and MEG while observers performed a task designed to engage VSTM and designed to reveal possible lateralization of brain activity during the retention phase of the task (Figure 1). As expected, the maintenance of information in VSTM was accompanied by a sustained posterior contralateral negativity (SPCN) in the ERP analysis of the EEG (Figure 2), replicating previous work (e.g., Jolicœur et al., 2006a, 2008; Klaver et al., 1999; Vogel & Machizawa, 2004).

Analyses of the MEG data contribute to our understanding of the neural sources participating in the maintenance of information in VSTM and revealed an MEG counterpart (SPCM) of the SPCN (Figures 3, 4, and 5). The MEG results revealed clear-cut effects of load and side over occipito-parietal regions, and a clear interaction of load and side for two clusters of sensors (SPCM).

Maps of the average magnetic field amplitudes during the retention interval, for each condition and for various subtractions between conditions, are shown in Figure 4. A careful inspection of these maps and how they differ across conditions (seen also in the subtraction maps) reveals how the experimental manipulations affected the sustained magnetic activity during the retention interval. Interestingly, the double subtractions map (Figure 4I), reproduced with its own scale in Figure 5, had a clear structure and revealed the MEG distribution for the SPCM that corresponds to the SPCN. Sensors near the maxima in this double subtraction map had activity patterns in which a load effect was found, but only for visual stimuli encoded from the contralateral side of visual space. Cortically-constrained local currents estimated using linear inverse methods (minimum norm) also showed a higher effect of load for stimuli encoded from the contralateral side (Figure 6c).

Interestingly, the SPCM tended to be stronger over left parietal cortex than over the corresponding right side (the right-sided extremum was actually nearly over the midline; Figure 5). In any case, the distribution of event-related MEG results and of their corresponding minimum norm source localization estimates were nicely convergent with the ERP SPCN results in pointing to a clearly posterior neural locus.

In the present work we examined brain activity shortly after the presentation and encoding of lateralized visual stimuli. One could argue that the activity we observed could reflect activity other than that required to maintain information in VSTM. For example, some of this activity could reflect the deployment of attention toward the stimuli. Indeed, it is likely that spatial attention was displaced toward the encoding hemifield following the presentation of the arrow cues (presented at the beginning of each trial) and that attention remained focused at this location in preparation for both the encoding and the test display. Therefore, one could reasonably presume that the SPCN/M we observed here was in fact a manifestation of spatial attention. However, the following considerations lead us to reject this interpretation. An increase of the amplitude of the SPCN was observed without a concomitant increase of the amplitude of the N2pc – an electrophysiological marker of transient shifts of spatial attention (Jolicoeur, Brisson, & Robitaille, 2008). The modulation of the SPCN (reflecting VSTM) in absence of modulation of the N2pc (spatial attention) suggests that the SPCN is indexing something other than spatial attention. Furthermore, if the SPCN was due to sustained deployment of attention at the location of the test display, which would occur during the retention period we studied here, then the SPCN should vanish when the test display is presented at fixation because it would now be counterproductive to maintain attention focused in the periphery. However, an SPCN was also observed in an experimental design similar to the one used here but with the notable difference that test displays were always presented at fixation (Perron et al., 2008). Together, these two sets of results suggest that the SPCN is a distinct component from the N2pc and that the SPCN does not merely reflect sustained attention in visual space.

In related work several researchers have provided evidence that visual stimuli encoded from the left or right hemifield produce a mnemonic trace in the contralateral cerebral hemisphere (or, at least, a trace that is stronger in the contralateral than in the ipsilateral hemisphere). The lateralization of the memory trace is revealed by lateralized brain activity observed during the retrieval phase of memory experiments, for both short-term (Fabiani, Ho, Stinard, & Gratton, 2003; Shin, Fabiani, & Gratton, 2006) and long-term visual memory (Gratton, Corballis, & Jain, 1997; Gratton, 1998). This encoding-hemisphere specific activity during retrieval was also observed using event-related optical signal (EROS; Gratton, Fabiani, Goodman-Wood, & Desoto, 1998). For these experiments, stimuli to be encoded were initially presented in the left or the right hemifield as we did, but memory was subsequently tested with stimuli at fixation. The presence of lateralized activity for these centrally-presented test stimuli indicates undoubtedly that a lateralized mnemonic trace was created following the original encoding of lateralized stimuli. These results provide strong converging evidence for the notion that visual short-term memory can sometimes be reflected by lateralized brain activity. Considering that a lateralized mnemonic trace can be formed (Gratton and collaborators) and that both sustained and transient shift of attention do not affect the SPCN (Jolicoeur et al., 2008; Perron et al., 2008), we conclude that the SPCN/M described in the present work was most likely due to brain activity required to maintain information in VSTM.

The memory load effects were observed both at contralateral and ipsilateral sensors relative to the side from which objects were encoded (Figure 3). In fact, ERMF waveforms at many sensors over parietal regions had additive effects of side and load. That is, the load effect was just as strong for ipsilateral as for contralateral encoding. Although the greater contralateral load effects have been the focus of previous research (e.g., Brisson & Jolicoeur, 2007a, 2007b; Jolicoeur et al., 2006a, 2006b, 2008; McCollough, Vogel, & Machizawa, 2007; Vogel, McCollough & Machizawa, 2005), here we want to highlight the relatively large concurrent ipsilateral load-related response which is not visible when computing the SPCN or SPCM components in the contralateral minus ipsilateral difference

waves. The magnitude of the ipsilateral load effect, for the MEG sensors and the EEG electrodes ipsilateral to the encoded stimuli, was of equivalent magnitude than the SPCN and SPCM. Together, these results suggest to us that there are two aspects to load-related brain activity associated with retention in VSTM. One aspect is the modulation of this response as a function of the visual field from which stimuli were encoded, producing greater activity in the contralateral hemisphere. The other aspect is the clear bilateral increase in brain activity measured both in the EEG and MEG results. Given the strong bilateral posterior brain responses in parietal regions, as a function of VSTM load, the current results call for caution in the exclusive use of ipsilateral activity as a control for contralateral activity (e.g. Vogel & Machizawa, 2004; Gratton, 1998) in electrophysiological paradigms used to study VSTM. The present results suggest the potential usefulness for a different type of control, such as an ignore (do not encode) condition, which could be used in subtractions from an active (encode) condition. Alternatively, regressions using the subject's psychometric performance curve as a function of the number of items, as used by Todd and Marois (2004), may be another technique that could provide converging evidence from electrophysiological experiments.

Conclusions

Several conclusions concerning the representation of information in VSTM can be drawn from the present MEG work. Firstly, we found a major contribution to the maintenance of information in VSTM from neural generators located in the parietal cortex, converging nicely with previous fMRI work (e.g., Todd & Marois, 2004). Secondly, we established the presence of a lateralized MEG load-dependent response, the SPCM, which appears to be the MEG counterpart to the SPCN, suggesting that further work using MEG will likely prove to be useful in furthering our understanding of VSTM. The SPCM was

left-hemisphere dominant. Further work will be required to determine whether this hemispheric dominance is general. Thirdly, the additional increase in activity associated with a higher memory load was about the same on the contralateral side as that observed on the ipsilateral side. Thus, results suggested that the predominant cortical response to increases in VSTM load was a bilateral parietal increase in neural activity, rather than primarily a contralateral response.

References

- Brisson, B., & Jolicœur, P. (2007a). Electrophysiological evidence of central interference in the control of visuospatial attention. *Psychonomic Bulletin & Review*, 14, 126–132.
- Brisson, B., & Jolicœur, P. (2007b). A psychological refractory period in access to visual short-term memory and the deployment of visual-spatial attention: Multitasking processing deficits revealed by event-related potentials. *Psychophysiology*, 44, 323–333.
- Brisson, B., & Jolicœur, P. (2007c). Cross-modal multitasking processing deficits prior to the central bottleneck revealed by event-related potentials. *Neuropsychologia*, 45, 3038–3053.
- Cohen, J. D., Perlstein, W. M., Braver, T. S., Nystrom, L. E., & et al. (1997). Temporal dynamics of brain activation during a working memory task. *Nature*, 386, 604–608.
- Courtney, S. M., Petit, L., Maisog, J. M., Ungerleider, L. G., & Haxby, J. V. (1998). An area specialized for spatial working memory in human frontal cortex. *Science*, 279, 1347–1351.
- Courtney, S. M., Ungerleider, L. G., Keil, K., & Haxby, J. V. (1997). Transient and sustained activity in a distributed neural system for human working memory. *Nature*, 386, 608–611.
- Cowan, N. (2001). The magical number 4 in short-term memory: A reconsideration of mental storage capacity. *Behavioral & Brain Sciences*, 24, 87–185.
- Cox, R.W. (1996). AFNI: Software for analysis and visualization of functional magnetic resonance neuroimages. *Computers and Biomedical Research*, 29:162-173.
- Curtis, C. E., & D'Esposito, M. (2003). Persistent activity in the prefrontal cortex during working memory. *Trends in Cognitive Science*, 7, 415–423.
- Dell'Acqua, R., Sessa, P., Jolicœur, P., & Robitaille, N. (2006). Spatial attention freezes during the attention blink. *Psychophysiology*, 43, 394–400.

- Delorme, A., & Makeig, S. (2004). EEGLAB: an open source toolbox for analysis of single-trial EEG dynamics including independent component analysis. *Journal of Neuroscience Methods*, 134, 9–21.
- Fabiani, M., Ho, J., Stinard, A., & Gratton, G. (2003). Multiple visual memory phenomena in a memory search task. *Psychophysiology*, 40(3), 472–485.
- Gratton, G. (1998). The contralateral organization of visual memory: a theoretical concept and a research tool. *Psychophysiology*, 35(6), 638–647.
- Gratton, G., Corballis, P. M., & Jain, S. (1997). Hemispheric organization of visual memories. *Journal of Cognitive Neuroscience*, 9(1), 92–104.
- Gratton, G., Fabiani, M., Goodman-Wood, M. R., & Desoto, M. C. (1998). Memory-driven processing in human medial occipital cortex: an event-related optical signal (EROS) study. *Psychophysiology*, 35(3), 348–351.
- Hämäläinen, M.S. and Ilmoniemi, R.J., (1994). Interpreting magnetic fields of the brain: minimum norm estimates. *Medical and Biological Engineering and Computing*, 32, 35–42.
- Jolicœur, P., Brisson, B., & Robitaille, N. (2008). Dissociation of the N2pc and sustained posterior contralateral negativity in a choice response task. *Brain Research*, 1215, 160 - 172.
- Jolicœur, P., Sessa, P., Dell'Acqua, R., & Robitaille, N. (2006a). On the control of visual spatial attention: Evidence from human electrophysiology. *Psychological Research*, 70, 414–424.
- Jolicœur, P., Sessa, P., Dell'Acqua, R., & Robitaille, N. (2006b). Attentional control and capture in the attentional blink paradigm: Evidence from human electrophysiology. *European Journal of Cognitive Psychology*, 18, 560–578.
- Klaver, P., Talsma, D., Wijers, A. A., Heinze, H.-J., & Mulder, G. (1999). An event-related brain potential correlate of visual short-term memory. *Neuroreport*, 10, 2001–2005.

- Linden, D. E., Bittner, R. A., Muckli, L., Waltz, J. A., Kriegeskorte, N., Goebel, R., et al. (2003). Cortical capacity constraints for visual working memory: dissociation of fMRI load effects in a fronto-parietal network. *Neuroimage*, 20, 1518–1530.
- McCollough, A. W., Machizawa, M. G., & Vogel, E. K. (2007). Electrophysiological measures of maintaining representations in visual working memory. *Cortex*, 43(1), 77-94.
- Pashler, H. (1988). Familiarity and visual change detection. *Perception and Psychophysics*, 44 369–378.
- Perron, R., Lefebvre, C., Robitaille, N., Brisson, B., Gosselin, F., Arguin M., Jolicoeur, P. (In press). Attentional and anatomical considerations for the representation of simple stimuli in visual short-term memory: Evidence from human electrophysiology. *Psychological Research*.
- Postle, B. R., Berger, J. S., & D'Esposito, M. (1999). Functional neuroanatomical double dissociation of mnemonic and executive control processes contributing to working memory performance. *Proceedings of the National Academy of Sciences of the USA*, 96, 12959–12964.
- Robitaille, N., & Jolicoeur, P. (2006). Fundamental properties of the N2pc as an index of spatial attention: Effects of masking. *Canadian Journal of Experimental Psychology*, 60, 101–111.
- Robitaille, N., Jolicoeur, P., Dell'Acqua, R., & Sessa, P. (2007). Short-term consolidation of visual patterns interferes with visuo-spatial attention: Converging evidence from human electrophysiology. *Brain Research*, 1185, 158-169.
- Rowe, J. B., Toni, I., Josephs, O., Frackowiak, R. S., & Passingham, R. E. (2000). The prefrontal cortex: response selection or maintenance within working memory? *Science*, 288, 1656–1660.
- Sereno, M. I., Pitzalis, S., & Martinez, A. (2001). Mapping of contralateral space in retinotopic coordinates by a parietal cortical area in humans. *Science*, 294, 1350–1354.

- Shin, E., Fabiani, M., & Gratton, G. (2006). Multiple levels of stimulus representation in visual working memory. *Journal of Cognitive Neuroscience*, 18(5), 844-858.
- Todd, J. J., Fougner, D., & Marois, R. (2005). Visual short-term memory load suppresses temporo-parietal junction activity and induces inattention blindness. *Psychological Science*, 16(12), 965-972.
- Todd, J. J., & Marois, R. (2004). Capacity limit of visual short-term memory in human posterior parietal cortex. *Nature*, 428, 751-754.
- Todd, J. J., & Marois, R. (2005). Posterior parietal cortex activity predicts individual differences in visual short-term memory capacity. *Cognitive, Affective, Behavioral Neuroscience*, 5, 144-155.
- Vogel, E. K. & Machizawa, M. G. (2004). Neural activity predicts individual differences in visual working memory capacity. *Nature*, 428, 748-751.
- Vogel, E. K., McCollough, A. W., & Machizawa, M. G. (2005). Neural measures reveal individual differences in controlling access to working memory. *Nature*, 438, 500-503.
- Xu, Y., & Chun, M. M. (2006). Dissociable neural mechanisms supporting visual short-term memory for objects. *Nature*, 440, 91-95.

Figure captions

Figure 1. Stimulation protocol. First, arrowheads indicated the side (left or right) of the display containing the disks (load of 2 or 4 disks) to be encoded. A test display appeared 1,200 ms afterward, and the task was to indicate if the disk presented had the same color as the one presented initially at this location. A load-4 left trial requiring the answer “same” is illustrated.

Figure 2. Electrophysiological results. Event-related potentials (row A) for the electrode over the left (PO7, left column) and the right (PO8, right column) hemisphere, averaged relative to the onset of the disks to be encoded. A separation of the waveforms for different memory load and side conditions is visible for the retention period (starting about 400 ms after the onset of the stimuli and lasting up to 1,400 ms). For both electrodes, the amplitude is more negative for the load-4 trials than for the load-2 trials. The most negative amplitude was obtained for the load-4 right trials, at the left electrode, and for the load-4 left trials, at the right electrode. In row B we show the contralateral minus ipsilateral difference waves showing the SPCN component. A clear effect of load on the SPCN was found at PO8, but not PO7.

Figure 3. Map of the magnetic activity, averaged over all conditions, during the retention period (400–1400 ms). Each magnetic peak had an equivalent one located on the other side of the map, but reversed in polarity. A sustained evoked response during the retention period was obtained for each condition from the peak sensor (shown in white) in each peak. The two temporal peaks (MLT22 and MRT22) showed higher absolute amplitude, during the retention period, for the load-2 conditions. The two central peaks (MLC31 and MRC31), however, did not exhibit clear modulations as a function of the experimental conditions. The two occipito-parietal peaks (MLO24 and MRO24) showed

the highest absolute amplitude for the load-4 conditions, when the stimuli were encoded from the contralateral visual hemifield, and the lowest absolute amplitude for the load-2 conditions, when the stimuli were encoded from the ipsilateral hemifield.

Figure 4. Average and subtraction magnetic field maps for the retention period (400–1400 ms). The four condition grand averages (E) present the same six magnetic extrema as the grand average map computed over all conditions (A). The two occipito-parietal peaks are visible for the memory load difference maps (load-4 – load-2, G and H). The Side difference maps (left – right, C and F) show mainly the left occipito-parietal peak. The Load X Side interaction difference map (I) was generated by subtracting the side effect (left – right) at load 2 from the side effect at load 4 (i.e., [left load-4 - right load-4] - [left load-2 - right load-2]). This map also showed a left posterior magnetic peak, but the location of this peak did not match exactly the location of the left occipito-parietal peak in the grand average map (A).

Figure 5. Interaction between Load and Side: Map and waveforms. Sensors with a significant interaction of Load and Side are shown in white. The evoked-response waveforms from the 13 left sensors showed higher (more positive) amplitude for the load-4 right trials. The evoked-response waveforms for the 7 right sensors, conversely, showed higher (more negative) amplitude for the load-4 left trials. These waveforms indicated a higher activation for the load-4 stimuli than for load-2 stimuli that was larger for stimuli encoded from the contralateral visual field.

Figure 6. Group results from minimum-norm cortically constrained source localization of the load effects, as a function of encoding side. A: Cortical sources for the load effect when encoding stimuli from the left visual field. B: Cortical sources for the load effect when encoding stimuli from the right visual field. C: Difference of the source

localization solutions highlighting the Load X Side interaction, associated with parietal, and occipital sources. Values are in nanoampere.

Table 1. Behavioral k values, for each combination of memory load and encoding side.

SEM in parentheses.

<u>Side</u>	<u>Load 2</u>	<u>Load 4</u>
Left	1.53 (.15)	1.91 (.25)
Right	1.55 (.14)	1.91 (.26)

Table 2. Average amplitude of the magnetic field during the retention interval, in

femtoTesla, for each combination of memory load and encoding side, for sensors used in the analyses, and averages for the two clusters, for the overall group of 16 subjects and for the subset of 5 subjects included in the detailed source localization analyses.

SEM in parentheses

	16 subjects				5 subjects			
	Load 2		Load 4		Load 2		Load 4	
	Left	Right	Left	Right	Left	Right	Left	Right
MLO24	8.7 (13)	-6.6 (13)	-5.0 (14)	-24.2 (17)	7.8 (21)	-8.2 (28)	-16.4 (24)	-36.3 (33)
MRO24	18.8 (11)	2.9 (10)	49.6 (15)	28.1 (15)	25.5 (18)	-1.1 (16)	65.6 (26)	39.1 (21)
MLT22	-74.8 (14)	-70.7 (14)	-82.1 (18)	-75.7 (18)	-88.2 (26)	-75.0 (24)	-76.9 (28)	-87.6 (31)
MRT22	38.4 (14)	32.7 (14)	28.4 (13)	29.2 (14)	70.5 (23)	67.8 (19)	52.9 (24)	53.8 (30)
MLC31	11.6 (11)	10.2 (14)	17.6 (16)	17.3 (17)	21.1 (22)	5.7 (22)	38.2 (33)	21.5 (32)
MRC31	-18.1 (10)	-14.6 (10)	-29.3 (13)	-25.8 (13)	-33.2 (26)	-20.9 (26)	-48.7 (33)	-37.4 (36)
Left cluster	0.5 (15)	-13.0 (16)	-4.6 (18)	-32.9 (18)	-29.8 (30)	-44.3 (32)	-32.0 (36)	-70.4 (35)
Right cluster	21.2 (10)	6.6 (9)	29.5 (13)	5.4 (12)	25.2 (20)	12.9 (21)	52.2 (22)	21.6 (22)

Figure 1

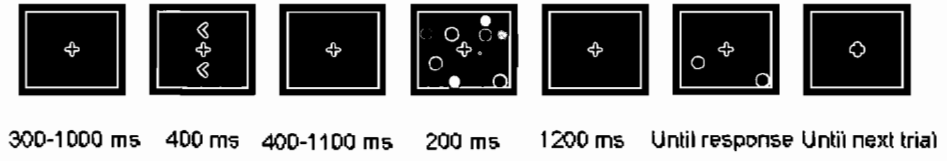


Figure 1

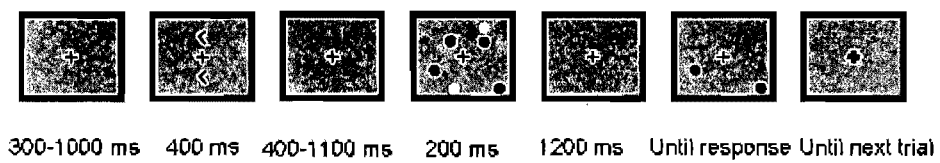
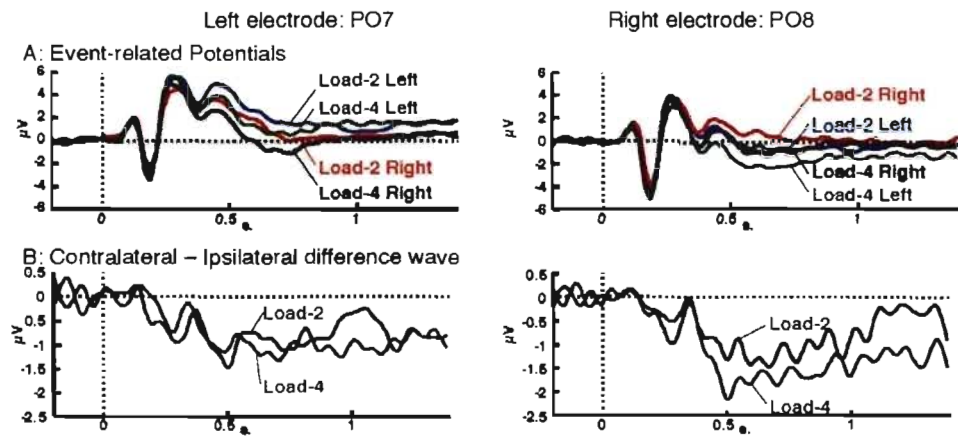
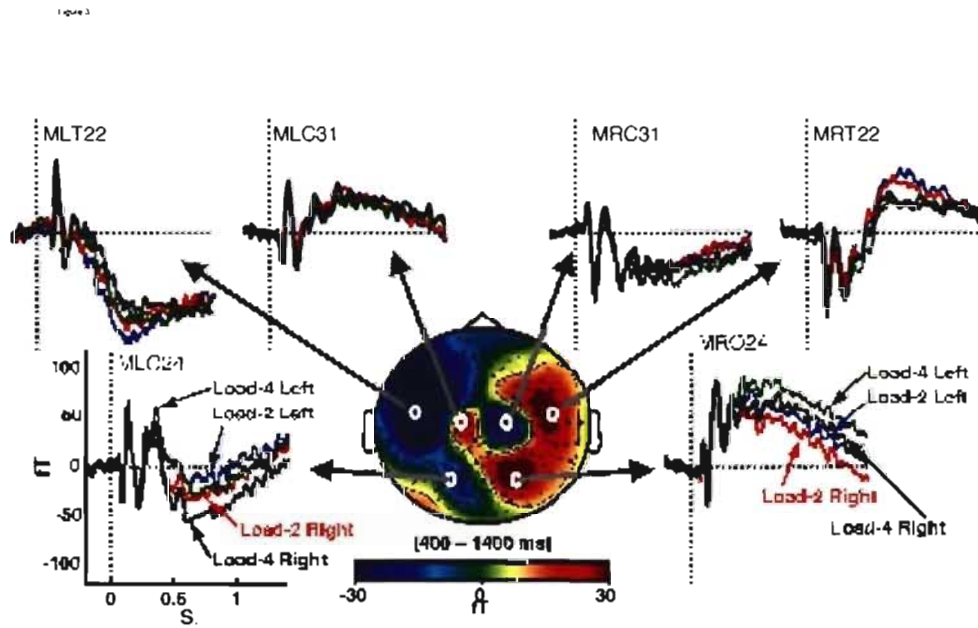


Figure 2





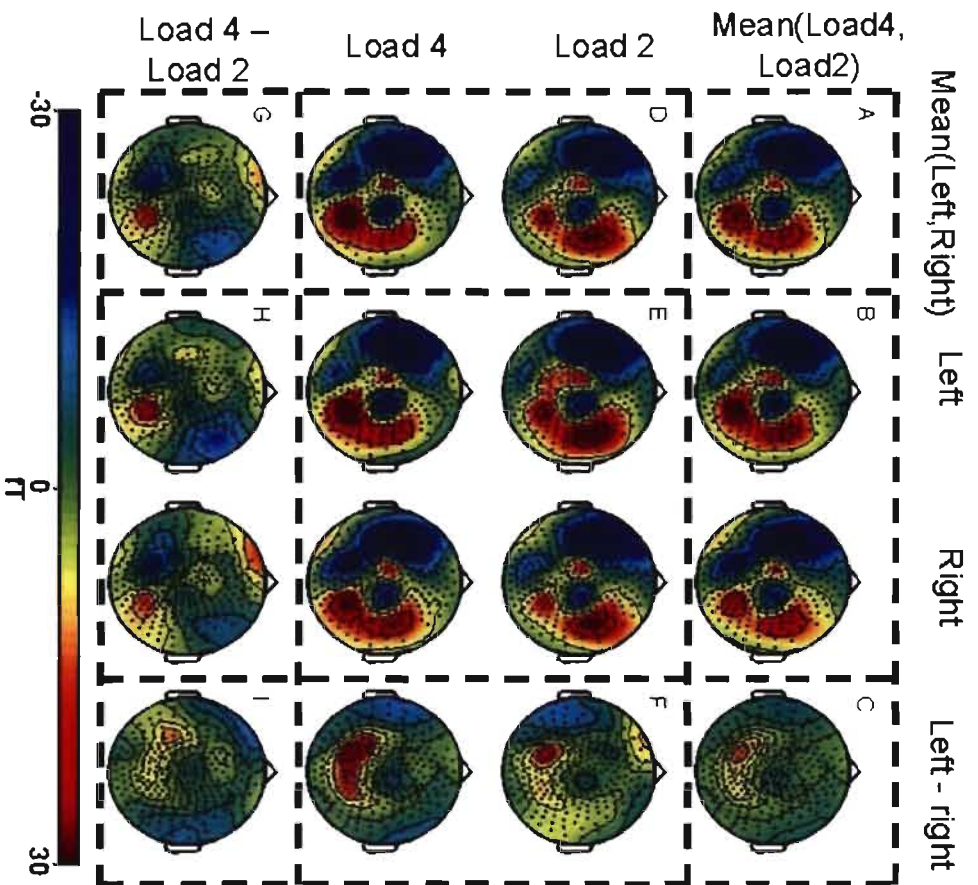


Figure 4

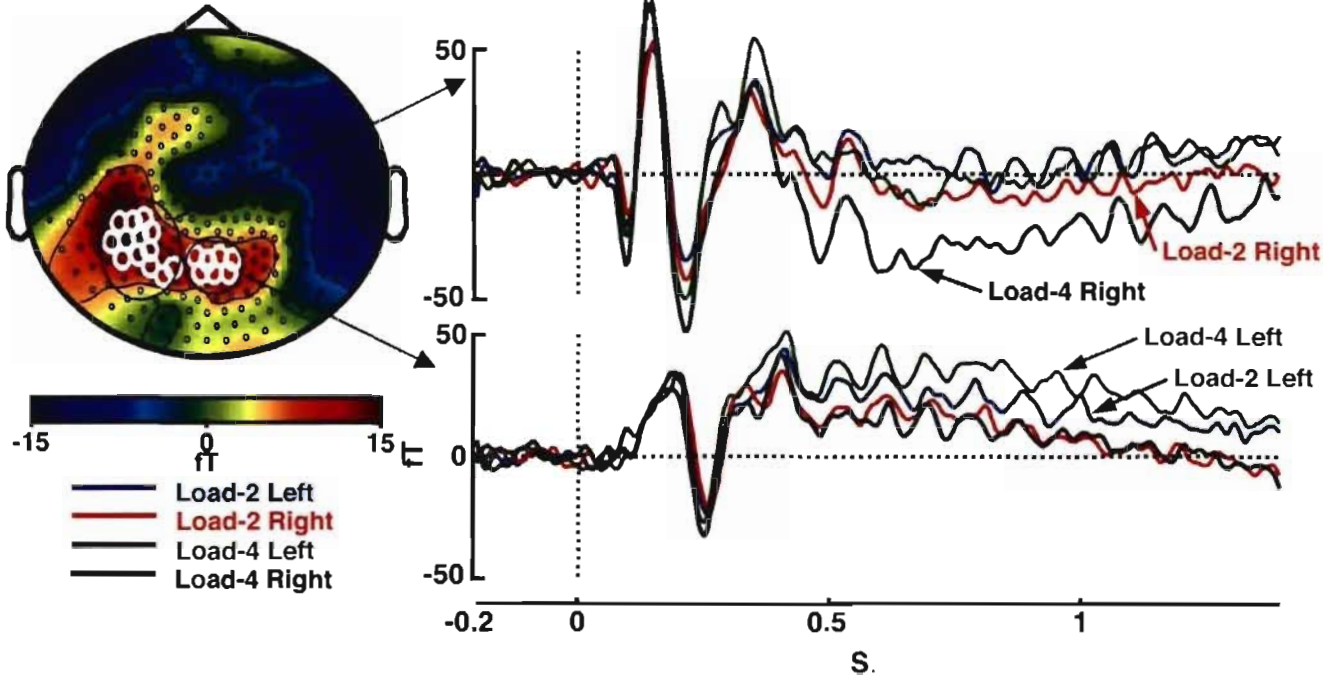
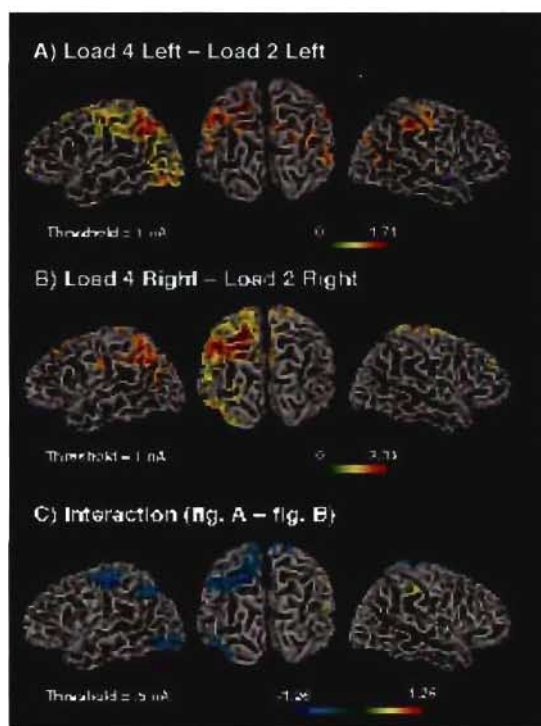


Figure 5



Chapitre 3 : Article 2

ARTICLE 2

Nicolas Robitaille, René Marois, Jay Todd, Stephan Grimault, Douglas Cheyne, et Pierre Jolicœur (en préparation). Distinguishing between lateralized and nonlateralized brain activity associated with visual short-term memory: fMRI, MEG, and EEG evidence from the same observers



**Distinguishing between lateralized and nonlateralized brain activity
associated with visual short-term memory: fMRI, MEG, and EEG
evidence from the same observers**

Nicolas Robitaille¹, René Marois², Jay Todd², Stephan Grimault^{1,3}, Douglas Cheyne⁴, and
Pierre Jolicœur¹

¹Centre de recherche en neuropsychologie et cognition, Département de psychologie, Université de Montréal,
Montréal, Québec, Canada.

²Vanderbilt Vision Research Center, Department of Psychology, Vanderbilt University, 530 Wilson Hall,
Nashville, Tennessee 37203, USA.

³Centre national de la recherche scientifique, France.

⁴Program in Neurosciences and Mental Health, Hospital for Sick Children, Toronto, Ontario, Canada.

Corresponding author :
Robitaille, Nicolas
Département de Psychologie
Pavillon Marie-Victorin
90, avenue Vincent d'Indy
Montréal, Québec
H2V 2S9
Tel.: 514 343-6111 #2631

E-Mail 

Abstract

Maintenance of centrally presented objects in visual short-term memory (VSTM) leads to **bilateral** increases of BOLD activations in IPS/IOS cortex, while maintaining stimuli encoded from a single hemifield leads to a sustained posterior **contralateral** negativity (SPCN) in electrophysiology. These two results (bilateral and contralateral activations) have never been investigated using the same physiological measures. We recorded the BOLD response using fMRI, and magnetoencephalography (MEG), and electrophysiology (EEG), while subjects encoded visual stimuli from a single hemifield. The EEG showed an SPCN, as did the MEG evoked fields originating from superior IPS. However, no SPCN-like activation was observed in the BOLD signals, contrary to the assumption that these BOLD, EEG, and MEG responses — that were each linked to the maintenance of information in VSTM — are markers of the same neuronal processes. A strong bilateral response was found in IPS/IOS cortex for BOLD activation and for MEG evoked fields (in addition to the bilateral MEG responses), despite the unilateral encoding of visual stimuli. Furthermore, left inferior occipital (IO) cortex, was distinguished by showing an unexpected interaction between load and side, the only BOLD activation having the SPCN-like pattern. The BOLD response in parietal cortex remained bilateral, even after unilateral encoding of the stimuli, but MEG showed both bilateral and contralateral activation, each likely reflecting a sub portion of the neuronal populations participating in the maintenance of information in VSTM.

Keywords: magnetoencephalography (MEG), functional magnetic resonance imaging (fMRI), visual short-term memory (VSTM), intra-parietal/intra-occipital cortex (IPS/IOS), sustained posterior contralateral negativity (SPCN), sustained posterior contralateral magnetic field (SPCM).

Introduction

While behaving in a constantly changing visual environment, the visual system must maintain, in a readily available form, a portion of what was seen; a process supported by visual short-term memory (VSTM). Recently, important insights about the neural representation of VSTM were obtained following the identification of several new physiological markers of VSTM. The maintenance of information in VSTM is likely supported by the intraparietal and intraoccipital cortex (IPS/IOS), given that the activity in these cerebral regions follows the amount of information held in memory¹. Conversely, lateralized visual stimuli, to be encoded and maintained for a brief period of time (e.g., one or two seconds), lead to sustained neural activity over the posterior regions of the cerebral cortex, contralateral to the stimuli to be encoded². An increase of the amplitude of this memory-related ERP component (labeled SPCN, for Sustained Posterior Contralateral Negativity) as the number of items remembered increased was found³, and was subsequently used in several investigations of VSTM⁴⁻⁷.

These two physiological markers of VSTM (the BOLD response, and the SPCN) have several features in common. The topographical distribution of the SPCN⁴⁻¹⁰ is very similar to that of the N2pc, for which parietal sources were identified¹¹. The amplitudes of the electrophysiological and hemodynamic markers increase monotonically with the number of items presented, but reach a maximum at the subject's maximal VSTM capacity (e.g., calculated using Cowan's K formula^{12, 13}), creating a plateau for higher numbers of items. Moreover, both markers were linked to individual differences in VSTM capacity^{14, 15}. The most prominent difference between the SPCN and the BOLD activation in IPS/IOS is the encoding field manipulation used to isolate the SPCN. Indeed, the SPCN, as other ERP components like the N2pc and the LRP, is based on a "contralateral minus ipsilateral" difference to isolate the lateralized portion of the brain response, where the ipsilateral side of the brain is used as a control "condition," or as a control activation¹⁶ for the contralateral activation. This manipulation is intended to remove the effect of any activity that is not lateralized according to the stimulus presentation side (or response-button side, for LRP). Studies of VSTM using fMRI so far have used bilateral stimulus presentations and found bilateral activation in IPS/IOS.

INSERT FIGURE 1 ABOUT HERE

The goal of the present study was to observe, directly, the relationship between the BOLD activation in IPS/IOS, the electrophysiological (SPCN) component, and the magnetoencephalographical (SPCM) marker of the maintenance of information in VSTM. We tested the same subjects both in fMRI and in MEG — with EEG recorded simultaneously with MEG — in very similar experiments designed to allow comparisons across brain imaging modalities. To allow the use of a regression on the numbers of items accurately held in memory¹⁵, we presented 1, 2, 4, or 6 visual objects. We used bilateral stimulus presentations, with an arrow indicating which stimuli (on the left or right side of the screen) had to be encoded^{14, 18, 19}. This allowed us to compute both a load-related activation (by collapsing trials with left-encoding and right-encoding) and an SPNC-like activation (using the “contralateral minus ipsilateral” approach) with the data from all imaging modalities. We recently coined the term SPCM, a magnetic equivalent of the SPCN (labeled SPCM for Sustained Posterior Contralateral Magnetic field)¹⁸. Sensors showing the SPCM were located on two separate clusters of sensors, over parietal cortex. A critical finding of that study was that on different sensor clusters (different than for the SPCM) we found an increase of amplitude with the increase in the numbers of items held in memory that was independent from the encoding hemifield (i.e., no interaction between hemifield and the increase in activation as a function of memory load). This led us to conclude that a more complex network of neural generators was active during the retention period than what was isolated as the SPCM. However, this previous study only used two loads, preventing the use of a parametric analysis based on estimated memory capacity across loads (e.g., regression using Cowan’s k^1). Furthermore, anatomical MRIs were available for only 5 participants, which limited the possibility of source localization. This limitation was overcome here because an anatomical MRI was acquired for every subject.

The specific hypothesis we will test is that both physiological markers (BOLD activation in IPS/IOS and the SPCN/M) reflect the same underlying neural processes. In other words, the generators of the SPCN/M would be the left and right IPS/IOS; each of them would increase in activation level more for stimuli encoded from the contralateral side of space,

relative to activation for stimuli encoded from the ipsilateral side. When stimuli are encoded from both side of the screen simultaneously, the result would be a bilateral activation, as found in fMRI and suggested by the results of Klaver². We consider that this is commonly assumed, as both papers^{1, 14} are often cited as though the SPCN/M and BOLD responses are different manifestations of the same underlying brain functions.

RESULTS

Behavior

The number of items effectively encoded (calculated with Cowan's k formula¹²) varied across set size and reached a plateau between 4 and 6 items, as shown in Figure 2a, $F(3,33) = 9.66, p < .0001$, see figure 2a. All other factors (presentation side, first or second day of recording, fMRI or MEG recording) did not have a significant effect on k , all $F_s < 1$. The group k values for each memory set size, averaged across both fMRI and MEG recording sessions (weighted by the number of trials in each), was used as the estimate of VSTM capacity at each load. These values were then used to create the load regressor, which will be used in the subsequent analyses of MEG, ERP, and fMRI data.

INSERT FIGURE 2 ABOUT HERE

ERP — event-related potentials

The SPCN waveform amplitude increased during the retention period as load increased from 1 to 4, and then plateaued (figure 2c). The SPCN is calculated by subtracting the activation at the ipsilateral electrode (i.e., PO8 when the arrows pointed to the right and PO7 when the arrows pointed to the left) from the activation at the contralateral electrode (i.e., the contralateral minus ipsilateral difference). Note that the same type of calculation will be performed with all the physiological signals used in the study, namely we will compute an SPCM for the magnetic evoked field and an SPCN-like activation for the BOLD signal to quantify the degree to which the contralateral brain response is greater than the ipsilateral response. The amplitude of the SPCN during the retention period (400 to 1200 ms after the onset of the display), is plotted with SEM in figure 2b (green dashed curve), was significantly predicted by k , $F(1,35) = 7.94, p < .008$. In order to compare to the fMRI analysis below, we also examined the overall effect of load in the average of the ipsilateral and contralateral ERP waveforms (rather than in the subtraction of these waves) (figure 2d). Robust initial visual components following the onset of the stimuli were present — this is because these waveforms are not subtraction waveforms. However, the amplitude

of the ERP was not consistent through the retention period, and not significantly predicted by k , $F(1,35) = .034$, $p > .85$; see blue curve in figure 2b. The unsubtracted ‘load’ results probably reflect the contribution of multiple generators (e.g., sustained posterior negativity, on the one hand, and P3, on the other), and highlight the usefulness and importance of using the SPCN (contralateral minus ipsilateral difference waves) in the analysis of the EEG data, in the study of VSTM.

ERF — event-related fields

Load-sensitive channels (figure 3a) were identified with multiple-regression of the MEG evoked fields. The two clusters of channels, each channel indicated with a bold dark circle, had a p -value inferior to .001 (uncorrected, channels evaluated independently). The left cluster contained 21 contiguous sensors with primarily ingoing (negative) fields during the sustained response and the right cluster of 20 contiguous sensors with primarily outgoing (positive) fields during the sustained response (the polarity of signals depends on the position and orientation of the neural generators relative to the sensors). The ERFs for the left cluster (figure 3b and 3c) showed evoked responses followed by sustained activity after the onset of the encoding-display. During the retention period, there was a clear differentiation of the waveforms according to the memory load conditions; the higher load showed higher amplitude from load 1 up to load 4, and no further increase from load 4 to load 6. The ERFs for the right cluster (figure 3e and f) showed again a clear differentiation as a function of memory load; higher load led to higher amplitude up to load 4 and a plateau across loads 4 to 6. For comparison between left and right sensors we inverted the polarity of left cluster channels. Combined activity of these waveforms during the retention period was significantly predicted by k , $F(1,35) = 27.34$, $p < .0001$, (figure 3d). However, the SPCMs calculated from these waveforms were not significantly predicted by k , $F(1,35) = 2.02$, $p > .16$.

INSERT FIGURE 3 ABOUT HERE

Side-sensitive channels were also identified using multiple-regression (figure 3g). The posterior midline cluster contained 28 sensors. To avoid cancellation of the ERFs, we computed the average activity separately for the left and the right sensors within this cluster

(midline sensors were ignored). The 14 sensors in the left portion of the cluster had higher amplitude for the contralateral trials (figure 3h) than for the ipsilateral trials (figure 3i). Conversely, the 11 sensors in the right portion of the cluster showed higher activity for the contralateral trials (figure 3l) than for the ipsilateral trials (figure 3k). Combined activity (again here we transformed the left sensors to be negative-going) of these waveforms during the retention period (figure 3j) indicated a modulation by the load, for the overall load effect $F(1,35) = 15.56, p < .0001$. In order to determine if we could replicate here the SPCN effect, we also calculated the SPCM from these sensors. The amplitude of the SPCM across the load was significantly modulated by k, $F(1,35) = 12.31, p < .002$. This indicates that there are cerebral regions (to be localized more precisely with the forthcoming source localization) that emit a higher magnetic field when there is an increase in the number of items encoded from their contralateral hemifield.

Activity in the two anterior-most clusters was not significantly modulated by Load (both F s $< 3.9, ps > .05$) or by the Load X Side interaction (both F s $< 1.4, ps > .05$). Given that activity in these clusters was not affected by the memory load manipulation, we did not analyze them further.

These analyses of the ERFs indicated that the effects we were interested in were visible at the sensor level, and this justified the source-localization analyses we present in subsequent sections of the article.

INSERT FIGURE 4 ABOUT HERE

fMRI -- Functional Magnetic resonance imaging

Load-related activity was found using a regression on k on the fMRI BOLD signal, as expected from previous research, and the results are shown in figure 4. We isolated a pair of symmetric posterior clusters containing the IPS/IOS coordinates previously described¹. Within each cluster, three maxima were visible. For each bilateral pair of maxima (we defined maxima as a sphere of 5 mm surrounding the position of the voxel having the highest local activation), we extracted the time-course using deconvolution (see figure 5 for an example time-course). To examine more closely the effect of load, we averaged together

the activity of both maxima, for both side-conditions (blue curves on the middle column of figure 4), at time 8.8 and 11 sec. This activation was submitted to a multiple-regression analysis, with k as the regressor of interest. This second analysis was intended as a direct test of the effect of mnemonic load for a specific pair of maxima located in homologous areas of the brain. It is indeed redundant in the present case (because these voxels were shown to follow k in the previous regression analysis), but it will allow a direct comparison of the effect of mnemonic load for different brain areas and most importantly for the SPCN-like BOLD signal described later in this paragraph. The numbers of items was also included as a covariate to remove any modulation of the response by the actual visual display. The superior IPS maxima (figure 4, row A) showed a clear modulation correlated with k , $F(1,34) = 5.11$, $p < .03$. The IOS maxima (figure 4, row B) were also significantly predicted by k , $F(1,34) = 12.01$, $p < .002$; as were the ventral-occipital (VO) maxima (figure 4, row C), $F(1,34) = 6.56$, $p < .02$. These results were expected because these maxima were identified on the load-effect map. In order to compare these results with the EEG and MEG results, an SPCN-like BOLD activation was also calculated (blue curves of the third column of figure 4) by subtracting the activation of the ipsilateral maximum (left maximum for left stimuli and right maximum for the right stimuli) from the contralateral one. Although we found increases in BOLD signal strength that were larger on the contralateral side, none of them had a clear plateau between load 4 and load 6, and hence none was modulated by k , all $F(1,34) < 1$, all $p > .6$. Overall, we found clear load effects that followed k when we averaged over left and right hemisphere maxima (replicating previous results¹). However, we did not find an SPCN-like BOLD response that followed behavioral load effects, as estimated by k .

INSERT table 1 ABOUT HERE

We also determined which brain areas showed a BOLD response significantly different across the encode-left and encode-right conditions, independently of the numbers of items encoded. This "side map" (figure 4d and 4e) showed clusters of significant activation (corrected for multiple comparisons using False Discovery Rate: $q < .05$). The inversion of polarity across hemisphere indicates a systematic modulation according to the position of the stimulus to be encoded: activation was higher for stimuli encoded from the contralateral

hemifield. We isolated three pairs of maxima in these maps. The first pair of maxima was located in the middle occipital gyrus, in Brodmann area 18; slightly more central and posterior than the IOS maxima (Figure 4D; see table 1 for the Talairach coordinates). Their activity was significantly predicted by k , $F(1,34) = 5.39$, $p < .03$. The activation in the second pair of maxima, located in the inferior occipital (IO) gyrus, was also significantly predicted by k , $F(1,34) = 8.84$, $p < .006$. Note that the arrows on Figure 4E indicate the maxima used. The medial activation in the left hemisphere did not have a homologous area to be compared with, so we did not include this region in the analysis. The third pair of maxima corresponded to the VO maxima described in the load maps. The SPNC-like BOLD activation, unlike what was found in any of the previously described maxima pairs, was significantly modulated by k for the IO maxima, $F(1,34) = 5.36$, $p < .03$. The time course of the BOLD response, estimated by deconvolution for this pair of maxima, is shown in figure 5. For the left IO (top row of figure 5), the response to the load was modulated by the position of the stimuli, leading to a significant Load X Side interaction, $F(1,80) = 11.92$, $p < .001$. The right IO BOLD response to the load, on the contrary, was not influenced by the position of the stimuli, $F(1,80) = .19$, $p < .66$. The SPNC-like activation for the two others pairs of maxima (MOG and VO) were not modulated by load, $F(1,34) < 1$.

INSERT FIGURE 5 ABOUT HERE

The interaction (Load X Side) SPM map did not exhibit any significant activation, either using FDR or cluster threshold²⁰ when correcting for multiple comparisons. Thus, among the significant activations found in the fMRI data, the only candidate cerebral region for creating a load-related asymmetry similar to what is commonly found in EEG and MEG was the left IO.

An increase of activation for contralateral trials relative to ipsilateral trials, proportional to the number of items presented (rather than on the numbers of items encoded, as measured with k), was visible for several of the maxima pairs in parietal and occipital cortex. Multiple regressions indicated a significant correlation with the numbers of items for all the maxima pairs, all $F_s > 5.5$, all $p_s < .025$, except for the superior IPS, $F(1,35) = 1.64$, $p >$

.20. Consequently, there are three occipital maxima pairs, IOS, middle occipital, and VO, that did not show a correlation with k , but that showed one with the numbers of items presented for encoding. Given that the same numbers of items were presented in both attended and ignored hemifield; this effect is likely attributable to attention or memory-related factors. However, the absence of a plateau when the capacity of VSTM was exceeded indicates a processing step that is distinct from a pure working memory-load effect and most likely corresponds to an attentional involvement in VSTM.

ER-SAM — SPM on the source-localization of the MEG signal.

For each condition and subject, activation volumes were created using three source-localization analyses (ER-SAM²¹, MEM²², and MNE²³). The ER-SAM (Event-Related Synthetic Aperture Magnetometry) analysis is a beamformer-based localization of the source of evoked-field. Beamformer analyses use the covariance across the sensors in the raw data (i.e., trial-by-trial, before creating ERF) to maximize the activation at the estimated sources and minimize activation from others sources. The specificity of the ER-SAM method is to maximize further the signal that is time-locked to an event — here the apparition of the stimuli to encodes. MNE and MEM analysis, on the contrary, consisted in projecting back the data from a single time point (in our case, from the averages of the time-points in the retention period) onto an ensemble of pre-determined sources oriented perpendicularly to the cortical surface (actually, the interface between the white and gray matter of the cortex). The obtained solution is then further constrained by maximizing the smoothness (MNE) or minimizing the entropy (MEM) of the solution. In the interest of space constraints, we show only the ER-SAM analysis here, but it should be noted that we found good agreement with MEM and MNE analyses. These methods are based on very different constraints and methods for source localization, and thus their convergence to the same source is a good indication of their reliability. The resulting 96 maps (12 subjects X 8 conditions) were then submitted to the same multiple linear regressions approach used for the fMRI data. To visualize the results, we overlaid them on a standard white-grey border surface, as shown in figure 6.

INSERT FIGURE 6 ABOUT HERE

Significant load effects (False Discovery Rate: $q < .05$, top row of figure 6) consisted of three main cerebral activations. An increase of activation with load for the left and the right IPS/IOS cortex was visible, and was confirmed with MNE and MEM. The right frontal decrease of activation associated with the increase in mnemonic load included the right infero-frontal gyrus and the right claustrum. This decrease in amplitude, however, was not visible in MNE or MEM. The ER-SAM map showing the effect of side showed less extended activations. Similar to the fMRI results, there is an inversion of the activation values for the left and right posterior cortex, although this inversion occurred at different horizontal planes for the left and right hemispheres and was generally superior to the fMRI foci (see areas indicated by arrows in figure 6, bottom row). Although the MEM and MNE maps did not reach significance, lowering the threshold in these maps revealed the same regions. The interaction maps (Load by Side) did not reach significance in the sources localization analyses.

In order to compare the MEG activation with the results found for fMRI, we used the previously identified maxima as ROIs. We averaged the activation in the ER-SAM maps, for a 7 mm radius sphere around the voxels of maximal activations in fMRI results (see figure 4, green curves). Statistical analyses were performed with multiple regression, and significance was assessed using permutation²⁴. Activation in all pairs of maxima was significantly predicted by k , all $ps < .009$. The same analysis conducted on the MEM and the MNE maps showed similar results. Thus, for every fMRI maximum found, the MEG activation showed an increase of activation as memory load increased. The SPCM was also calculated for these pairs of maxima. The SPCM for the superior parietal cortex was significantly predicted by k , $p < .022$. The IO gyrus showed a marginal SPCM, $p < .07$; while all other SPCM calculations were not influenced by load, p 's $> .11$. The SPCM on MNE and MEM maps did not reached significance. The parietal activations, thus, showed a higher response when the stimuli maintained in VSTM were encoded from their contralateral hemifield. This results contrast with the absence of SPCN-like activation in the BOLD signal for the same cerebral regions.

INSERT FIGURE 7 ABOUT HERE

Literature-based inferior IPS ROI

Inferior IPS has been linked to processing of information in VSTM^{25,26}, but did not reveal itself in our maxima-based fMRI analysis. As we considered it important to describe the behaviour of this region in our task, we defined ROIs base on Talairach coordinates from previous reports (see table 1). They are located more lateral and inferior than our superior IPS, which is consistent with the physiology of the IPS. The BOLD activation for this ROI is shown in figure 7. An increased of the BOLD activation as the numbers of items maintained in VSTM increased, thus showing a modulation by k , $F(1,34) = 7.87$, $p < .009$, but the SPCN-like BOLD activation was not modulated by k , $F < .58$, $p > .44$. This pattern of results is identical to what was found for the superior IPS. The numbers of items, however, showed a significant correlation with the SPCN-like activation, $F(1,35) = 5.23$, $p < .03$. Thus, the inferior IPS was the only cerebral region not in occipital cortex that showed a linear increase of activation for contralateral presentation of stimuli to be encoded. ER-SAM activation for these regions followed the same pattern: increase of activation with k , $p < .00001$, but the SPCN-like activation of ER-SAM activation was not predicted by k , $p > .21$. However, the SPCM pattern for the MNE activation in inferior IPS was significantly predicted by k , $p < .02$. Superior and inferior IPS are thus showing high concordance of activation, having a strong bilateral BOLD responses and magnetic evoked field increasing with the numbers of items held in VSTM. However, they also showed differences of activation for the SPCN-like BOLD response and SPCM activations, mainly a linear increase in contralateral BOLD responses that was present for inferior IPS only.

Discussion

We determined the mnemonic-load related activation pattern and the SPCN-like activation pattern for various physiological markers linked to VSTM. The hemifield manipulation had limited impact on BOLD signal, while this manipulation was particularly useful to isolate the effect of mnemonic load in the ERPs. The evoked magnetic fields showed both a load-related increase and an SPCM effect.

Role of parieto-occipital areas in supporting VSTM

The superior IPS is likely one of the more important cerebral sources of the SPCM identified in the MEG sensor data, given it was the only cluster showing a significant increase of activation (as estimated with ER-SAM) with load, for contralateral stimuli. Superior IPS also showed an increase in BOLD signal for increasing memory load, consistent with previous study^{1, 15, 17, 25-27}. However, unlike what was expected, no SPCN-like activation pattern was found for the BOLD signal in IPS. That is, the increase in BOLD signal in the IPS was about the same in left and right IPS regardless of the side of visual space from which stimuli were encoded. This pattern of response is quite unlike what is found in the EEG and MEG results. It could be argued that we did not have the statistical power necessary to isolate such lateralized activity (although we did find significant lateralized activity, but this activity was linearly increasing with the numbers of items rather than limited by a plateau corresponding with VSTM capacity). However, the magnitude of the load-related manipulation was ten times higher than the magnitude of the (nonsignificant) SPCN-like BOLD activation, so even if the SPCN-like responses turned out to be statistically significant, the most predominant effect would still be a bilateral increase in activation. It is possible that the presence of ipsilateral stimuli reduced the lateralization of activity within IPS/IOS. Indeed, one may consider that ignored stimuli would also elicit a response, albeit smaller than for encoded stimuli. Using the same stimuli as for their VSTM experiment, two papers (Todd & Marois¹ and Mitchell & Cusack²⁸) investigated the BOLD activation in IPS using an iconic-memory task. Unfortunately, their results are not consistent: IPS showed a modulation of BOLD activation following k (as calculated for the VSTM task) in an iconic-memory task for Cusack and Mitchell, but not for Todd and Marois. Consequently, we cannot rule-out the possibility that the BOLD response

in the ipsilateral IPS reflects the non-mnemonic activation found by Cusak and Mitchell instead of a bilateral encoding of the stimuli. If the absence of SPCN-like response is indeed caused by iconic activation of the ignored stimuli, this would, however, indicate that the BOLD response is sensitive to this iconic activation while the evoked magnetic field is not.

The disagreement of the results for the superior IPS across MEG evoked-fields and the BOLD signal is surprising given the strong agreement previously found between these two measures (Dales et al., 2000; Logothetis 2001; see Arthur et al., 2000, 2003, for similar finding for ERPs and fMRI). However, these studies used mainly the response of primary sensory areas, with transient and short-duration evoked-fields (usually less than 100 ms) response to sensory stimuli, while here the evoked magnetic fields are of longer duration (1000 ms) and are related to higher cognitive functions. However, it was also shown that different modulations of the magnetic fields (DC shift, evoked-potential, and oscillatory activity for the alpha and gamma-band) show spatio-temporal covariance with the BOLD responses²⁹. In the current paradigm, we previously showed a bilateral decrease of alpha-band oscillatory activity originating from parietal cortex in a very similar task¹⁹, and it is known that the displacement of spatial attention, as occurring here following the presentation of the arrowheads, does modulate parietal alpha-band oscillatory activity³⁰⁻³². It then appears that the SPCM observed here reflects the activity of a subpopulation of the neurons in superior IPS, but that the BOLD responses recorded from this region integrate the activity of more neurons, who do not all exhibit the same modulation of activation.

Inferior IPS showed a clear pattern here, the BOLD and ER-SAM overall load activations followed k, but not their SPCN-like activations. In a retention interval of 8,300 ms, inferior IPS did not show a BOLD activation following the k-pattern, but rather a linear increase with the numbers of items (Experiment 3 of Xu & Chun, 2006)²⁶. It was also found that sequentially presented stimuli at the center of the screen led to an equivalent BOLD response for loads 1 to 4, while sequentially presented stimuli at different eccentric locations led to an increase in activation with higher number of stimuli and therefore of spatial location, (Experiment 4 of Xu & Chun, 2006)²⁶. Although these results suggested a dissociation between superior and inferior IPS based on the spatial content of the encoded information, the simple spatial manipulation used here (restricting encoding to one

hemisphere) did not create differential memory-related activations between superior and inferior IPS. In addition, the IOS activations followed closely inferior IPS: increased mnemonic load led to an increase of the BOLD response, and of ER-SAM activations. Furthermore, a bilateral response to unilaterally-encoded stimuli was found for all of IPS/IOS cortex. Thus, our experimental manipulations did not allow us to find differences in BOLD activation patterns across the examined subportions of the IPS/IOS.

The ventral occipital cortex activation isolated here was described earlier¹, but a specific role of this region for VSTM was discarded because this area, unlike the IPS/IOS cortex, showed an equivalent increase of activation with the behavioral k for an iconic memory task as for the VSTM task, and did not show a sustained activity with a longer 9200 ms retention interval. Furthermore, a linear increase of BOLD activation in VO following the increase of items presented to the subject (up to 8 items, well above VSTM capacity) was also found for an iconic memory task²⁸. Although we did not perform such manipulations ourselves, their interpretation should apply to our situation, so we do not consider VO as playing a critical role in VSTM here. The middle occipital gyrus also showed a load-related activation pattern in our data, but only after being identified on the side SPM maps. ROI analyses are much more powerful than general SPMs — not being corrected for multiple comparisons — which could explain why it has not been identified previously. No SPCN-like activation was found for these maxima, however.

A linear increase of contralateral BOLD activation was found for occipital areas, as for the inferior IPS. Because this effect did not follow the behavioral memory pattern with a plateau following k , this likely does not reflect a process specific to VSTM. However, the presence of ipsilateral distractors (i.e., not-encoded stimuli) also indicates that this effect is not related to the simple increase in the numbers of stimuli, but rather indicates an effect of attention. An interesting implication of this result is that sufficient statistical power was present to capture a systematic modulation of the SPCN-like BOLD activation, thus providing support to our conclusion drawn on the absence of a SPCN-like activation tightly following the number of items encoded in VSTM.

Spatial attention vs spatial location

Using fMRI, Sereno and colleagues identified a retinotopic map of spatial position encoded in short-term memory for IPS³³, a result that was further expanded to several maps along the IPS sulcus³⁴. Like usual retinotopic maps, this one represents contralateral space, creating a significantly higher activation for contralateral than ipsilateral positions. Because our visual objects were created by the conjunction of a spatial location and a color, we were expecting to trigger a similar contralateral hemisphere bias in parietal activation to the one identified in Sereno and colleagues' work. Furthermore, the retinotopic organization found by Sereno and colleagues implies that different spatial positions are encoded by different groups of neurons, which should lead to a high summed activation when multiple locations are encoded. However, encoding several objects, each defined by the conjunction of a spatial location and a color, did not create asymmetries proportional to the numbers of items encoded (i.e., we did not find SPCN-like pattern in the BOLD response from IPS), but only a bilateral increase in BOLD activation. Some differences are evident across Sereno et al.'s design and ours. In their work, the target for which position was encoded was presented alone, thus possibly creating an initial stimulus-driven laterality. This would hardly be creating their effect because this retinotopic map was not identified with bright visual stimuli that did not require encoding in spatial short-term memory³⁵. However, the presentation of the target alone could also create an exogenous shift of spatial attention,^{36,37} which was not the case in the current study. The linear increase of contralateral BOLD activation that we found for inferior IPS (figure 7, blue curve of left panel) suggest an effect of attention proportional to the number of items presented, which could create the results found by Sereno and colleagues. Because they used a fixed mnemonic load (1 item), they could not distinguish between attention-related and memory-related activity using the plateau effect as we did here.

Another critical difference between their study and ours is the presence of a visual object to-be-encoded at each of the spatial locations to-be-encoded. Consequently, it is possible that the creation of an object-file by the binding of different features (spatial position and color were the only feature relevant to the task, but the stimuli also had a disk shape), which we know has strong impact on VSTM performance³⁸, would also modify the neural pathway supporting the maintenance of spatial position.

Inferior occipital cortex – unexpected activation

An SPCN-like pattern of activation was found in the BOLD response for the inferior occipital (IO) cortex isolated in the side fMRI activation map (figure 4E). The actual pattern of activation, however, was a modulation by load for the contralateral stimuli only in the left IO; the right IO had a load-related activation pattern for both encoding sides. The stimulation was equivalent for the left and right trials so this difference in activation can only be attributed to either spatial attention or to visual short-term memory. Previous reports using a control task^{1, 28} or a long retention period^{1, 26} did not investigate the specific involvement of IO in VSTM. Given that we were predicting, based on previous results, either a bilateral increase of activation or a contralateral increase of activation within each hemisphere for analogous cerebral regions, we do not have an empirically-supported interpretation for this activation. Further studies will be required to determine the functional role of IO in the task.

Strengths and limitations

A good concordance of source activation was visible across the different evoked-field localization methods, with two main exceptions. First, the SPCN-like activation of the MNE for inferior IPS did follow k , which was not the case for the MEM or the ER-SAM. However, superior IPS did follow the SPCN-like pattern in ER-SAM, so this discrepancy is likely a difference in the precision of localization across methods. However, the right infero-frontal gyrus and the right claustrum decrease was only visible in ER-SAM, while other methods showed a non-significant increase of activation with the increase of mnemonic load at this location. For this reason, we do not wish to postulate a role for these regions in VSTM, although we consider worthwhile to report this result. Accordingly, despite the numerous advances in source localization of MEG signals, the use of multiple methods is still advised, along with careful interpretation of the results.

Conclusion

We studied several physiological markers of VSTM during maintenance of laterally-encoded stimuli. The BOLD activation in parietal cortex showed a bilateral increase in activation, independent of the location of the stimuli. The magnetic fields also showed a

bilateral increase in activation, together with a contralateral increase in activation for IPS. Finally, we found an asymmetric load effect in IO cortex, which, to our knowledge, was not expected based on current literature, and is worthy of future study.

Methods

Subject

13 subjects were recorded in this experiment. One subject was excluded for a failure to keep fixation during the task. The twelve remaining subjects (7 females) were between 19 and 31 years old (average 23.3), reported having no neurological problem and were able to discriminate easily the colors used in the memory task. For the first six subjects we counterbalance the order of MEG and fMRI sequences, as it is often done whenever two experimental sessions are required. However, the three subjects who perform the fMRI first showed strong artifact in their MEG signal. To avoid further contamination of the MEG signal (of magnitude around $3e-14$ Tesla) following the ~75 minutes exposure to the 3 Tesla magnetic field of the MRI, the remaining subjects did the MEG experiment first. The ICA artifact removal procedure (see below) successfully cleaned the signals of the three subjects tested first with fMRI, so they could be included in the experiment.

MEG procedure

Stimuli were presented on a back-projected translucent screen, located 75 cm in front of the subject. The area containing all the possible stimuli subtended 14° (width) by 7° (height) of visual angle centered within the display. Each trial started with the presentation for 200ms of two arrowheads directly above and below the fixation point (see figure 1), with the arrowheads pointing to the left or the right of the screen. The fixation cross was then presented alone for 600 to 700 ms (varied randomly across trials). The random values were added so activity related to the arrows would not systematically overlap activity related to the memory array. On each side of the screen, 1, 2, 4, or 6 colored disks were presented for 200 ms (always an equal number on each side), at randomly selected positions within a 3 X 4 imaginary grid. Colors were selected among 8 highly discriminable colors (black, dark

blue, green, light blue, pink, red, white, yellow). Color was never repeated on one side of the screen, but selection was independent for each side. The retention period was 1000 to 1100 ms (randomly selected from a rectangular distribution), followed by the test display. The test display consisted of a colored disk (one on each side of the screen), located at the position of one disk presented for encoding. This display was presented for 1500 ms. On 50% of the trials, the test disk had the same color as the one previously presented at this location; otherwise it was of one of the 7 remaining colors. Subjects had 1500 ms to produce their answer by pressing one of two keys on an optically coupled response pad (right index for “same,” right middle finger for “different”). A colored disk was always presented simultaneously on the other side of the screen, with color and position varied in the same way as for the test disk, but independently. Feedback was provided after each trial by changing the fixation cross to a + or – sign, for a correct or an incorrect answer, respectively. The feedback was presented for 600 to 900 ms, chosen on the basis of the previous random interval to create an average interval of 4400 ms (range: 4350 to 4450, selected from a rectangular distribution) between the onset of each trial. Trials were presented in 20 blocks of 40 trials. Subjects initiated the block manually, allowing for rest period as needed. Trial order was counterbalanced as in the fMRI recording.

The amount of information maintained in VSTM was assessed using Cowan's k formula¹² based on the behavioural results: (proportion of hits - proportion of false alarms) * the number of items presented. This formula is useful because it corrects for possible biases in the propensity to respond 'same' or 'different' (see also¹³ Pashler, 1988).

MEG and EEG recording

A CTF-VSM whole-head 275-sensor MEG system in a magnetically shielded room was used for the recordings. Data were filtered with a 150 Hz low-pass filter and digitalized at 600 Hz during the recording. Bad MEG channels (3 or 4, depending on the subject) were excluded from the recording. EEG (PO7, PO8, right mastoid) was also recorded with reference to the left mastoid, and later algebraically re-referenced to the average of the mastoids. Bipolar EOG (electrodes placed at the left and right canthi for horizontal EOG and above and below the left eye for vertical EOG) was recorded in order to monitor eye

blinks and eye movements. Bipolar ECG was also recorded. Trials with a correct or an incorrect response were included in the brain signal analyses.

The ERP and MEG analyses were done using CTF software, EEGLAB⁴⁷, Fieldtrip, Brainvisa, Brainstorm, AFNI, and custom programs.

EEG analysis

The data were screened in order to remove trials containing eye blinks or eye movements, or artifacts in the electric signals. Trials were baseline-corrected based on the mean activity during the pre-encoding period (-200 to 0 ms, time relative to the onset of the memory array) and averaged. Amplitude of the SPCN was measured as the average of the activation during the retention period (400 to 1200 ms). The SPCN was calculated as usual (amplitude for the contralateral sensor (PO7 for encode-right trials and PO8 for encode-left) minus the ipsilateral), for each load. A multiple regression was then performed for these values. The regression matrix contain a single predictor of interest (the behavioral k , centered), and dummy coding to remove the overall mean for each subject. The effect of load was also calculated by averaging the amplitude for both electrodes and stimulus location, for each load, and was submitted to the same type of regression.

MEG analysis

Trials with eye movements were removed because they could have been systematically correlated with the task (i.e., left movement for encode-left trials and right movement for encode-right trials). For each subject, we then performed an independent components analysis (ICA) of the entire data set. Components isolating activity from eye blinks, cardiac, or respiratory activity, were selected based on their topographies, their time-course, and their frequency signatures. Data were then back-transformed in signal-space (without these components), baseline-corrected (-200 to 0 ms) and averaged by conditions, producing event-related fields (ERFs). Statistical analyses were performed on the retention period on a sensor-by-sensor basis using the multiple linear regression analysis described earlier.

Beamformer analyses (ER-SAM) were performed using the raw data (prior to ICA), again with trials where subjects failed to keep fixation removed. This was deemed appropriate as beamformers can effectively reduce spatially stable noise, and data in which the artifacts were removed by ICA cannot be effectively used in the beamformer calculations due to reducing the rank of the data matrix. For each subject, a single weight matrix was calculated on the raw data of the entire experiment. Activation images were then produced for each conditions, averaged over the entire retention period. Use of a single weight matrix prevented any differences across conditions being attributed to differences in the weights with changing noise conditions. For ER-SAM, we used broadband activity (DC to 150 Hz) and the weights matrix was calculated from the onset of the memory array stimuli to the end of the retention period (0 to 1400 ms), after baseline correction (-200 to 0 ms). Images were calculated (spatial sampling resolution of 3 mm) at every time-point of the retention period before being averaged.

Sources of the evoked magnetic fields were also estimated using cortically constrained weighted minimum norm (MNE; Brainstorm, and MEEG software tools from LENA-CNRS-UPR640, Cognitive Neuroscience and Cerebral imaging Laboratory) and Maximum of Entropy on the Mean (MEM^{22, 48}). The cortical surface was extracted from the anatomical MRI scan using BrainVisa software. Approximately 8000 sources, oriented perpendicularly relative to the cortical surface, were distributed over the cortical surface, and these local sources were used in distributed source localization analyses. Event-related field for each condition, after being cleaned with ICA, were used as input for these analyses. MNE surfaces were computed with a Tikhonov parameter value of 10. MEM surfaces used activity during the baseline (-200 to 0) for a Multivariate source pre-localization (MSP). Images were computed for every time point in the retention period (400 to 1,200 ms) before being averaged. Resulting images were interpolated back in the anatomical MRI space (voxels size: 4 mm³) of each subject, transformed in Talairach space using AFNI⁴⁹ and spatially smoothed (FWHM 12 mm). For ROI analysis, activation within a 7-mm radius sphere centered on the coordinate of interest was averaged in each map.

fMRI procedure

The procedure was identical as for the MEG recordings except for two manipulations added to account for the overlap of the BOLD response across trials. First, random blank intervals were added between trials (52% without interval, 26% with one volume, 13% with two, 6% with three, 3% with four), which allowed deconvolution analysis. Second, two blank conditions were added (arrow pointing to the left or right, but without stimuli or test afterward), for which time-course will also be extracted and subtracted from the time-course of experimental conditions. Each run consisted of 102 trials to allow counterbalancing of the order of the 10 trial types (2 sides X 4 loads, + 2 blanks), with a supplemental trial at the beginning and the end to ensure that all analyzed trials are preceded and followed by a trial of each possible type. Stimuli were back-projected on a translucent screen, visible via a mirror fixed onto the antenna. T2-weighted EPI images were acquired in AC-PC orientation, TR = 2200 ms, TE = 30 ms, FOV 24 cm, Flip Angle 70°, 28 axial slices of 64 X 64 voxels, 5 mm thick without slice gap, interleaved. Each subject performed 4 functional runs, followed by a high-resolution 3D anatomical scan. Data acquisition was performed with a 3T Trio Siemens scanner at l'Unité de Neuroimagerie Fonctionnelle de l'Institut de Gériatrie de l'Université de Montréal. The first 8 subjects were tested with an 8-channel antenna on the Trio platform, the 4 last with a 12-channel antenna, on the Trio TIM platform after scanner upgrades.

fMRI analysis

Analyses were performed using AFNI⁴⁹ and in-house Matlab routines. Preprocessing consisted of slice-timing alignment, motion-correction, 8 mm FWHM spatial smoothing and within-run normalization. For each subject and condition, an SPM map was created using multiple regression analysis, with regressors defined for each trial type and convolved with a canonical hemodynamic function (1 parameter gamma function). Influence of within-run trends (linear and higher-order) was removed by including regressors following Legendre polynomial trends (degree 5). This created 96 maps (12 subjects X 8 conditions), which were transformed into Talairach space before being submitted to a multiple regression analysis with regressors defined for k (balanced), for the Side factor, and for the interaction of k by Side, with a random-effect model. A false discovery rate (FDR) threshold of $q < .001$ was used to control for multiple comparisons in

the Load maps, and of $q < .05$ for the Side map. We used a more liberal statistical threshold for the Side map because this is the first investigation of the effect of this manipulation in fMRI. Maxima were defined manually as the voxels with the highest activations in the corrected statistical maps. The time course of the activation was extracted for a sphere (radius = 5 mm) centered on the maxima, using deconvolution. The activation time course for the trials without stimuli to encode was subtracted from the time course for experimental trials.

REFERENCES

1. Todd, J.J. & Marois, R. Capacity limit of visual short-term memory in human posterior parietal cortex. *Nature* 428, 751-754 (2004).
2. Klaver, P., Talsma, D., Wijers, A.A., Heinze, H.-J. & Mulder, G. An event-related brain potential correlate of visual short-term memory. *Neuroreport: For Rapid Communication of Neuroscience Research* 10, 2001-2005 (1999).
3. Brisson, B., Leblanc, E. & Jolicoeur, P. Contingent capture of visual-spatial attention depends on capacity-limited central mechanisms: Evidence from human electrophysiology and the psychological refractory period. *Biol Psychol* (2008).
4. Robitaille, N., Jolicoeur, P., Dell'Acqua, R. & Sessa, P. Short-term consolidation of visual patterns interferes with visuo-spatial attention: converging evidence from human electrophysiology. *Brain Res* 1185, 158-169 (2007).
5. Robitaille, N. & Jolicoeur, P. Fundamental properties of the N2pc as an index of spatial attention: effects of masking. *Canadian journal of experimental psychology = Revue canadienne de psychologie experimentale* 60, 101-111 (2006).
6. Jolicoeur, P., Brisson, B. & Robitaille, N. Dissociation of the N2pc and sustained posterior contralateral

- negativity in a choice response task. *Brain Res* 1215, 160-172 (2008).
7. Brisson, B. & Jolicoeur, P. A psychological refractory period in access to visual short-term memory and the deployment of visual-spatial attention: multitasking processing deficits revealed by event-related potentials. *Psychophysiology* 44, 323-333 (2007).
 8. McCollough, A.W., Machizawa, M.G. & Vogel, E.K. Electrophysiological measures of maintaining representations in visual working memory. *Cortex; a journal devoted to the study of the nervous system and behavior* 43, 77-94 (2007).
 9. Perron, R., et al. Attentional and anatomical considerations for the representation of simple stimuli in visual short-term memory: Evidence from human electrophysiology. *Psychological Research* (in press).
 10. Brisson, B. & Jolicoeur, P. Express Attentional Re-Engagement but Delayed Entry into Consciousness Following Invalid Spatial Cues in Visual Search. *PLoS ONE* 3, e3967 (2008).
 11. Hopf, J.M., et al. Neural sources of focused attention in visual search. *Cerebral Cortex* 10, 1233-1241 (2000).
 12. Cowan, N. The magical number 4 in short-term memory: A reconsideration of mental storage capacity. [References]. *Behavioral & Brain Sciences* 24, 87-185 (2001).
 13. Pashler, H. Familiarity and visual change detection. *Perception & Psychophysics* 44, 369-378 (1988).

14. Vogel & Machizawa. Neural activity predicts individual differences in visual working memory capacity. *Nature* 428, 748-751 (2004).
15. Todd, J.J. & Marois, R. Posterior parietal cortex activity predicts individual differences in visual short-term memory capacity. *Cogn Affect Behav Neurosci* 5, 144-155 (2005).
16. Gratton, G. The contralateral organization of visual memory: a theoretical concept and a research tool. *Psychophysiology* 35, 638-647 (1998).
17. Song, J.-H. & Jiang, Y. Visual working memory for simple and complex features: An fMRI study. *NeuroImage* 30, 963-972 (2006).
18. Robitaille, N., Grimault, S. & Jolicoeur, P. Bilateral parietal and contralateral responses during maintenance of unilaterally-encoded objects in visual short-term memory: Evidence from magnetoencephalography. *Psychophysiology* (2008).
19. Grimault, S., et al. Oscillatory activity in parietal and dorsolateral prefrontal cortex during retention in visual short-term memory: Additive effect of spatial attention and memory load. *Human brain mapping* (2008).
20. Forman, S.D., et al. Improved assessment of significant activation in functional magnetic resonance imaging (fMRI): use of a cluster-size threshold. *Magn Reson Med* 33, 636-647 (1995).
21. Douglas Cheyne, L.B.W.G. Spatiotemporal mapping of cortical activity accompanying voluntary movements using

- an event-related beamforming approach. Human brain mapping 27, 213-229 (2006).
22. Grova, C., et al. Evaluation of EEG localization methods using realistic simulations of interictal spikes. NeuroImage 29, 734-753 (2006).
 23. Hamalainen, M.S. & Ilmoniemi, R.J. Interpreting magnetic fields of the brain: minimum norm estimates. Medical & biological engineering & computing 32, 35-42 (1994).
 24. Anderson, M.J. & Legendre, P. An empirical comparison of permutation methods for tests of partial regression coefficients in a linear model. Journal of Statistical and Computer Simulation 62, 271-303 (1999).
 25. Xu, Y. The Role of the Superior Intraparietal Sulcus in Supporting Visual Short-Term Memory for Multifeature Objects. J. Neurosci. 27, 11676-11686 (2007).
 26. Xu, Y. & Chun, M.M. Dissociable neural mechanisms supporting visual short-term memory for objects. Nature 440, 91-95 (2006).
 27. Kawasaki, M., Watanabe, M., Okuda, J., Sakagami, M. & Aihara, K. Human posterior parietal cortex maintains color, shape and motion in visual short-term memory. Brain Res 1213, 91-97 (2008).
 28. Mitchell, D. & Cusack, R. Flexible, Capacity-Limited Activity of Posterior Parietal Cortex in Perceptual as well as Visual Short-Term Memory Tasks. Cereb Cortex doi:10.1093/cercor/bhm205 (2007).
 29. Brookes, M.J., et al. GLM-beamformer method demonstrates stationary field, alpha ERD and gamma ERS co-

- localisation with fMRI BOLD response in visual cortex. *NeuroImage* 26, 302-308 (2005).
30. Thut, G., Nietzel, A., Brandt, S.A. & Pascual-Leone, A. Alpha-band electroencephalographic activity over occipital cortex indexes visuospatial attention bias and predicts visual target detection. *J Neurosci* 26, 9494-9502 (2006).
 31. Wyart, V. & Tallon-Baudry, C. Neural Dissociation between Visual Awareness and Spatial Attention. 2667-2679 (2008).
 32. Medendorp, W.P., et al. Oscillatory activity in human parietal and occipital cortex shows hemispheric lateralization and memory effects in a delayed double-step saccade task. *Cerebral Cortex* 17, 2364-2374 (2007).
 33. Sereno, M.I., Pitzalis, S. & Martinez, A. Mapping of contralateral space in retinotopic coordinates by a parietal cortical area in humans. *Science* 294, 1350-1354 (2001).
 34. Konen, C.S. & Kastner, S. Representation of eye movements and stimulus motion in topographically organized areas of human posterior parietal cortex. *J Neurosci* 28, 8361-8375 (2008).
 35. Sereno, M.I., et al. Borders of multiple visual areas in humans revealed by functional magnetic resonance imaging. *Science* 268, 889-893 (1995).
 36. Posner, M.I. Orienting of attention. *Quarterly Journal of Experimental Psychology A* 32, 3-25 (1980).

37. Posner, M. & Cohen, Y. Components of visual orienting. (1984).
38. Vogel, E.K., Woodman, G.F. & Luck, S.J. Storage of features, conjunctions and objects in visual working memory. *Journal of experimental psychology* 27, 92-114 (2001).
39. Clark, V.P., et al. Functional magnetic resonance imaging of human visual cortex during face matching: a comparison with positron emission tomography. *NeuroImage* 4, 1-15 (1996).
40. Ishai, A., Schmidt, C.F. & Boesiger, P. Face perception is mediated by a distributed cortical network. *Brain research bulletin* 67, 87-93 (2005).
41. Kanwisher, N., McDermott, J. & Chun, M.M. The fusiform face area: a module in human extrastriate cortex specialized for face perception. *J Neurosci* 17, 4302-4311 (1997).
42. Grill-Spector, K., Knouf, N. & Kanwisher, N. The fusiform face area subserves face perception, not generic within-category identification. *Nat Neurosci* 7, 555-562 (2004).
43. Mangun, G.R., Buonocore, M.H., Girelli, M. & Jha, A.P. ERP and fMRI measures of visual spatial selective attention. *Human brain mapping* 6, 383-389 (1998).
44. Kawashima, R., O'Sullivan, B.T. & Roland, P.E. Positron-emission tomography studies of cross-modality inhibition in selective attentional tasks: closing the "mind's eye". *Proc Natl Acad Sci U S A* 92, 5969-5972 (1995).

45. Heilman, K.M., Watson, R.T. & Valenstein, E. Neglect and related disorders. in *Clinical Neuropsychology* 243-293 (Oxford University Press, New York, 1985).
46. Sakurai, Y., et al. Pure alexia for kana. Characterization of alexia with lesions of the inferior occipital cortex. *Journal of the neurological sciences* 268, 48-59 (2008).
47. Delorme, A. & Makeig, S. EEGLAB: an open source toolbox for analysis of single-trial EEG dynamics including independent component analysis. *Journal of neuroscience methods* 134, 9-21 (2004).
48. Amblard, C., Lapalme, E. & Lina, J.M. Biomagnetic source detection by maximum entropy and graphical models. *IEEE transactions on bio-medical engineering* 51, 427-442 (2004).
49. Cox, R.W. AFNI: software for analysis and visualization of functional magnetic resonance neuroimages. *Computers and biomedical research, an international journal* 29, 162-173 (1996).

Figure legends

Figure 1

Sequence of events in each trial. Stars refer to random intervals of 0–100 ms, which were compensated as needed after the response production to have a total duration of 4,400 ms. A load 4, encode-left trial, requiring the answer "same" is illustrated, which received a positive feedback.

Figure 2

A) The number of items maintained in VSTM (k) increased from load 1 up to load 4 and then decreased slightly at load 6. The amplitude of the SPCN waveform (C) during the retention period, 400–1200 ms, followed k (green dashed line in B), but not the waveforms averaged for each load not taking side into account, shown in D (blue dashed line in B). SEM illustrated with vertical bars in A and B.

Figure 3

The two posterior clusters of MEG sensors significantly modulated by k (A) showed robust activation throughout the retention period (B-C, E-F). The averages waveform for these sensor (with polarity adjusted) show an activation pattern during the retention period that was predicted by k (blue solid line in D), but they did not have a systematic modulation by side, which led to a flat amplitude across load for the SPCM (green dash line in D). The posterior cluster of MEG sensors significantly modulated by the side (G) was divided in a left (H-I) and a right (K-L) cluster. The averages waveform for these sensors (with polarity adjusted) show an activation during the retention period that was predicted by k (blue solid line in J), as did the SPCM calculated from these sensors (dashed green line in J).

Figure 4

Bilateral maxima found in the k -regression map in fMRI (first column) were the superior IPS (A), the IOS (B), and VO (C). The side map revealed the middle occipital cortex (D)

and the inferior occipital (IO) cortex (E). The average amplitude of every maxima pair was predicted by k , either for the fMRI BOLD (blue curve) or the ER-SAM source analysis of the MEG signal (green curve). However, the SPCN-like activations calculated from these maxima were only significantly predicted by k for the ER-SAM in superior IPS (row A) or the fMRI BOLD in IO cortex (row E).

Figure 5

Time course of the BOLD activation in IO. Left IO showed a modulation of activation across load for contralateral trials (upper-left panel) but not for ipsilateral trials (upper-right panel). Right IO, however, showed a modulation for both ipsilateral and contralateral trials (lower panels).

Figure 6

Regression on k (top row) and on the stimulus presentation side (bottom row) for the event-related beamformer source reconstruction, displayed on a template brain surface. The load activation was concentrated in the IPS/IOS area. Side-related activations (red for higher activation for encode-left trials and blue for higher activation for encode-right trials) were less extensive but visible for both left and right IPS (indicated with arrows) and in the left occipital cortex.

Figure 7

Activations for the inferior IPS, as identified based on Xu and Chun's (2006) coordinates. A significant effect of load was found for the fMRI BOLD activation and the ER-SAM. The SPCN-like activation was not significant.

Table 1. Talairach coordinate of regions investigated

	RH	LH
Superior IPS	16, -67, 49	-14, -69, 46
Inferior IPS (Xu and Chun, 2006)	26, -65, 34	-25, -70, 29
IOS	35, -85, 14	-31, -81, 15
Middle occipital	24, -86, 16	-21, -86, 18
IO (inferior occipital)	39, -72, -7	-40, -72, -7
VO	34, -69, -16	-26, -75, -15

Figure 1

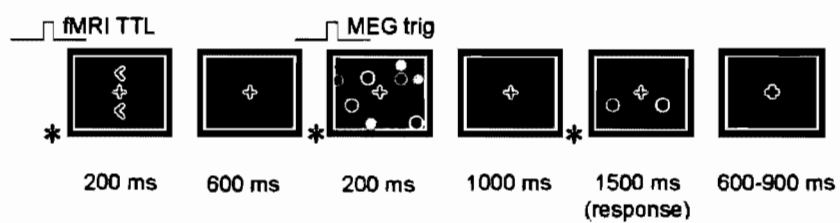


Figure 2

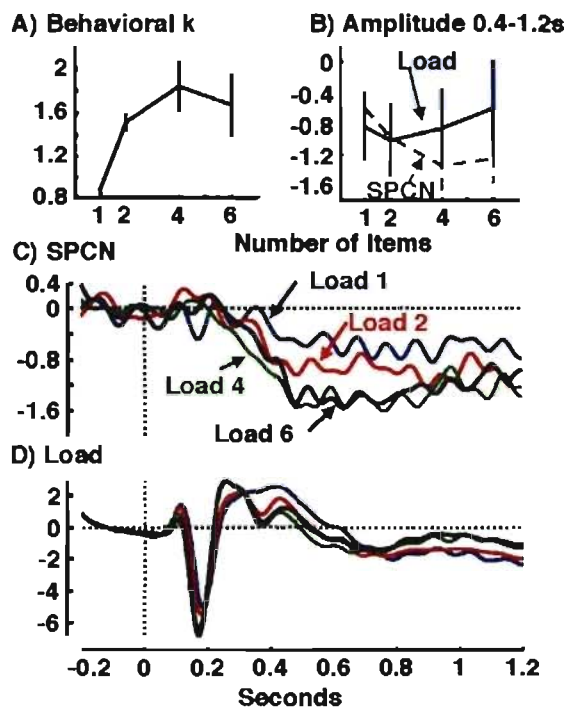


Figure 3

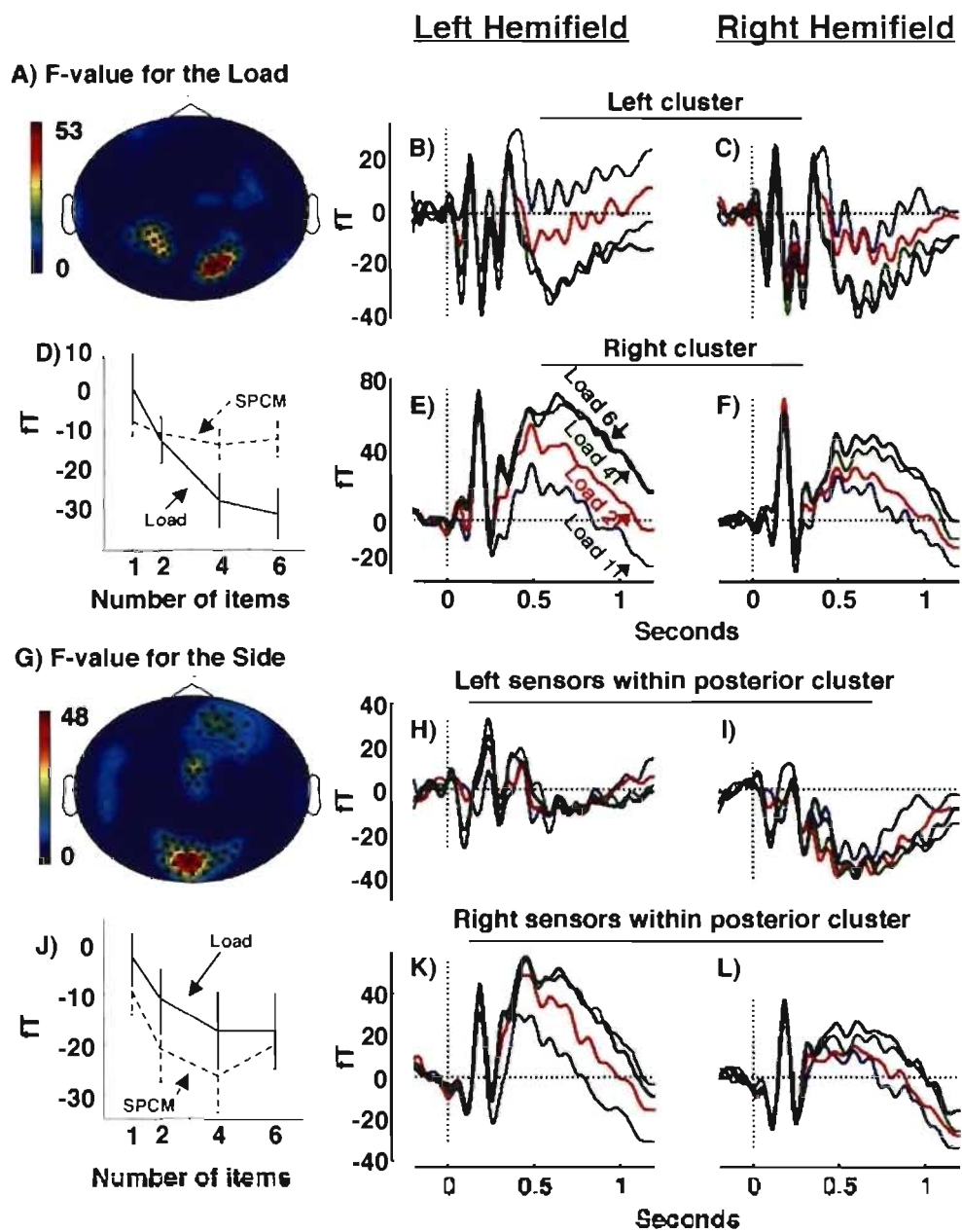
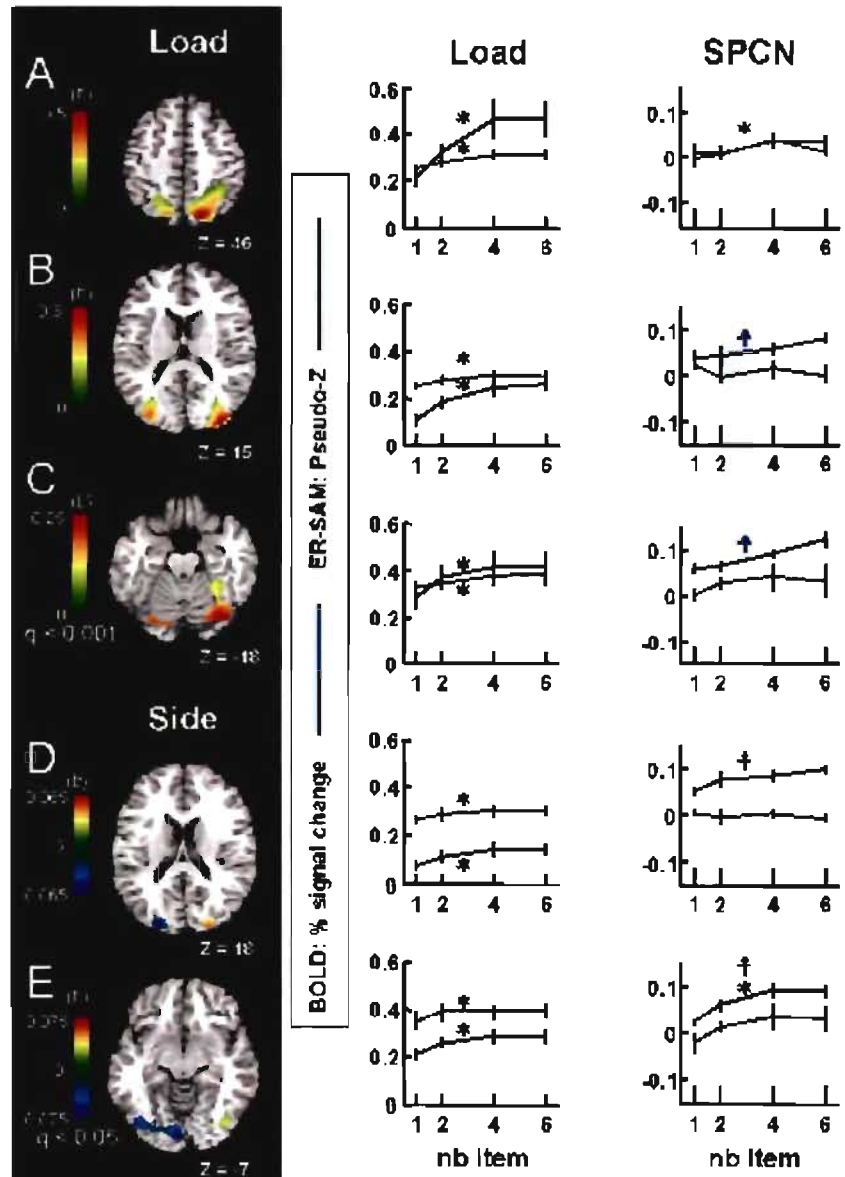


Fig. 64



* Significantly predicted by behavioral k (Figure 2A)
 † Significantly predicted by the number of items

Figure 5

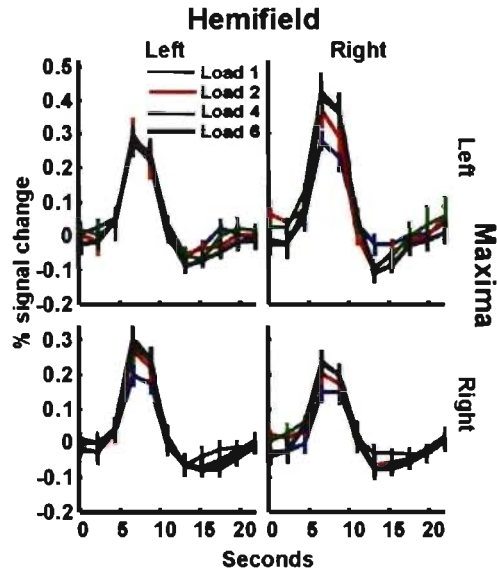


Figure 6

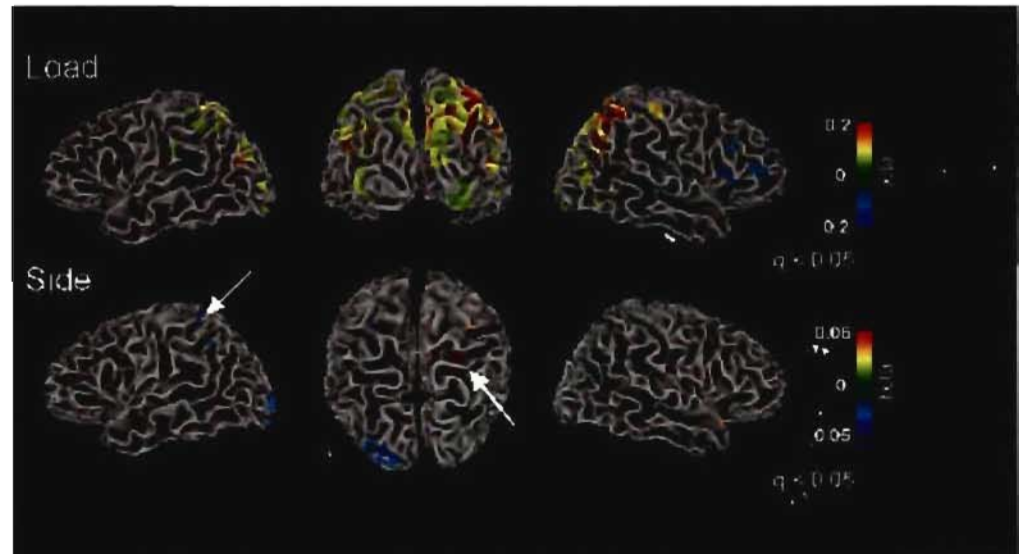
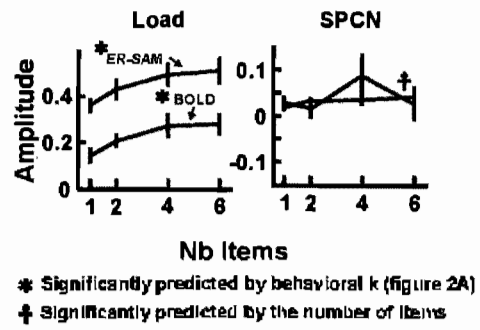


Figure 7



Conclusions

Article 1

Dans le premier article, nous avons présenté aux participants des disques de couleur à encoder pour environ une seconde. Il y avait 2 ou 4 stimuli à encoder, qui étaient présentés soit à gauche soit à droite du point de fixation. Cela nous a permis d'identifier une composante des potentiels évoqués magnétiques, la SPCM, qui est l'équivalent de la SPCN. Bien qu'attendu, ce résultat n'était pas à prendre pour acquis étant donné les différences d'orientation du signal MEG et EEG. De plus, nous n'avons en rien prouvé ici qu'une seule source neurale était responsable des SPCN et SPCM. L'analyse de la distribution de l'activation sur les capteurs et l'analyse des sources indiquent un générateur pariétal de la SPCM.

Le nombre d'items encodés en mémoire a également créé une activation bilatérale. En effet, les capteurs MLO24 et MRO24 montrent une augmentation de l'amplitude de leur activation avec l'augmentation de la charge, mais de façon additive avec l'effet de position. Cet effet indique donc une augmentation de l'activité ipsilatérale lors de l'augmentation de la charge mnésique, augmentation qui par ailleurs est d'amplitude équivalente à la SPCM.

Les résultats de l'article 1 indiquent qu'un patron d'activation neuronale complexe est à l'œuvre. En effet, l'explication la plus simple aurait été que dans chaque hémisphère, un seul générateur cérébral soit influencé par l'augmentation de la charge mnésique. Ces générateurs auraient une augmentation de leur activation plus grande lorsque des stimuli provenant de l'hémisphère qui leur est controlatéral sont maintenus en mémoire. Par contre, le fait d'observer à la fois des capteurs qui montrent un effet additif de la charge avec la position des stimuli et d'autres capteurs qui montrent une interaction entre ces deux facteurs ne peut pas s'expliquer par une paire de générateurs montrant une activité symétrique l'un vis-à-vis de l'autre.

Une fois que le modèle simple constitué d'une paire de générateurs neuronaux est réfuté, il devient plus difficile de déterminer le patron de générateurs impliqués. En effet, il existe une infinité de combinaisons possibles de générateurs qui vont parfaitement reproduire le même patron d'activation sur les capteurs (Helmholtz, 1853). De plus, il n'est pas possible de déterminer si le patron obtenu entre les conditions est le résultat d'une modulation de l'activation de générateurs ou de l'addition de nouveaux générateurs (Urbach & Kutas, 2002). Donc, la conclusion du premier article est la présence de deux effets, un effet additif entre le côté de présentation et la charge mnésique sur un groupe de capteurs, et une interaction entre le côté de présentation et la charge mnésique sur un autre groupe de capteurs.

Article 2

Puisque l'activation MEG uniquement n'a pas réussi à identifier clairement les générateurs neuronaux responsables du maintien de l'information en MCTV, nous avons décidé de reproduire cette expérience en y ajoutant plusieurs éléments. D'abord, afin de pouvoir utiliser la régression sur k (le nombre d'items encodés en mémoire), nous sommes passés de deux niveaux de charge (2 et 4) à quatre niveaux (1, 2, 4 et 6). Un effet de plateau est attendu dans ce cas, soit une augmentation de l'activité cérébrale lorsque la charge passe de 1 item à 2 et de 2 items à 4, mais avec une activation pour 6 items qui est la même que pour 4. Cette manipulation a l'avantage de permettre de dissocier l'activité reliée directement au traitement visuel des items présentés (qui augmenterait de façon linéaire avec le nombre d'items présentés) de l'activité reliée à l'encodage en mémoire. De plus, chaque participant a fait deux enregistrements, un en MEG (avec EEG simultané) et un en IRMf, avec des protocoles pratiquement identiques.

Les avantages d'enregistrer les mêmes participants dans les deux protocoles (MEG et fMRI) sont nombreux. Premièrement, les groupes de participants seront toujours équivalents, éliminant la possibilité d'avoir des différences liées à la constitution des groupes. De plus, l'analyse de sources en MEG bénéficie de l'utilisation de l'image anatomique haute résolution habituellement acquise lors d'une expérience en IRM. En effet, l'image anatomique haute résolution permet de visualiser les solutions de localisation des sources MEG projetées sur le cerveau de ce participant, permettant l'identification des structures cérébrales. De plus, il est possible de créer des moyennes de groupes dans des espaces communs (comme l'espace Talairach, par exemple) en transformant d'abord les images anatomiques dans l'espace commun, et ensuite en appliquant, pour chaque sujet, la même transformation à la solution de localisation de sources MEG. L'information anatomique permet enfin de restreindre les solutions de localisations de source à l'interface entre la matière grise et la matière blanche, matières qui peuvent être extraites de ces images. Également, puisque l'analyse du signal IRMf devrait permettre d'identifier des régions d'intérêt, il sera possible de regarder l'activation magnétoencéphalographique pour ces régions spécifiquement.

Nous avons trouvé deux groupes de capteurs en magnétoencéphalographie, un au-dessus du cortex pariétal gauche et un au-dessus du cortex pariétal droit, dont les amplitudes augmentent en fonction de la charge mnésique, jusqu'à l'atteinte d'un plateau avec quatre items. Comme pour la première étude, l'activité de ce groupe de capteurs était affectée par la position des stimuli, ayant une plus grande activité lorsque les stimuli étaient présentés dans l'hémichamp controlatéral. Également en accord avec la première étude, ces deux effets étaient additifs, donc la latéralisation de l'activation n'était pas influencée par la charge mnésique. Un autre ensemble de capteurs en MEG ont permis d'identifier une deuxième fois la SPCM. Tel qu'attendu, cette SPCM était située sur des capteurs plus

postérieurs que ceux précédemment identifiés. De plus, l'activation de cette SPCM a montré une saturation de l'activation entre les charges 4 et 6, confirmant le lien entre la SPCM et le maintien de l'information en mémoire à court terme visuelle.

La localisation des sources de l'activité cérébrale MEG a permis de déterminer qu'une grande portion du cortex pariétal, incluant l'IPS/IOS, montrait une augmentation de son activité lors de l'augmentation de la charge mnésique. De plus, parmi les régions d'intérêt identifiées, le cortex IPS supérieur montrait une SPCM, indiquant donc que la SPCM serait générée par cette région cérébrale.

L'activation BOLD, par contre, n'a pas montré un tel patron d'activation. En effet, il n'a pas été possible d'identifier une seule paire de régions cérébrales (donc une région dans l'hémisphère gauche et son homologue dans l'hémisphère droit) montrant une activation de type SPCN : une réponse cérébrale de plus grande amplitude pour le maintien de l'information visuelle provenant de l'hémichamp controlatéral. Par contre, une région cérébrale, le cortex occipital inférieur gauche, a montré une augmentation de l'amplitude de sa réponse lorsque le nombre de stimuli présentés à l'écran augmentait, mais seulement lorsque ces stimuli provenaient de l'hémichamp droit; aucune modulation n'était visible lorsque les stimuli provenaient de l'hémichamp ipsilatéral (i.e., gauche).

Le cortex occipital inférieur est une région cérébrale peu étudiée. En effet, il existe environ vingt fois plus d'articles portant sur une région connexe, le gyrus fusiforme. Puisque des stimuli étaient toujours présents dans l'hémichamp ipsilatéral, l'activation dans le cortex inférieur occipital résulte soit d'un effet attentionnel, soit de l'encodage et du maintien de l'information provenant de l'hémichamp controlatéral. Des études en tomographie par émission de positrons ont montré une modulation de cette région cérébrale par l'attention spatiale (Mangun, Buonocore, Girelli, & Jha, 1998), ainsi qu'une diminution de son

activation lorsque des participants effectuaient une tâche tactile difficile (Kawashima, O'Sullivan, & Roland, 1995). Ces résultats favorisent la piste de l'effet attentionnel sur le cortex occipital inférieur gauche. Par contre, le patron de modulation asymétrique est plus difficile à expliquer. Il est intéressant de noter la ressemblance dans le patron d'activation du cortex occipital inférieur et le phénomène de l'héminégligence, (Heilman, Watson, & Valenstein, 1985). En effet, l'héminégligence est un déficit dans le traitement de l'information provenant de l'hémichamp visuel controlatéral à la suite d'une lésion du cortex pariétal. Par contre, l'héminégligence se manifeste principalement à la suite d'une lésion dans l'hémisphère droit ; une lésion de l'hémisphère gauche cause rarement de l'héminégligence. Dans le cas du cortex occipital inférieur, nous avons observé que celui dans l'hémisphère gauche modulait son activité en fonction de ce qui se passe dans l'hémichamp droit uniquement, tandis que le cortex occipital inférieur droit modulait son activité en fonction des événements se produisant des deux côtés. Donc, si nous reformulons ceci du point de vue des hémichamps visuels, le maintien en mémoire de stimuli provenant de l'hémichamp droit provoque une activation bilatérale dans le cortex occipital inférieur, donc une lésion de l'un ou l'autre des cortex occipitaux inférieurs n'empêchera pas le traitement de l'information provenant de cet hémichamp. Par contre, les stimuli encodés en MCTV provenant de l'hémichamp visuel gauche modifient l'activation dans le cortex occipital inférieur droit uniquement, donc une lésion de l'hémisphère droit entraînerait une absence de traitement de l'information de l'hémichamp visuel gauche. Donc, bien qu'une lésion du cortex occipital inférieur (gauche ou droit) n'entraîne pas le phénomène de l'héminégligence, il semble qu'un biais fondamental en faveur de l'hémichamp droit soit à l'œuvre tant dans nos résultats que pour le phénomène de l'héminégligence.

Discussion générale

Le principal résultat de ces travaux est la découverte de l'activation bilatérale suite à l'encodage de stimuli visuels provenant d'un seul hémichamp. Cette activation bilatérale était visible en magnétoencéphalographie ainsi qu'en imagerie par résonance magnétique fonctionnelle.

Une activation à dominance bilatérale est surprenante. En effet, en électrophysiologie (Klaver et al., 1999 ; Vogel et Machizawa, 2004), il est essentiel de soustraire la réponse ipsilatérale à la réponse controlatérale pour isoler la SPCN. Par contre, en MEG et en IRMf, nous avons observé des effets de charges mnésiques visibles sans la soustraction « ipsilatérale moins controlatérale ». Nous devons donc réfuter un modèle simple où un seul processus neuronal est responsable à la fois de la SPCN, de la SPCM et de l'activation BOLD obtenues pour l'IPS/IOS.

En utilisant une méthodologie totalement différente, Gratton et ses collègues (Fabiani, Ho, Stinard, & Grattona, 2003; Gratton, 1998; Gratton, Corballis, & Jain, 1997; Gratton, Fabiani, Goodman-Wood, & Desoto, 1998; Klaver, Talsma, Wijers, Heinze, & Mulder, 1999; Shin, Fabiani, & Gratton, 2006) ont investigué les traces mnésiques latéralisées suite à l'encodage de stimuli en mémoire visuelle à court terme. Ils ont utilisé une méthode d'analyse de délais de phase du signal en imagerie optique. En effet, le temps pris par les photons pour traverser le tissu cérébral entre l'émetteur de lumière infrarouge et le récepteur est modifié par l'état des tissus cérébraux. Il est possible de mesurer ces délais en mesurant le délai de phase de la lumière lorsque celle-ci est modulée à très haute fréquence (e.g. 112 MHz). Ils ont présenté des stimuli visuels de nature abstraite (donc difficilement verbalisables) à mémoriser pendant 2 secondes. Ces stimuli étaient toujours présentés en paires, un dans chaque hémichamp visuel. Ils ont ensuite mesuré la réponse à

des stimuli-test présentés au centre de l'écran, qui étaient identiques ou non aux stimuli présentés deux secondes plus tôt. Lorsque le stimulus avait déjà été présenté initialement, la réponse de l'hémisphère cérébral controlatéral à la présentation initiale (donc de l'hémisphère ayant participé à l'encodage du stimulus visuel) était différente de celle de l'hémisphère ipsilatéral. Ce résultat indique que l'encodage de stimuli en mémoire visuelle à court terme laisse une trace mnésique dans l'hémisphère ayant traité le stimulus à encoder. Ils ont également reproduit ce résultat avec des potentiels évoqués visuels. Ce résultat de l'activation unilatérale semble en opposition avec l'activation bilatérale que nous avons obtenue ici. Par contre, une différence cruciale entre leurs manipulations et les nôtres vient du fait qu'ils ont fait un encodage bilatéral pour chaque essai. En effet, leurs participants encodent les deux stimuli, celui de gauche et celui de droite, tandis que dans notre cas, l'encodage était limité à un hémichamp. Nous aurions pu croire de prime abord que cette manipulation aurait augmenté le niveau de latéralisation en tentant de « forcer l'oubli » des stimuli présentés dans l'hémichamp ipsilatéral. Par contre, puisqu'une forte activité bilatérale a été observée dans nos résultats, nous pourrions réinterpréter les résultats obtenus par Gratton et collègues comme reflétant un encodage préférentiel des stimuli présentés dans l'hémichamp controlatéral. Par contre, si aucun stimulus à encoder n'est présent dans un hémichamp visuel, l'hémisphère qui lui est controlatéral semblerait participer au maintien en MCTV des stimuli ipsilatéraux.

Une différence intéressante entre les différents travaux existe au niveau de la disposition des stimuli. En effet, Xu et Chun, (2007, 2007; Xu, 2007) disposent les stimuli sur un seul cercle de rayon 6,8°, tandis que Vogel et Machizawa (2004), Todd et Marois (2004) et nous disposons les stimuli sur des grilles imaginaires. À la lumière des résultats présentés ici, il serait justifié de s'interroger sur l'influence de ce facteur. La disposition en cercle est également celle qui a été utilisée par Sereno et al., (2001) pour étudier la mémoire

spatiale à court terme. Il serait possible de reconsidérer dans ces cas l'encodage de la position spatiale comme étant un encodage de la direction par rapport au point de fixation. La présentation de stimuli sur une grille aurait comme conséquence de parfois disposer les stimuli à encoder sur une même ligne par rapport au point de fixation, réduisant donc le nombre de directions à encoder.

Conclusion

En conclusion, nous avons observé plusieurs fois que pour une tâche complexe d'encodage en mémoire visuelle à court terme de stimuli visuels présentés de façon latéralisée, un ensemble d'activations bilatérales et controlatérales survient. Il n'a pas été possible de fusionner directement les différents résultats en identifiant un nombre limité de régions cérébrales qui auraient été enregistré via les différentes méthodes d'imagerie. Il ne serait donc pas avisé d'utiliser une seule de ces méthodes dans ce paradigme de recherche. La suite de l'avancement des connaissances dans ce champ consistera à diviser la tâche en ses différentes composantes (sélection et encodage des stimuli provenant d'un seul hémisphère, maintien de l'information spatiale ou des caractéristiques de l'objet visuel, récupération de l'information en mémoire pour faire la comparaison avec les stimuli-test) afin d'isoler les activations cérébrales en lien avec chaque composante de la tâche.

Bibliographie

- Alvarez, G. A., & Cavanagh, P. (2004). The capacity of visual short-term memory is set both by visual information load and by number of objects. *Psychological Science*, *15*(2), 106-111.
- Anders M. Dale, R. L. B. (1997). Selective averaging of rapidly presented individual trials using fMRI. *Human Brain Mapping*, *5*(5), 329-340.
- Atkinson, & Shiffrin. (1968). Human memory: A proposed system and its control processes. In K. W. Spence and J. T. Spence (Eds.), *The psychology of learning and motivation* (Vol. 2, pp. 89-195). Orlando, FL: Academic press.
- Atkinson, & Shiffrin. (1971). The control of short-term memory. *Scientific American*, *225*(2), 82-90.
- Baddeley, A. D. (1988). When long-term learning depends on short-term storage. *Journal of memory and language*, *27*(5), 586-595.
- Baddeley. (2000). The episodic buffer: A new component of working memory? *Trends in cognitive sciences*, *4*(11), 417-423.
- Bellec, P., Perlbarg, V., Jbabdi, S., Pelegriani-Issac, M., Anton, J. L., Doyon, J., et al. (2006). Identification of large-scale networks in the brain using fMRI. *Neuroimage*, *29*(4), 1231-1243.
- Burock, M. A., Buckner, R. L., Woldorff, M. G., Rosen, B. R., & Dale, A. M. (1998). Randomized event-related experimental designs allow for extremely rapid presentation rates using functional MRI. *Neuroreport*, *9*(16), 3735-3739.
- Chen, A. C., Feng, W., Zhao, H., Yin, Y., & Wang, P. (2008). EEG default mode network in the human brain: spectral regional field powers. *Neuroimage*, *41*, 561-574.
- Cohen, J. D., Perlstein, W. M., Braver, T. S., Nystrom, L. E., & et al. (1997). Temporal dynamics of brain activation during a working memory task. *Nature*, *386*, 604-608.
- Courtney, S. M., Ungerleider, L. G., Keil, K., & Haxby, J. V. (1997). Transient and sustained activity in a distributed neural system for human working memory. *Nature*, *386*, 608-611.
- Dell'Acqua, R., Sessa, P., Jolicoeur, P., & Robitaille, N. (2006). Spatial attention freezes during the attention blink. *Psychophysiology*, *43*(4), 394-400.

- Epstein, C. M., Sekino, M., Yamaguchi, K., Kamiya, S. (2002). Asymmetries of prefrontal cortex in human episodic memory: effects of transcranial magnetic stimulation on learning abstract patterns. *Neuroscience Letters*, 320(1-2), 5-8.
- Fabiani, M., Ho, J., Stinard, A., & Gratton, G. (2003). Multiple visual memory phenomena in a memory search task. *Psychophysiology*, 40, 472-485.
- Gratton, G. (1998). The contralateral organization of visual memory: a theoretical concept and a research tool. *Psychophysiology*, 35, 638-647.
- Gratton, G., Corballis, P. M., & Jain, S. (1997). Hemispheric organization of visual memories. *Journal of Cognitive Neuroscience*, 9, 92-104.
- Gratton, G., Fabiani, M., Goodman-Wood, M. R., & Desoto, M. C. (1998). Memory-driven processing in human medial occipital cortex: an event-related optical signal (EROS) study. *Psychophysiology*, 35, 348-351.
- Grill-Spector, k., Kourtzi, Z., & Kanwisher, N. G. (2001). The lateral occipital complex and its role in object recognition. *Vision Research*, 41(10-11), 1409-1422.
- Haber, R. N., & Standing, L. G. (1969). Direct measures of short-term visual storage. *The Quarterly journal of experimental psychology*, 21(1), 43-54.
- Hadland, K. A., Rushworth, M. F. S., Passingham, R. E., Jahanshahi, M., & Rothwell, J. C. (2001). Interference with performance of a response selection task that has no working memory component: An rTMS comparison of the dorsolateral prefrontal and medial frontal cortex. *Journal of Cognitive Neuroscience*, 13(8), 1097-1108.
- Hämäläinen, M., Hari, R., Ilmoniemi, R. J., Knuutila, J., & Lounasmaa, O. V. (1993). Magnetoencephalography -- theory, instrumentation, and applications to noninvasive studies of the working human brain. *Reviews of Modern Physics*, 65(2), 413.
- Heilman, K. M., Watson, R. T., & Valenstein, E. (1985). Neglect and related disorders. In *Clinical Neuropsychology* (pp. 243-293). New York: Oxford University Press.

- Helmholtz, H. (1853). Ueber einige Gesetze der Vertheilung elektrischer Ströme in körperlichen Leitern mit Anwendung auf die thierisch-elektrischen Versuche. *Annalen der Physik und Chemie*, 89, 211-233, 354-377.
- Jolicoeur, P. (1999). Concurrent response-selection demands modulate the attentional blink. *Journal of Experimental Psychology: Human Perception and Performance*, 25, 1097-1113.
- Jolicoeur, P., Sessa, P., Dell'Acqua, R., & Robitaille, N. (2006). Attentional control and capture in the attentional blink paradigm: Evidence from human electrophysiology. *European Journal of Cognitive Psychology*, 18, 560-578.
- Jolicoeur, P., Sessa, P., Dell'Acqua, R., & Robitaille, N. (2006). On the control of visual spatial attention: evidence from human electrophysiology. *Psychological Research*, 70, 414-424.
- Kanwisher, N., Chun, M., McDermott, J., & Ledden, P. J. (1996). Functional imaging of human visual recognition. *Brain research. Cognitive brain research*, 5, 55-67.
- Kanwisher, N., Woods, R. P., Iacoboni, M., & Mazziotta, J. C. (1997). A locus in human extrastriate cortex for visual shape analysis. *Journal of Cognitive Neuroscience*, 9, 133-142.
- Kapoula, Z., Isotalo, E., Muri, R. M., Bucci, M. P., & Rivaud-Pechoux, S. (2001). Effects of transcranial magnetic stimulation of the posterior parietal cortex on saccades and vergence. *Neuroreport*, 12, 4041-4046.
- Kawasaki, M., Watanabe, M., Okuda, J., Sakagami, M., & Aihara, K. (2008). Human posterior parietal cortex maintains color, shape and motion in visual short-term memory. *Brain Research*, 1213, 91-97.
- Kawashima, R., O'Sullivan, B. T., & Roland, P. E. (1995). Positron-emission tomography studies of cross-modality inhibition in selective attentional tasks: closing the "mind's eye". *Proc Natl Acad Sci U S A*, 92, 5969-5972.
- Kelley, W. M., Miezin, F. M., McDermott, K. B., Buckner, R. L., Raichle, M. E., Cohen, N. J., et al. (1998). Hemispheric specialization in human dorsal frontal cortex and

- medial temporal lobe for verbal and nonverbal memory encoding. *Neuron*, 20, 927-936.
- Kessels, R. P., d'Alfonso, A. A., Postma, A., & de Haan, E. H. (2000). Spatial working memory performance after high-frequency repetitive transcranial magnetic stimulation of the left and right posterior parietal cortex in humans. *Neuroscience Letters*, 287, 68-70.
- Klapp, S. T., Marshburn, E. A., & Lester, P. T. (1983). Short-term memory does not involve the. *Journal of experimental psychology. General*, 112, 240-264.
- Klaver, P., Talsma, D., Wijers, A. A., Heinze, H.-J., & Mulder, G. (1999). An event-related brain potential correlate of visual short-term memory. *Neuroreport: For Rapid Communication of Neuroscience Research*, 10(10), 2001-2005.
- Klaver, P., Talsma, D., Wijers, A. A., Heinze, H.-J., & Mulder, G. (1999). An event-related brain potential correlate of visual short-term memory. *Neuroreport*, 10, 2001-2005.
- Kourtzi, Z., & Kanwisher, N. (2000). Cortical regions involved in perceiving object shape. *J Neurosci*, 20, 3310-3318.
- Kwong, K. K., Belliveau, J. W., Chesler, D. A., Goldberg, I. E., Weisskoff, R. M., Poncelet, B. P., et al. (1992). Dynamic magnetic resonance imaging of human brain activity during primary sensory stimulation. *Proc Natl Acad Sci U S A*, 89, 5675-5679.
- Luck, S. J. (2006). *An Introduction to the Event-Related Potential Technique*. New York: MIT press.
- Luck, S. J., & Vogel, E. K. (1997). The capacity of visual working memory for features and conjunctions. *Nature*, 390, 279-281.
- Mangun, G. R., Buonocore, M. H., Girelli, M., & Jha, A. P. (1998). ERP and fMRI measures of visual spatial selective attention. *Human Brain Mapping*, 6, 383-389.
- Mazza, V., Turatto, M., Umiltà, C., & Eimer, M. (2007). Attentional selection and identification of visual objects are reflected by distinct electrophysiological responses. *Experimental Brain Research*, 181, 531-536.

- McCollough, A. W., Machizawa, M. G., & Vogel, E. K. (2007). Electrophysiological measures of maintaining representations in visual working memory. *Cortex*, *43*, 77-94.
- Miller. (1956). The magical number seven, plus or minus two: some limits on our capacity for processing information. *Psychological review*, *63*, 81-97.
- Mottaghy, F. M., Gangitano, M., Sparing, R., Krause, B. J., & Pascual-Leone, A. (2002). Segregation of areas related to visual working memory in the prefrontal cortex revealed by rTMS. *Cerebral Cortex*, *12*, 369-375.
- Mottaghy, F. M., Pascual-Leone, A., Kemna, L. J., Toepper, R., Herzog, H., Mueller-Gaertner, H.-W., et al. (2003). Modulation of a brain-behavior relationship in verbal working memory by rTMS. *Cognitive Brain Research*, *15*, 241-249.
- Mull, B. R., & Seyal, M. (2001). Transcranial magnetic stimulation of left prefrontal cortex impairs working memory. *Clinical Neurophysiology*, *112*, 1672-1675.
- Muri, R. M., Gaymard, B., Rivaud, S., Vermersch, A., Hess, C. W., & Pierrot-Deseilligny, C. (2000). Hemispheric asymmetry in cortical control of memory-guided saccades. A transcranial magnetic stimulation study. *Neuropsychologia*, *38*, 1105-1111.
- Muri, R. M., Vermersch, A. I., Rivaud, S., Gaymard, B., & Pierrot-Deseilligny, C. (1996). Effects of single-pulse transcranial magnetic stimulation over the prefrontal and posterior parietal cortices during memory-guided saccades in humans. *J Neurophysiol*, *76*, 2102-2106.
- Norman, D. A., & Shallice, T. (1986). Attention to action: Willed and automatic control of behaviour. In R. J. Davidson, G. E. Schwartz & D. Shapiro (Eds.), *Consciousness and self-regulation* (Vol. 4, pp. 1-18). New York: Plenum.
- Nyffeler, T., Pierrot-Deseilligny, C., Felblinger, J., Mosimann, U. P., Hess, C. W., & Muri, R. M. (2002). Time-dependent hierarchical organization of spatial working memory: A transcranial magnetic stimulation study. *European Journal of Neuroscience*, *16*, 1823-1827.

- Nyffeler, T., Pierrot-Deseilligny, C., Pflugshaupt, T., von Wartburg, R., Hess, C. W., & Muri, R. M. (2004). Information processing in long delay memory-guided saccades: further insights from TMS. *Experimental Brain Research*, 154, 109-112.
- Ogawa, S., Tank, D. W., Menon, R., Ellermann, J. M., Kim, S. G., Merkle, H., et al. (1992). Intrinsic signal changes accompanying sensory stimulation: functional brain mapping with magnetic resonance imaging. *Proc Natl Acad Sci U S A*, 89, 5951-5955.
- Petrides, M. (1995). Functional organization of the human frontal cortex for mnemonic processing: Evidence from neuroimaging studies. *Grafman, Jordan (Ed); Holyoak, Keith James (Ed); et al. (1995). Structure and functions of the human prefrontal cortex. Annals of the New York Academy of Sciences, Vol. 769. (pp. 85-96). New York, NY, US: New York Academy of Sciences. ix, 411 pp.*
- Petrides, M. (2000). The role of the mid-dorsolateral prefrontal cortex in working memory. *Experimental Brain Research*, 133, 44-54.
- Phillips, (1974). On the distinction between sensory storage and short-term visual memory. *Perception & psychophysics*, 16, 283-290.
- Picton, T. W., Bentin, S., Berg, P., Donchin, E., Hillyard, S. A., Johnson, R. J., et al. (2000). Guidelines for using human event-related potentials to study cognition: recording standards and publication criteria. *Psychophysiology*, 37, 127-152.
- Rami, L., Gironell, A., Kulisevsky, J., Garcia-Sanchez, C., Berthier, M., & Estevez-Gonzalez, A. (2003). Effects of repetitive transcranial magnetic stimulation on memory subtypes: A controlled study. *Neuropsychologia*, 41, 1877-1883.
- Raymond, J. E., Shapiro, K. L., & Arnell, K. M. (1992). Temporary suppression of visual processing in an RSVP task: An attentional blink? *Journal of Experimental Psychology: Human Perception & Performance*, 18, 849-860.
- Robitaille, N., Jolicoeur, P., Dell'Acqua, R., & Sessa, P. (2007). Short-term consolidation of visual patterns interferes with visuo-spatial attention: converging evidence from human electrophysiology. *Brain Research*, 1185, 158-169.

- Serences, J. T. (2004). A comparison of methods for characterizing the event-related BOLD timeseries in rapid fMRI. *Neuroimage*, *21*(4), 1690-1700.
- Sereno, M. I., Pitzalis, S., & Martinez, A. (2001). Mapping of contralateral space in retinotopic coordinates by a parietal cortical area in humans. *Science*, *294*, 1350-1354.
- Shallice, T., & Warrington, E. K. (1970). Independent functioning of verbal memory stores: A neuropsychological study. *The Quarterly journal of experimental psychology*, *22*, 261-273.
- Shin, E., Fabiani, M., & Gratton, G. (2006). Multiple levels of stimulus representation in visual working memory. *Journal of Cognitive Neuroscience*, *18*, 844-858.
- Smyrnis, N., Theleritis, C., Evdokimidis, I., Muri, R. M., & N., K. (2003). Single-pulse transcranial magnetic stimulation of parietal and prefrontal areas in a memory delay arm pointing task. *Journal of Neurophysiology*, *89*, 3344-3350.
- Song, J.-H., & Jiang, Y. (2006). Visual working memory for simple and complex features: An fMRI study. *NeuroImage*, *30*, 963-972.
- Sperling. (1960). The information available in brief visual presentation. *Psychological monographs*, *74*(11, Whole No. 498), 29.
- Squire, R. L., & Zola, S. M. (1996). Structure and function of declarative and nondeclarative memory systems. *Proceedings of the National Academy of Sciences of the United States of America*, *93*, 13515-13522.
- Squire, R. L., Knowlton, B. B., & Musen, G. G. (1993). The structure and organization of memory. *Annual review of psychology*, *44*, 453-495.
- Talairach, J., & Tournoux, P. (1989). *Co-planar stereotaxic atlas of the human brain* (M. Rayport, Translator). New York: Thieme Medical.
- Todd, J. J., & Marois, R. (2004). Capacity limit of visual short-term memory in human posterior parietal cortex. *Nature*, *428*, 751-754.
- Tulving. (1972). Episodic and semantic memory. In E. Tulving & W. Donaldson (Eds.), *Organization of memory* (pp. 381-403). New York: Academic Press.

- Urbach, T. P., & Kutas, M. (2002). The intractability of scaling scalp distributions to infer neuroelectric sources. *Psychophysiology*, *39*, 791-808.
- Vogel, & Machizawa. (2004). Neural activity predicts individual differences in visual working memory capacity. *Nature*, *428*, 748-751.
- Vogel, E. K., McCollough, A. W., & Machizawa, M. G. (2005). Neural measures reveal individual differences in controlling access to working memory. *Nature*, *438*, 500-503.
- Vogel, E. K., Woodman, G. F., & Luck, S. J. (2001). Storage of features, conjunctions and objects in visual working memory. *Journal of Experimental Psychology: Human Perception and Performance*, *27*, 92-114.
- Wagner, A. D., Poldrack, R. A., Eldridge, L. L., Desmond, J. E., Glover, G. H., & Gabrieli, J. D. E. (1998). Material-specific lateralization of prefrontal activation during episodic encoding and retrieval. *Neuroreport*, *9*, 3711-3717.
- Xu, Y. (2007). The Role of the Superior Intraparietal Sulcus in Supporting Visual Short-Term Memory for Multifeature Objects. *Journal of Neuroscience*, *27*, 11676-11686.
- Xu, Y., & Chun, M. M. (2006). Dissociable neural mechanisms supporting visual short-term memory for objects. *Nature*, *440*, 91-95.
- Xu, Y., & Chun, M. M. (2007). Visual grouping in human parietal cortex. *Proc Natl Acad Sci U S A*, *104*, 18766-18771.
- Zhang, W., & Luck, S. J. (2008). Discrete fixed-resolution representations in visual working memory. *Nature*, *453*, 233-235.

Annexe 1 : autres travaux réalisé au cours de la thèse

Fundamental Properties of the N2pc as an Index of Spatial Attention: Effects of Masking

Nicolas Robitaille and Pierre Jolicoeur
Centre de Recherche en Neuropsychologie et Cognition
Université de Montréal

Abstract Masking is an important tool in many paradigms used to study the cognitive architecture. The N2pc is an electrophysiological event-related potential (ERP) that has been used as a tool to study the deployment of visual spatial attention. The aim of this paper was to study the effects of masking on the N2pc. Two stimuli were presented on the screen, one to left and one to right of fixation, and subjects reported the identity of one of them. The targets could be discriminated both by their category (letters vs. digit) and by their colour (pink vs. green). Backward masking was produced by presenting a second pair of bilateral stimuli after the offset of the first pair. The second stimuli were characters of the same colour and category as in the first pair. Forward masking was produced by using the very same stimuli as in the backward masking condition, but by instructing subjects to report the second stimulus. The forward mask trials had longer response times compared to no-mask trials, and backward mask trials had even longer response times, and also a higher error rate. Although the different masking procedures lead to clear behavioural effects, the N2pc was not affected, suggesting that the deployment of visual spatial attention, per se, was not affected by pattern masking. A sustained posterior contralateral negativity (SPCN) following the N2pc was also found (300 ms post-target, and beyond), and the amplitude of the SPCN was strongly modulated by the number of presented stimuli and the duration of the SPCN was positively correlated with RT in the behavioural task. We hypothesize that the SPCN reflects neural activity associated with the passage of information through visual short-term memory.

The N2pc is a lateralized event-related potential (ERP) component that reflects the locus of attention in the

This article was accepted by the previous editorial team, headed by Peter Dixon.

Cet article a été accepté par l'équipe de rédaction précédente dirigée par Peter Dixon.

visual field (Luck & Hillyard, 1994a). It usually occurs in the temporal window of the N2 component and is measured at posterior electrode sites, over the hemisphere contralateral to the target. Usually the N2pc is measured by taking the difference in the ERP observed at electrode sites contralateral to the visual field of a target and the ERP observed at a corresponding electrode on the ipsilateral side, for visual displays that are physically equivalent across the left and right visual fields. By physically equivalent, we mean displays that should produce equivalent bottom-up sensory activation in each hemisphere, as a function of purely sensory factors. The observation of a difference in electrophysiological response across cerebral hemispheres for such displays, therefore, must reflect differential processing of the initially equivalent display. Luck and Hillyard (1994a) found that the amplitude of the N2pc was higher for more attention-demanding tasks, and they argued that the N2pc reflects neuronal activity associated with filtering out of distractors in visual search tasks. Luck, Girelli, McDermott, and Ford (1997) found that adding nearby distractors increased the amplitude of the N2pc, which provided converging evidence for the hypothesis that the N2pc reflects a process of distractor suppression. More generally, these results suggest that increasing the perceptual difficulty of visual search might increase the amplitude of the N2pc.

Backward masking renders visual tasks more difficult by superimposing new contours over the location previously occupied by visual targets. This type of masking often increases response time and increases error rates. If increasing task difficulty increases the amplitude of N2pc and if masking increases task difficulty, we hypothesized that backward masking might also increase the amplitude of the N2pc. This hypothesis was tested in the present experiment.

Woodman and Luck (2003a) showed that a particular form of masking, four-dot masking, did not modulate the N2pc, although this masking lowered the accuracy

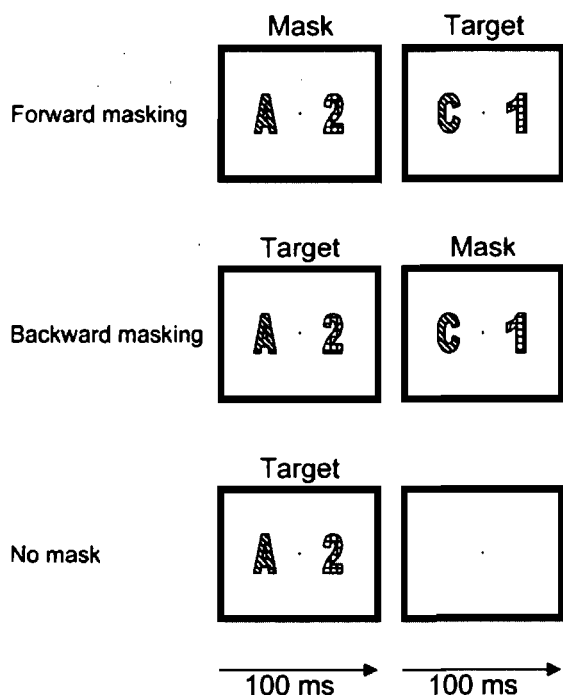


Figure 1. Experimental paradigm. One character was green and one was pink (represented here with different textures).

of the report of the targets. Apparently, spatial attention can engage on a target, but later processing may fail to produce a conscious percept of the target. Four-dot masking requires particular conditions to be effective (Enns & Di Lollo, 1997), and most particularly that the attention of the subject not be focused at the location of the masked object. This implies that spatial uncertainty about target location is a prerequisite for four-dot masking. Perhaps a form of masking that does not require these conditions to be effective, such as a backward mask, would modulate the N2pc. It is perhaps surprising that the presence of the four dots, in the four-dot masking condition in Woodman and Luck (2003a) experiment did not cause an increase in the size of the N2pc, given that these dots were close to the target, and presumably acted as a form of distractor. On the other hand, there were many other visual forms present in the visual display used by Woodman and Luck (2003a), so adding four dots may not have been sufficient to have the same effect as adding distractors to a sparse display, as in the Luck et al. (1997) study.

Masking is commonly used in cognitive psychology. For example, it is a key factor in the attentional blink (AB) paradigm (Raymond, Shapiro, & Arnell, 1992). The AB occurs when two targets (T1, T2) follow each other within a short interval. The report of the second one,

T2, is impaired relative to the report of the first one (T1). The masking of T1 (e.g., Raymond, Shapiro & Arnell, 1992) and T2 (Giesbrecht & Di Lollo, 1998; Jolicoeur, 1999b; Vogel & Luck, 2002) is important for the paradigm, and both modulate the magnitude of the observed AB effect. Some models of the AB (e.g., Chun & Potter, 1995; Jolicoeur, 1998, 1999a) hypothesize that the treatment of the second target is delayed because central resources are engaged and less available while the first target undergoes processing. This hypothesis received good support from electrophysiological evidence reported by Vogel and Luck (2002). During this delay, the second target can be degraded by a trailing mask, leading to a lower accuracy of report for T2. Given the critical importance of backward masking in many paradigms, and particularly the AB paradigm, and our desire to use the N2pc to investigate spatial attention in the AB paradigm, we wished to investigate effects of masking on the N2pc in a very simple situation involving masking. The aim of this paper was to investigate if a masking procedure commonly used in AB paradigm would modulate the N2pc.

To assess the effect of masking on the ERP, good control over the physical properties of the stimuli was required. This was done by comparing two kinds of masking: backward masking and forward masking using exactly the same stimulus (see Figure 1). This was accomplished by asking the observers to report either the first or the second of two successive stimuli presented rapidly at the same location. This design allowed us to equate perfectly for the physical properties of stimuli in the forward versus backward masking conditions, because the two masking conditions could be created simply by changing the instruction to the subject while using identical stimuli. Based on prior work, we anticipated that reporting the first of two stimuli (backward masking) would be more difficult than reporting the second (forward masking). In general, it is very easy to report the last stimulus in a sequence of stimuli at the same location but much more difficult to report the second-to-last stimulus (e.g., see Giesbrecht & Di Lollo, 1998; Vogel & Luck, 2002). The backward masking condition could be considered as a target followed by a pattern mask, where the mask is another character of the same category and colour. Conversely, the forward-masking condition could be considered as a pattern mask followed by a target, where the pattern mask is another character of the same category and colour. According to classical work (Breitmeyer, 1984) on the masking phenomenon, a pattern mask is more effective when the target and the mask share physical characteristics. Furthermore, a 100 SOA was found highly effective under those conditions. We also included a control condition, containing only

one stimulus, in which the target was neither forward nor backward masked. This condition should produce a typical N2pc ERP, that we could then compare with the ERP measured in the two masking conditions.

Method

Subjects

Twelve volunteers, nine women, aged between 19 and 24, were paid for their participation. They reported no neurological problems, normal or corrected-to-normal vision, and normal colour vision. We obtained informed consent from each subject at the beginning of the experiment. No subject was rejected based on various trial screening criteria that are explained in the electrophysiological recordings and analysis section and at the beginning of the results section.

Stimuli

The stimuli were presented on a 17-inch colour cathode-ray tube (CRT) driven by a microcomputer running MEL 2.01 software at 60 HZ in 640 × 480 pixel mode. The stimuli were digits (1, 2, 3, and 4) and letters (A, B, C, and D), shown in pink or green. The characters were 1.2° of visual angle high and 1.1° wide. A fixation point (0.2°) was present at the centre of the display. Two characters were presented at the same time, centred on a point 3° to the left and the right of the fixation point. The luminance and chromaticity of the stimuli were measured with a Minolta CS-100 chroma meter. The luminance of the green was 19.7 cd/m² ($x = .292$, $y = .550$; CIE (x , y) chromaticity coordinates (Wyszecki & Stiles, 1982); that of the pink was 18.5 cd/m² ($x = .386$, $y = .279$), the fixation point was 30.8 cd/m² ($x = .280$, $y = .302$), and the background was 0.10 cd/m² ($x = .449$, $y = .442$). Counterbalancing (explained below) ensured that the small difference in luminance across the green and pink stimuli could not have influenced the measured N2pc.

Procedure

Each trial began with a fixation symbol at the centre of the display, indicating if the last answer was correct (+) or incorrect (-). The subject started each trial by pressing the space bar on a standard computer keyboard. The + or - sign was then replaced by a small fixation point. The fixation point remained alone on the screen for 500 ms. The two characters then appeared. One character was a letter and the other was a digit. One was pink and the other was green. The colour for a character category (letter vs. digit) was kept constant for all trials for each subject, but was counterbalanced across subjects.

Each condition was tested in a different block because the backward mask and the forward mask

involved the same stimuli but different instructions. The order of the blocks was counterbalanced across subjects using a Latin square.

The task was to report the identity of the pink character, for half of the subjects, or of the green character, for the other half. The pink character was a digit for half of the subjects and a letter for the other half. The target character appeared with equal probability to the left or to the right of fixation, with left and right trials intermixed at random within each block of trials. Given that the colour paired with a stimulus category was kept constant for any given subject, the subject could use character identity to select which character to process, but subjectively, colour appeared to be the effective selection feature.

For the two blocks involving masking, two characters were presented on each side, one after the other in rapid succession. During the forward masking block, the task was to report the second stimulus. During the backward-masking block, the task was to report the first stimulus. Finally, for the no-mask block, a single character was presented on each side of fixation. Each stimulus was presented for 100 ms, leading to a 200-ms total presentation time for the two conditions involving masking. After the offset of the characters, the fixation dot remained alone on the screen.

The subjects reported the identity of the target character using four response keys, as quickly as possible, while keeping errors to a minimum. The keys [j], [k], [l], and [;] were to be pressed with fingers of the right hand for the stimuli 1, 2, 3, 4, or the stimuli A, B, C, D, respectively.

After the response, the fixation dot disappeared. A blank screen was then presented for a variable amount of time, ranging between 1,000 and 1,500 ms (selected at random from a uniform distribution), preventing subjects from initiating the next trial in the same action sequence as for their response. Each trial was initiated by a press of the space bar. The reaction times (calculated relative to the onset of the target) and accuracy were recorded by the stimulation computer.

Each block contained 16 practice trials and 288 experimental trials, except the first practice block, which included 24 practice trials, the first 8 of which had a longer presentation time, to ensure that the task was understood.

Electrophysiological Recordings and Analysis

The recordings were made with a Biosemi Active-two system, with 64 active AG-AGCL scalp electrodes positioned using the extended International 10-20 system. Subjects were seated in a dimly lit electrically shielded room. The EEG was algebraically re-referenced to the average of the left and right mastoids. The elec-

troculogram (EOG) was recorded with active AG-AGCL electrodes placed at the left and right canthi and above and below the left eye. HEOG was obtained by subtracting the signal at the left electrode from the signal recorded at the right electrode. VEOG was obtained by subtracting the signal at the electrode above the left eye from the signal at the electrode below the left eye. The signals were amplified, low-pass filtered with a cut-off frequency of 67 Hz, and digitized at 256 Hz during the recording. They were filtered again, during postrecording analysis, using a high-pass filter with a cut-off frequency of 0.05 Hz and a low-pass frequency of 80 Hz. A deviation of more than 100 μ V in any 200-ms period in the VEOG was considered as an eye blink. A deviation of more than 35 μ V in any 200-ms period in the HEOG (low-pass filtered using a 5 Hz cut-off, 48 dB, Butterworth zero phase filter) was considered as an eye movement. Trials with eye blinks and eye movement (24.6%) were removed during postrecording analysis for all electrodes. Furthermore, if an electrode contained a recording artefact (a derivation of more than 100 μ V in any 200-ms period) during a trial, this trial was also removed from the average for this electrode.

As a further precaution to ensure that subjects did not move their eyes in the direction of the target (despite screening trials on the basis of the HEOG), separate average HEOG curves were computed for left-target trials and for right-target trials. Any residual tendency of the subject to move his/her eyes toward the target, for the trials included in the analysis, would produce systematic deviations in these average HEOG waveforms.

Average waveforms were computed at each scalp electrode site for each condition with a 200-ms prestimulus baseline and a 500-ms poststimulus period relative to the onset of the characters. The epochs were baseline corrected based on the mean activity during the 200-ms prestimulus period, for each electrode site.

The average ipsilateral and contralateral waveforms were computed for all lateralized posterior electrode pairs. However, given that the results were similar across several sites, and that we are more interested in differences between masking conditions rather than differences between electrode sites, we focused our analyses on the waveforms observed at the PO7 and PO8 electrodes. We first computed an average ipsilateral waveform by averaging the waveform for the left electrode (PO7) for trials in which the target was on the left with the waveform for the right (PO8) electrode for trials in which the target was on the right. Similarly, we computed an average contralateral waveform by averaging the right-sided response (PO8) to left targets with the left-sided response (PO7) to right targets. These

TABLE 1
Proportion of Correct Response and Reaction Time (ms)

Mask Type	Accuracy	Reaction Time
No mask	98% (0.87)	601 (18.6)
Forward mask	97% (0.58)	718 (15.3)
Backward mask	87% (1.41)	1,000 (26.8)

Note. The Standard Error (with between-subject variability removed) is shown in parenthesis.

waveforms were then subtracted (contralateral – ipsilateral) to produce the N2pc difference waveform.

A quantitative evaluation of the amplitude of the N2pc component was obtained by computing the mean amplitude of the N2pc difference waveform in a 180–280 ms window. The presence of the N2pc was assessed by computing a *t*-test against zero for each condition. A repeated measure ANOVA with masking type as three-level within-subject factor was used to assess differences between conditions. This statistical model was also applied to the subsequent time window, as well as to the measures assessing behavioural performance.

Results

Behaviour

Response times for trials with a correct response were screened for outliers. For each condition and subjects the average reaction time and the standard deviation was calculated. The observation furthest from the mean was then temporarily excluded and the standard deviation and mean were re-calculated. If the mean was lower than the mean minus $C \times$ the standard deviation or greater than the mean plus $C \times$ the standard deviation, it was excluded permanently, and the process was repeated until no observation was rejected. The criterion, C , was 3.0 or greater, and was adjusted as a function of sample size, as explained in Van Selst and Jolicoeur (1994). This resulted in the loss of 2.35% of the correct trials. The means of the screened response times for the different masking conditions are shown in Table 1.

The mean response times were submitted to a repeated-measures ANOVA with masking condition as a within-subjects factor. As can be seen in Table 1, response times were longest in the backward-mask condition, intermediate in the forward-mask condition, and shortest in the no-mask condition, $F(2, 22) = 59.75$, $MSE = 7,589.39$, $p < .0001$, showing that the backward-mask condition was, as expected, the most difficult. The accuracy results corroborated this prediction because accuracy was the lower in the backward-mask condition than in other two conditions, which produced equivalent results, $F(2, 22) = 22.78$, $MSE = 0.00189$, $p < .0001$.

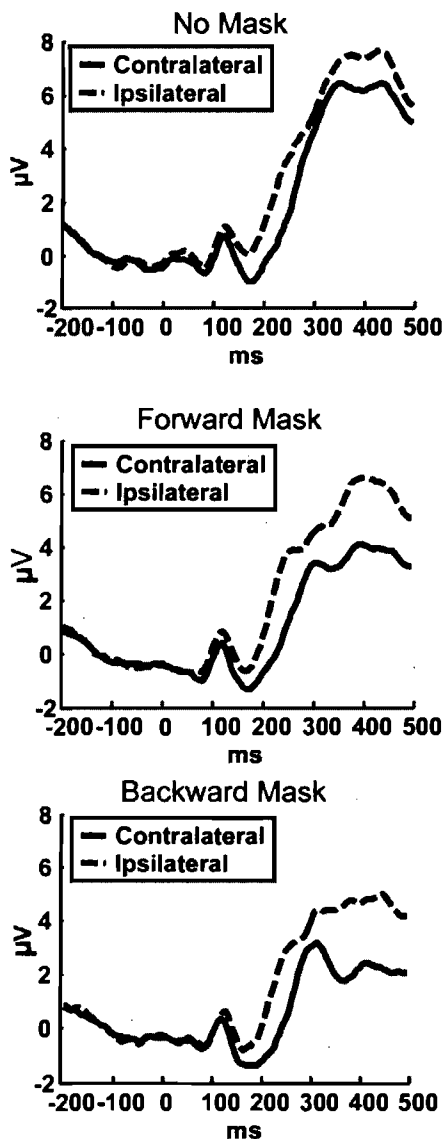


Figure 2. Average ipsilateral and contralateral waveforms for the no-mask condition, the backward-mask condition, and the forward-mask condition at the PO7 and PO8 electrodes.

Electrophysiology

Only the trials with a correct response were analyzed. Together with the artefact rejection procedures, 31.8% of the trials were lost. For the trials kept, the maximum mean deviation of the horizontal EOG for any given subject was 3.5 μV , in the N2pc time window, showing that, for the worst case, the eyes moved no more than about $.2^\circ$ (Lins, Picton, Berg, & Scherg, 1993) in the direction of the target, with most subjects having residual movements of less than $.1^\circ$. Consequently, all subjects were kept for further analy-

sis, without further ocular artefact correction.

The average ipsilateral and contralateral waveforms from the no-mask condition, the forward-mask condition, and the backward-mask condition are shown in Figure 2. The N2pc difference waveforms (computed by subtracting the ipsilateral waveform from the contralateral waveform) for the three masking conditions are shown in Figure 3. There was a clear and statistically significant (t-test against 0) N2pc in each of the three masking conditions, $t(11) > 2.998$, $p < .012$, in all cases. A repeated-measure ANOVA with mask condition as a within-subjects factor was also carried out. No differences in the amplitude in the N2pc waveforms during the 180-280 ms interval were found, $F(2, 22) = 0.533$, $MSE = 0.765$, $p > 0.59$. As noted earlier, the above analyses were performed on mean amplitudes in the N2pc time window. We also performed analyses using an automated peak detection algorithm (finding the minimum value in the 0-280 ms time window) and found the amplitude of the peak of the N2pc waveform for each condition for each subject. Inspection of the individual N2pc waveform for each condition for each subject confirmed that the 180-280 time window was appropriate for every subject. Furthermore, as can be seen in Figure 3, there was no difference in latency of the components, and thus it was not the case that the N2pc could fall outside the analysis window in one condition but not the others – this was true for individual subjects also. We do not believe that our failure to find statistically significant differences across conditions was due to a lack of power because we have observed clear and significant effects on the amplitude of the N2pc in several other studies, using similar numbers of subjects (16) and trials per condition (200; e.g., Jolicoeur, Sessa, Dell'acqua, & Robitaille, in press a, b) and in several other studies in our laboratory.

Note that N2pc curves were computed relative to the occurrence of the first stimulus, without regard as to whether the first stimulus was a target (backward masking condition) or a mask (forward-masking condition). Thus, we observed that the onset of the N2pc was linked to the occurrence of the selection cue for the stimuli, namely the colour. This observation was reproduced and extended in another experiment (Robitaille & Jolicoeur, 2005).

Sustained Posterior Contralateral Negativity (SPCN)

Consider again the results shown in the bottom panel of Figure 3. In all three conditions, the contralateral minus ipsilateral waveforms exhibited a sustained negativity that had an onset at about 300 ms after the presentation of the stimuli. We refer to the lateralized ERP component observed after 300 ms as the SPCN, for sustained posterior contralateral negativity.

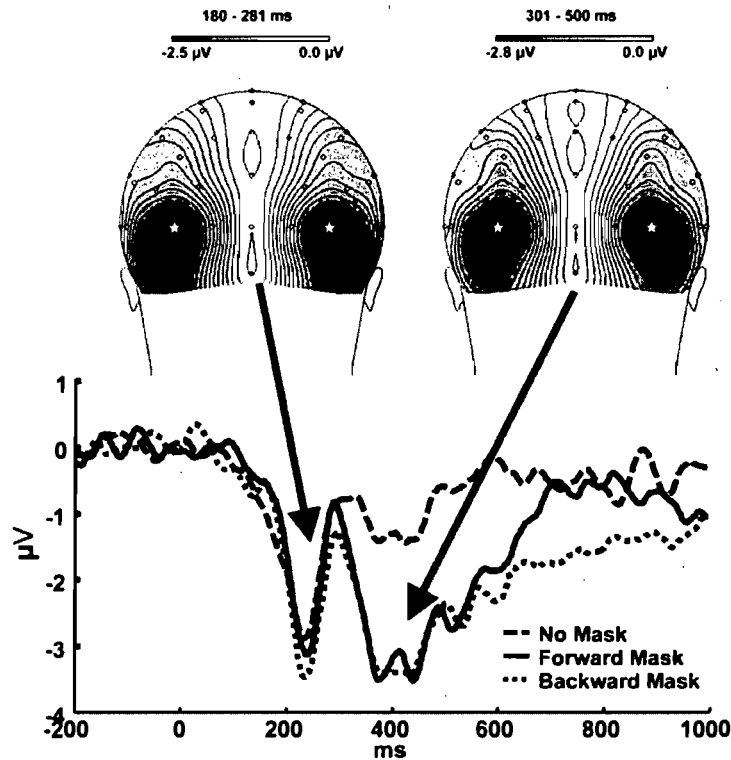


Figure 3. Contralateral minus ipsilateral difference waveforms, at PO7 and PO8, for the three conditions and scalp distributions in two time windows. The left scalp distribution shows the voltage map for the mean activity in the 180–280 ms time window for posterior electrodes, for the backward-mask condition. The right scalp distribution map shows the mean activity in the 300–500 ms time window for the same condition. The white stars show the location of the PO7 (left) and PO8 (right) electrodes used for the statistical analyses and for the waveforms shown in Figures 2 and 3. Because the N2pc difference waveform was computed for each electrode pair, the resulting scalp distribution maps are symmetric.

In contrast with the absence of differences between conditions for the N2pc time window, there were clear differences across conditions for the SPCN in amplitude and duration. From 300 ms to about 500 ms, the ERPs for the two masked conditions produced a larger SPCN than the ERPs for the no-mask condition, implying a difference in the lateralization of cerebral activity relative to the side of the target depending on the condition. In this time window (300–500 ms), this difference was clearly statistically significant, $F(2, 22) = 7.88$, $MSE = 1.361$, $p < .003$. A subsequent repeated-measure ANOVA with only the two masked conditions comparing mean amplitude in the 300–500 ms time window revealed no significant difference, $F < 1$. The mean amplitudes are graphed in Figure 4.

We hypothesize that the SPCN could reflect neural activity associated with the passage of the stimuli

through visual short-term memory (VSTM). Vogel and Machizawa (2004) reported that such a sustained contralateral negativity is observed when subjects held information in VSTM and the amplitude of the negativity was proportional to the number of elements held in memory (as long as the number of items was less than or equal to the observer's VSTM storage capacity). They called their component the CDA, for contralateral delay activity. In the no-mask condition, there was only one stimulus to be encoded and processed, but there were two in the masking conditions. We hypothesize that the two stimuli were somewhat difficult to distinguish because of their rapid successive presentation. For the conditions in which there were two stimuli, subjects had to determine which one came first and which one came second, in order to report the correct one at the end of the trial. It is likely that both stimuli were initial-

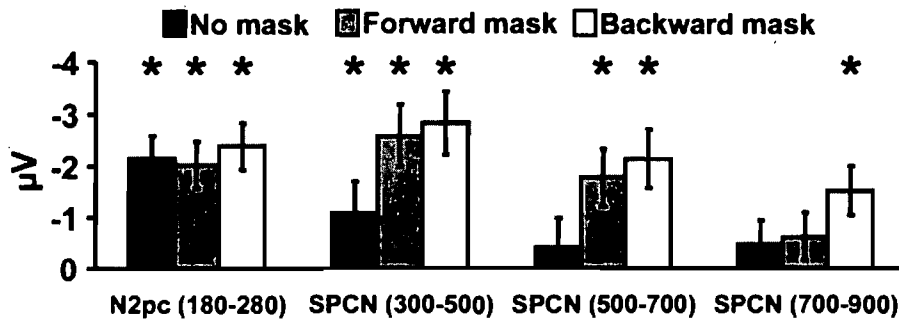


Figure 4. Mean amplitude of the contralateral minus ipsilateral difference waveforms for fixed time windows, with confidence intervals (Masson & Loftus, 2003) allowing comparisons across masking conditions. The asterisks indicate amplitude significantly different from zero.

ly encoded and represented in VSTM for some time, while subjects determined which one to process further in order to make the correct response. In this view, two object representations likely transited through VSTM in the forward-mask and backward-mask conditions, but only one representation transited through VSTM in the no-mask condition. Our results thus dovetail nicely with those of Vogel and Machizawa (2004), and the present results suggest that the SPCN could provide a useful index for the involvement of VSTM in more complex cognitive tasks.

If the SPCN reflects the maintenance of the stimuli in VSTM, a set of predictions could be made regarding the timing of the return to baseline of this component. Indeed, there were large differences in reaction time across the different masking conditions that indicate that processing the stimuli required more time in the forward-mask condition than in the no-mask condition, and even more time in the backward-mask condition. If part of these RT differences were associated with different durations of transit through VSTM, and if the SPCN reflects the time during which stimuli are maintained in VSTM, then we should see the SPCN return to baseline at different times for the different conditions. More specifically, the SPCN in the backward-mask condition should be present for a longer amount of time than in the forward-mask condition, and the SPCN for the forward-mask condition should be present for longer than for the no mask condition.

These predictions were tested by reanalyzing the data using a longer time window (up to 1,000 ms post-stimulus onset, plotted in Figure 3). The results clearly confirmed the predictions. The SPCN in the backward-masking condition was still visible up to 800 ms post stimulus, in contrast with what was observed in the forward-masking condition or the no-mask condition. In

Figure 4, we show the mean amplitude of the SPCN for each condition in different time windows to show that the differences across conditions that are apparent by eye in the 300-1,000 ms time period reflect statistically reliable differences.

We already showed in a foregoing analysis that the mean amplitude of the SPCN differed across conditions in the 300-500 ms window. Subsequent tests also showed that the mean amplitude was significantly different from 0 in all three conditions.

The mean amplitude of the SPCN in the 500-700 ms time window was also different across conditions, $F(2, 22) = 8.406$, $MSE = 1.168$, $p < .002$. Subsequent analyses confirmed that the amplitude was lower for the no-mask condition relative to the other two (all $F_s > 9$; $p < .02$), and there was no difference in amplitude between the two masked conditions, $F(1, 11) = 0.995$; $MSE = 0.769$; $p > .30$. Furthermore, the mean amplitude of the SPCN for the no-mask condition was not significantly different from 0 in this time window.

The mean amplitude of the SPCN for the 700-900 ms time window was also statistically different across conditions, $F(2, 22) = 4.472$, $MSE = 0.845$, $p < .023$. Subsequent analyses confirmed that the amplitude was higher for the backward-mask condition relative to the others (all $F_s > 5$; $p < .05$), and there was no difference in amplitude between the forward-mask condition and the no-mask condition, $F(1, 11) = 0.19$, $MSE = 0.60$, $p > .60$. The SPCN was not different from 0 for the no-mask and the forward-mask conditions in this time window, whereas it was still significant for the backward-mask condition.

These analyses suggest that the amplitude of the SPCN tracks the number of items held in VSTM (Vogel & Machizawa, 2004) while the time course of the component tracks how long the items are held in VSTM.

Discussion

Our principal goal was to examine the effects of masking on the N2pc component. We compared forward-mask, backward-mask, and no-mask conditions, using stimuli that were identical for the two former conditions. We found no effects on the amplitude or latency of the N2pc across conditions (Figure 3). Although changing masking conditions produced clearly different success rates and substantial mean response time differences, visual spatial attention appeared to engage on the target based on the selection cue (most likely colour) with equal latency and probability in all conditions. These results justify the use of the N2pc as an index of spatial deployment of attention in the AB paradigm, or in other cognitive paradigms that require the use of masking (Jolicoeur et al., in press a,b). Our conclusion regarding the minimal or null effects of masking on the N2pc must naturally be confined to the conditions we used in the present study, namely, a presentation condition in which the location of the target was not known in advance.

Interestingly, we note that, like Eimer (1996), we observed a substantial N2pc under conditions in which one target was presented to the left of fixation and one was to the right of fixation. Luck and his colleagues (e.g., Luck & Hillyard, 1994a, b; Luck et al., 1997) have argued that the N2pc reflects a process of distractor suppression. In this view, no N2pc should be observed in the absence of distractors. One account for the presence of an N2pc, despite the absence of distractors in the same hemifield (in our no-mask condition, and in some conditions in Eimer, 1996) could be that the stimulus in the opposite hemifield, somehow, is sufficient to trigger a distractor-suppression mechanism. Such a mechanism could, for example, attempt to block unwanted stimulation originating in the opposite hemisphere but contributing to activation in the hemisphere contralateral to the target via connections crossing through the corpus callosum. In this view, callosal inputs generated by the distractor in the opposite hemifield could compromise target processing, and the N2pc would reflect a process designed to suppress this activity in order to minimize the contaminating input to the mechanisms that process the desired target. In our preparation, and in that of Eimer (1996), the stimuli were presented symmetrically about the fixation point, making it possible for symmetric cortical links to carry unwanted signals (to be suppressed, thereby engaging the mechanisms that produce the N2pc). Despite very large effects on mean response time across conditions and highly significant effects on accuracy, we found no significant effects on the amplitude of the N2pc in its usual time window (180-280 ms), suggesting that "task difficulty," per se, does not modulate the N2pc.

In the Results section, we motivated additional analyses of the SPCN based on the hypothesis that this response could reflect a distinct ERP component from the N2pc. We suggested that the SPCN could reflect a process of maintenance in VSTM, as suggested by the elegant work of Vogel and Machizawa (2004). In this view, the N2pc would reflect a mechanism of target selection (perhaps via distractor suppression) whereas the SPCN would reflect a subsequent process of activation in VSTM. The results support a dissociation between N2pc and SPCN because the N2pc was not different across the three masking conditions, whereas the SPCN showed clear amplitude and duration differences across conditions.

Before we accept the hypothesis that the SPCN is a distinct component, however, we need to consider the possibility that the larger SPCN observed for the two conditions that involved masking reflected an N2pc to the second stimulus when two items were presented one after the other. In Figure 3, we show the scalp distribution of the N2pc and the SPCN (in the 300-500 ms window) and it is clear that these distributions are very similar. This suggests that the neural generator(s) for the N2pc and for the SPCN could be the same. One interpretation of these results is that the SPCN may be nothing more than a second N2pc to the second stimulus in the forward-mask and backward-mask conditions. Another interpretation is that there is a single N2pc lasting for much longer than the usual 180-280 ms period, and that a contralateral positivity (or ipsilateral negativity) with a peak at about 300 ms gives the appearance that there are two separate negative components. Certainly, the very similar scalp distributions shown in Figure 3 are consistent with this hypothesis.

Nonetheless, there are several arguments that militate against these accounts. First, the two-N2pc hypothesis provides no account for the sustained response observed in the no-mask condition, in which a substantial sustained response was observed, but this condition had only one stimulus. The no-mask condition thus had no second stimulus to produce a second N2pc, yet this condition produced a significant SPCN 300-500 ms post stimulus. Second, and more importantly, the hypothesis of an N2pc to the second stimulus would not predict different durations of SPCN across the forward-mask and backward-mask conditions. However, we observed that the SPCN returned to baseline earlier in the forward-mask condition than in the backward-mask condition. Third, according to the two-N2pc hypothesis, one would expect the second N2pc to have the same duration as the first N2pc. As in many other experiments in which the N2pc was measured, the duration of the N2pc is about 100 ms (Hopf, Boelmans, Schoenfeld, Heinze, & Luck, 2002; Luck, Girelli, McDermott, &

Ford, 1997; Luck & Hillyard, 1994a, 1994b; Hopf et al., 2000; Woodman & Luck, 2003b). Thus the second N2pc, which appears to begin at about 300 ms, should have returned to baseline at about 400 ms. However, instead, the observed SPCN continued long after that.

Another hypothesis that could explain why the posterior contralateral negativity extended well beyond 400 ms is that it reflected different probabilities of rechecking the stimuli across the three conditions. The long duration of the SPCN could be explained, in part, by the idea that subjects focus on the target once and then recheck it to make sure they made the correct decision. This could explain the fact that the SPCN was also observed in the no-mask condition, but was smaller (because less rechecking is needed for this simpler task). This could also explain the difference in the offset time: Subjects were less certain of their decision in the backward-mask condition, and therefore engaged in prolonged rechecking. A problem for this view, however, is that stimuli were presented only briefly and were no longer on the screen when rechecking would presumably need to take place to produce long-lasting hemispheric asymmetries (especially in the backward-mask condition, for which the SPCN lasted beyond 1,000 ms, as can be seen in Figure 3). Given that the conditions were blocked, subjects would quickly learn that there is no point in attending to the screen because there is simply no stimulus present and thus no information to be extracted from this location that can help to guide response selection.

If rechecking was taking place, it could not have been for a physical stimulus on the screen. Rather, any rechecking would require processing a representation of the stimulus in memory. Our view is that this stimulus was most likely in VSTM and that the sustained activity we called SPCN reflected neural activity required to maintain the VSTM representation, rather than sustained attention on the computer screen.

In order to provide a stronger link between the SPCN and VSTM, we have since performed several new experiments. In one of them we presented four digits on each trial (two to the left and two to the right of fixation; Perron, Brisson, Robitaille, & Jolicoeur, 2005). One was red and one was green (in opposite hemifields) and two were yellow (one in each hemifield). These stimuli were shown for 150 ms. Half of the subjects were instructed to encode both characters on the side of the red character and half on the side of the green character. After a delay (ISI) of either 600 ms or 1,200 ms, a single probe digit was shown at fixation. The task was to decide whether the probe matched (both in form and colour) one of the digits on the encoded side. We found that the duration of the SPCN was determined by the duration of the probe delay,

and in particular the SPCN was observed for at least 1,400 ms in the 1,200 ms probe-delay condition. As in the present experiment, the SPCN was preceded by an N2pc in the usual time window. Interestingly, this experiment required processing a probe character at fixation, which presumably would require a shift of visual spatial attention away from the peripheral location where characters were initially encoded, back to the centre. Nonetheless, we observed an SPCN during the entire retention interval as subjects prepared to encode the probe character, suggesting strongly that the SPCN is tied to maintenance in VSTM rather than maintained visuo-spatial attention at the level of the visual display (Perron et al., 2005).

For these reasons, and because we have begun to observe other dissociations between the N2pc and the SPCN in other work in our laboratory (e.g., Perron et al., 2005), we hypothesize that the SPCN is likely a distinct component, tied to activity in VSTM (Vogel & Machizawa, 2004), rather than a second, or sustained, N2pc when there were two sequential stimuli. More work will be required to confirm this hypothesis. Finally, even if our speculations concerning the SPCN failed to stand the test of time, the fact that both the N2pc and the initial phase of the SPCN had the same mean amplitude across the two masking conditions supports our hypothesis that masking did not strongly modulate the N2pc, at least in the usual time window for this component.

We find the differences in the duration of the SPCN across conditions to be particularly interesting and suggestive of differential durations of retention in VSTM. Based on present results and others in recent work (Jolicoeur et al., in press a, b; Perron et al., 2005), we suggest that the SPCN likely reflects the passage through VSTM of the representations of the stimuli selected for further processing by visual-spatial attention. Furthermore, the duration of the SPCN is consistent with the reaction time measured for the task, perhaps reflecting a longer retention time of the stimuli in VSTM in the backward-masking condition. The similarity of the scalp distributions observed in the N2pc and early SPCN time windows suggests the possibility that the same neural tissue may be performing different functions at different times. The initial response could reflect target enhancement, distractor suppression, or perhaps the initial encoding of information into VSTM, whereas the same cells could later participate in a sustained response required to maintain a representation in VSTM. The notion that a given cell can participate in different psychological functions at different times has been elegantly demonstrated for cells in early visual cortex (Lamme & Roelfsema, 2000). The present results suggest that something similar may be taking place fur-

ther in the visual system where circuits for the attentional selection and encoding of stimuli may be implemented using the same neural tissue that is later used for the maintenance of information in VSTM. In any case, we believe that future study of the SPCN will likely provide a powerful tool to study the neural fate of information selected for further processing in complex cognitive tasks.

References

- Breitmeyer, B. (1984). *Visual masking: An integrative approach*. New York: Oxford University Press.
- Chun, M., & Potter, M. C. (1995). A two-stage model for multiple target detection in rapid serial visual presentation. *Journal of Experimental Psychology: Human Perception & Performance*, *21*(1), 109-127.
- Dell'Acqua, R., Jolicoeur, P., Pesciarelli, F., Job, R., & Palomba, D. (2003). Electrophysiological evidence of visual encoding deficits in a cross-modal attentional blink paradigm. *Psychophysiology*, *40*, 629-639.
- Donchin, E. (1981). Surprise!... Surprise? *Psychophysiology*, *18*, 493-513.
- Donchin, E., & Coles, M. G. H. (1988). Is the P300 component a manifestation of context updating? *Behavioral & Brain Sciences*, *11*, 357-374.
- Eimer, M. (1996). The N2pc component as an indicator of attentional selectivity. *Electroencephalography and Clinical Neurophysiology*, *99*, 225-234.
- Enns, J. T., & Di Lollo, V. (1997). Object substitution: A new form of masking in unattended visual locations. *Psychological Science*, *8*(2) 135-139.
- Giesbrecht, B., & Di Lollo, V. (1998). Beyond the attentional blink: Visual masking by object substitution. *Journal of Experimental Psychology: Human Perception & Performance*, *24*(5), 1454-1466.
- Hopf, J. M., Luck, S. J., Girelli, M., Hagner, T., Mangun, G. R., Scheich, H., et al. (2000). Neural sources of focused attention in visual search. *Cerebral Cortex*, *10*(12), 1233-1241.
- Jolicoeur, P. (1998). Modulation of the attentional blink by on-line response selection: Evidence from speeded and unspeeded Task1 decisions. *Memory & Cognition*, *26*, 1014-1032.
- Jolicoeur, P. (1999a). Concurrent response selection demands modulate the attentional blink. *Journal of Experimental Psychology: Human Perception and Performance*, *25*, 1097-1113.
- Jolicoeur, P. (1999b). Dual-task interference and visual encoding. *Journal of Experimental Psychology: Human Perception and Performance*, *25*, 596-616.
- Jolicoeur, P., & Dell'Acqua, R. (1998). The demonstration of short-term consolidation. *Cognitive Psychology*, *36*, 138-202.
- Jolicoeur, P., Sessa, P., Dell'acqua, R., & Robitaille, N. (in press a). On the control of visual spatial attention: Evidence from human electrophysiology. *Psychological Research*.
- Jolicoeur, P., Sessa, P., Dell'acqua, R., & Robitaille, N. (in press b). Attentional control and capture in the attentional blink paradigm: Evidence from human electrophysiology. *European Journal of Cognitive Psychology*.
- Lamme, V. A. F., & Roelfsema, P. R. (2000). The distinct modes of vision offered by feedforward and recurrent processing. *Trends in Neuroscience*, *23*, 571-579.
- Lins, O. G., Picton, T. W., Berg, P., & Scherg, M. (1993). Ocular artifacts in EEG and event-related potentials I: Scalp topography. *Brain Topography*, *6*, 51-63.
- Luck, S. J. (1998). Sources of dual-task interference: Evidence from human electrophysiology. *Psychological Science*, *9*, 223-227.
- Luck, S. J., Girelli, M., McDermott, M. T., & Ford, M. A. (1997). Bridging the gap between monkey neurophysiology and human perception: An ambiguity resolution theory of visual selective attention. *Cognitive Psychology*, *33*(1), 64-87.
- Luck, S. J., & Hillyard, S. A. (1994a). Electrophysiological correlates of feature analysis during visual search. *Psychophysiology*, *31*(3), 291-308.
- Luck, S. J., & Hillyard, S. A. (1994b). Spatial filtering during visual search: Evidence from human electrophysiology. *Journal of Experimental Psychology: Human Perception and Performance*, *20*(5), 1000-1014.
- Masson, M. E., & Loftus, G. R. (2003). Using confidence intervals for graphically based data interpretation. *Canadian Journal of Experimental Psychology*, *57*(3), 203-220.
- Miller, J., Patterson, T., & Ulrich, R. (1998). Jackknife-based method for measuring LRP onset latency differences. *Psychophysiology*, *35*, 99-115.
- Perron, R., Brisson, B., Robitaille, N., & Jolicoeur, P. (2005). Dissociating N2pc and SPCN. *15th annual meeting of the Canadian Society for Brain, Behaviour and Cognitive Science/Société Canadienne des Sciences du Cerveau, du Comportement et de la Cognition*, Montréal, QC.
- Raymond, J. E., Shapiro, K L., & Arnell, K M., (1992). Temporary suppression of visual processing in an RSVP task: An attentional blink? *Journal of Experimental Psychology: Human Perception and Performance*, *18*(3), 849-860.
- Robitaille, N., & Jolicoeur, P. (2005). *Dissociating target onset from selection cue onset: Effects on the onset of the N2pc*. Manuscript in preparation.
- Vogel, E. K., & Luck, S. J. (2002). Delayed working memory consolidation during the attentional blink. *Psychonomic Bulletin & Review*, *9*, 739-743.
- Vogel, E. K., Luck, S. J., & Shapiro, K. L. (1998). Electrophysiological evidence for a postperceptual locus

- of suppression during the attentional blink. *Journal of Experimental Psychology: Human Perception and Performance*, 24, 1656-1674.
- Van Selst M., & Jolicoeur, P. (1994). A solution to the effect of sample size on outlier elimination. *Quarterly Journal of Experimental Psychology: Human Experimental Psychology*, 47A, 631-650.
- Vogel, E. K., & Machizawa, M. G. (2004). Neural activity predicts individual differences in visual working memory capacity. *Nature*, 458, 748-751.
- Woodman, G. F., & Luck, S. J. (2003a). Dissociations among attention, perception, and awareness during object-substitution masking. *Psychological Science*, 14(6), 605-611.
- Woodman, G. F., & Luck, S. J. (2003b). Serial deployment of attention during visual search. *Journal of Experimental Psychology: Human Perception and Performance*, 29(1), 121-138.
- Wyszecki, G., & Stiles, W. S. (1982). *Color science: Concepts and methods, quantitative data and formulae* (2nd Ed.). New York: John Wiley & Sons.

Sommaire

Le masquage est un outil utilisé dans plusieurs paradigmes de recherche étudiant l'appareil cognitif humain. Habituellement, le masquage consiste à augmenter le niveau de difficulté perceptuelle d'un item visuel en présentant un deuxième item, dans des conditions de très grande proximité spatiale et temporelle. La N2PC est une composante des potentiels évoqués visuels (PEV) fréquemment utilisée afin d'étudier le déploiement de l'attention visuo-spatiale. Elle consiste en une plus grande négativité dans l'hémisphère controlatérale que dans l'hémisphère ipsilatérale à une cible visuelle. Un distracteur visuel est présenté simultanément à l'hémisphère ipsilatérale. Puisque la cible et le distracteur sont visuellement équivalents, cette différence peut donc être interprétée comme reflétant la sélection et/ou le traitement de la cible. Le but de cet article est de découvrir les effets du masquage sur la N2PC. Deux stimuli étaient présentés sur l'écran, à droite et à gauche du point de fixation. Les participants devaient rapporter l'identité de l'un d'entre eux, le plus rapidement possible, tout en faisant le moins d'erreur possible. La cible pouvait être identifiée à la fois par la catégorie (lettre vs chiffre) ainsi que par la couleur (rose vs vert). Un masquage rétroactif a été produit en présentant une deuxième paire de stimuli bilatéraux (de même couleur et de même catégorie que le stimulus présentés au même endroit) immédiatement après la disparition de la première. Le deuxième ensemble de stimuli agissait donc comme un masque par motif pour le premier. Dans une seconde condition, un masquage proactif a été produit en utilisant les mêmes stimuli que

pour le masquage rétroactif, mais en demandant aux participants de rapporter l'identité du deuxième stimulus de la séquence plutôt que du premier. Dans ce cas, le premier stimulus agit comme un masque par motif pour le deuxième stimulus. Enfin, des essais sans masque ont également été présentés aux participants, afin de servir de condition contrôle. Les essais avec masquage proactif ont engendré un temps de réaction plus long que les essais sans masquage. Les essais avec masquage rétroactif ont engendré un temps de réaction plus long encore, ainsi qu'un taux d'erreurs plus élevé. Ces résultats indiquent que la séquence de stimuli utilisée a créé les effets de masquage escompté. Par contre, bien que les différentes conditions de masquage aient clairement produit des patrons de performance comportementale différents, la N2PC était identique pour toutes les conditions. Ce résultat suggère que le déplacement de l'attention visuo-spatiale en soi n'était pas affecté par le masquage. Une négativité soutenue, controlatérale et postérieure (SPCN, *sustained posterior contralateral negativity*), a également été observée. Cette composante avait une distribution spatiale semblable à la N2PC et commençait 300 ms après l'apparition des stimuli. Son amplitude était fortement modulée par le nombre de stimuli présentés de chaque côté (un dans la condition sans masque, deux dans les autres conditions), tandis que sa durée était plus grande lorsque les temps de réactions moyens observés étaient plus longs. Nous posons l'hypothèse que la SPCN reflète l'activité neuronale associée au passage de l'information en mémoire visuelle à court terme.

Effect of cue–target interval on the N2pc

Nicolas Robitaille and Pierre Jolicœur

Centre for Research in Neuropsychology and Cognition, Department of Psychology, University of Montreal, Montreal, Quebec, Canada

Correspondence and requests for reprints to Nicolas Robitaille, Centre de Recherche en Neuropsychologie et Cognition, Département de Psychologie, Université de Montréal, Montréal, Québec, Canada
Tel: + 1 514 343 6111 ext. 2631; fax: + 1 514 343 5787; e-mail: [REDACTED]

Sponsorship: This research was supported by a grant from the Natural Sciences and Engineering Research Council of Canada (CRSNG), by the Canada Research Chairs Program, by support from l'Université de Montréal, and le Centre de Recherche en Neuropsychologie et Cognition to Pierre Jolicœur and by a postgraduate scholarship from NSERC to Nicolas Robitaille.

Received 7 July 2006; accepted 14 July 2006

The N2pc component of the event-related potential occurs when participants must select and process a lateralized visual target, often in the presence of one or more distractors. The goal of this research was to determine whether the N2pc reflects unique processing related to the treatment of the target or whether it reflects processing related to the presence of a distractor. The selection cue for the target was presented 100 ms earlier, at the

same time as, or 100 ms later than the target itself. An earlier cue allowed earlier spatial selection, leading to less interference from the distractor. The results indicated that the offset of the N2pc was delayed when more interference from the distractor was expected. *NeuroReport* 17:1655–1658 © 2006 Lippincott Williams & Wilkins.

Keywords: discrimination, event-related potential, flanker effects, N2pc, spatial selection

Introduction

The N2pc is a component of the event-related potential that indexes the deployment of attention across visual space [1]. It consists of a larger negativity over the hemisphere contralateral to a visual target compared with the voltage over the ipsilateral hemisphere. This lateralized event-related potential component often occurs approximately in the N2 time range (180–280 ms) and is observed at posterior electrode sites, which led Luck and Hillyard [1] to name the component N2pc (pc for posterior contralateral). Most experiments use bilateral stimuli designed to create equal stimulus-driven responses from the two visual fields, and hence the N2pc reflects purely attentional processes acting differentially in the hemisphere contralateral to a visual target compared with the hemisphere ipsilateral to the target. The systematic differential inter-hemispheric response in the visual cortex [2,3] contingent on the location of a target in visual space makes the N2pc a useful tool in the study of visual spatial attention [4–10].

In previous experiments designed to observe the N2pc, the selection cue and the target have been part of the same stimulus. For example, the cue could be the colour of the stimulus (e.g. red), and the task to make a discriminative response based on the shape of the stimulus (e.g. vertical vs. horizontal). The goal of the present study was to test whether the deployment of attention, as measured by the N2pc, would be equivalent if spatial attention could be deployed at a slightly different time relative to the onset of the target. We devised a paradigm in which we separated the selection cue from the stimuli (target and distractor),

which allowed us to present them at different times, instead of always simultaneously (see Fig. 1).

One interpretation of the N2pc is that it could reflect solely the deployment of attention per se, without reflecting further processing of the stimuli. This interpretation predicts an absence of differences in the N2pc waveforms according to our manipulations. The information used to deploy attention is exactly the same in each condition.

It is possible, however, that the N2pc also reflects the effect of attention on the processing of the target, which would be enhanced relative to processing of the distractor. Chronometric studies have shown that spatial cueing can lead to faster target processing, even in sparse visual displays [11]. According to this hypothesis, presenting the cue before the target should allow the spatial attention to move earlier to the target location. Spatial attention, however, would have to wait for the target to be presented in order to engage processing mechanisms on the target. Consequently, the N2pc would begin at the same time, but it would last 100 ms relative to the simultaneous cue condition. Conversely, presenting the selection cue after presenting the target should produce a shorter N2pc, because the target would already be present and stable as soon as attention could engage on it.

The N2pc could also reflect a process related to the interference caused by the presence of a distractor. Shiu and Pashler [12] found that an invalid spatial cue increased the identification error percentage, but only when multiple locations were occupied by distractors. In their single location condition, no effects of cueing were observed. Luck and Hillyard [1] and Luck *et al.* [13] have shown that, under

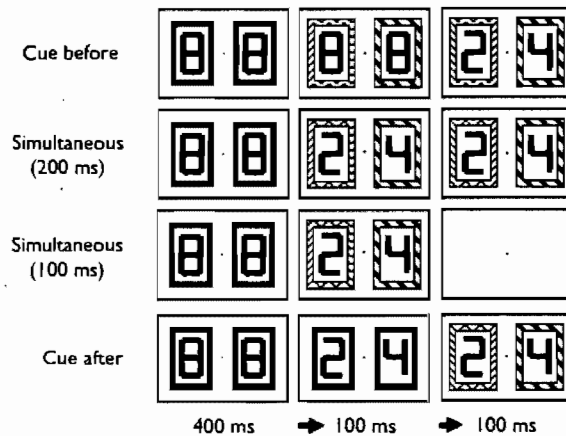


Fig. 1 Experimental conditions. The target and distractors were digits created by removing segments from an initial figure-8 pattern. The selection cue was a red (for half of the participants) or green (for the other half) frame presented around the digits. Red and green are represented here by different textures (which were not present in the actual experiment).

some conditions, adding distractors to the visual display increases the amplitude of the N2pc. Together with several other findings [1], this finding has been used to support the hypothesis that the N2pc is an electrophysiological manifestation of a distractor-suppression mechanism. Furthermore, Yantis and Johnston [14] demonstrated that pre-cuing the location of a target reduced the interference from distractors in the flanker paradigm [15,16]. Flanker interference is commonly assumed to reflect a conflict in response selection. Taken together, these results suggest that spatial attention can mediate the interference caused by distractors at different processing levels [17]. Accordingly, the N2pc should be larger when the colour-cue is presented after the target-distractor display, because the distractor would have time to activate corresponding representations in memory, later creating greater opportunity for interference with target processing. Conversely, the N2pc should be smaller when the selection cue is presented before the target, because spatial attention would start to act earlier, and thus reduce or prevent processing of the distractor, which would reduce the potential for distractor interference.

Participants

Seven volunteers, four women, aged between 19 and 29 years, were paid for their participation. They reported no neurological problems, and had normal or corrected-to-normal vision and normal color vision. We obtained informed consent from each participant at the beginning of the experiment. The procedure was vetted by the appropriate ethics committee at Université de Montréal.

Stimuli and procedure

The stimuli were presented on a 17-inch colour cathode-ray tube driven by a microcomputer running MEL 2.01 software [18]. Study participants were seated in a dimly lit electrically shielded room. The stimuli were presented on a near-black background (1.1 cd/m^2). The cue consisted of two outline rectangles (3.6° high and 2.4° wide), centered 3.6° left and

right of the fixation point. The rectangles were initially grey (21.1 cd/m^2). One turned pink (21.8 cd/m^2) and the other turned green (21.3 cd/m^2). A target colour was assigned to each participant for the whole experiment. The target and distractor were digits (2.4° high and 1.2° wide) taken from the set {1, 2, 3, 4}. Initially, a grey figure-8 was in the center of each rectangle. These figure-8s were composed of seven straight lines of equal length. The target digit (1, 2, 3, or 4) and a distractor digit were created by removing appropriate lines from each figure-8. The task of the participants was to report the identity of the digit located in the rectangle of the target color. The target was located in the left visual field on 50% of the trials and in the right visual field on 50% of the trials, randomly varied from trial to trial. The identity of the target digit was reported using four adjacent keyboard keys using fingers of the right hand. Participants were instructed to respond as fast as possible while making as few errors as possible.

Each trial began with a fixation and feedback symbol at the center of the display, indicating whether the previous answer was correct (+) or incorrect (-). The participant started each trial by pressing the space bar. The fixation/feedback symbol was then replaced by a small fixation point. The two grey figure-8s, each surrounded by a grey rectangle, appeared on the screen for 400 ms. In the 'cue before' condition, the cue occurred first (change of color of the rectangles), followed 100 ms later by the appearance of the digits (Fig. 1). The target and distractor digits and the cue remained on the screen together for 100 ms. In the 'simultaneous' condition, both the cue and the digits appeared simultaneously. All remained on the screen for 100 or 200 ms (randomly varied with equal probability). In the 'cue after' condition, the target and distractor digits appeared first, followed 100 ms later by the cue. The cue remained on the screen for 100 ms, together with the digits. The fixation dot remained on the screen until the response. The next trial began after a short interval of time (between 800 and 1000 ms, randomly selected) with a blank screen. Each participant performed one practice block of 24 trials, followed by 10 blocks of 72 trials. Each block was followed by a pause of 10 s or more. The three conditions were randomly intermixed within each block.

Electrophysiological recordings and analysis

The recordings were made with a BioSemi Active-two system (BioSemi Inc., Amsterdam, The Netherlands), with 64 active Ag-AgCl scalp electrodes positioned using the extended International 10-20 System. The electroencephalogram was algebraically re-referenced to the average of the left and right mastoids. The signals were amplified, filtered (low-pass cut-off at 67 Hz) and digitized at 256 Hz. Trials with eye blinks and eye movement were removed during post-recording analysis (see [19] for details of the procedure). Furthermore, if data from an electrode contained a recording artefact (a deviation of more than $100 \mu\text{V}$ over 200 ms) during a trial, this trial was removed from the average for this electrode. In addition, only the trials with a correct response were analysed. Overall, 82.2% of the trials were included in the analysis.

Average waveforms were computed for each scalp electrode site for each condition, with a 200-ms pre-stimulus baseline and a 500-ms post-stimulus interval relative to the onset of the selection cue. The epochs were baseline

Table 1 Behavioural results

Selection cue	Accuracy (%)	Reaction time (ms)
Before	96.2	660
Simultaneous	96.0	684
After	93.9	667

corrected on the basis of the mean activity during the 200-ms pre-stimulus interval. A pool of posterior electrodes in the region where the N2pc is usually observed was used, to increase the stability of the N2pc waveforms. The formula [(left electrode when the target was on the right + right electrode when the target was on the left) - (left electrode when the target was on the left + right electrode when the target was on the right)] was used to calculate the N2pc waveform for each lateralized electrode pair. In the resulting waveform, a negative deflection corresponds to a greater negativity over the hemisphere contralateral to the target. The latency of the onset and the offset of the N2pc were estimated using a jackknife procedure [20].

Results

Behaviour

The mean accuracy and response time in each condition are listed in Table 1. An analysis of variance treating conditions as within-subjects factors revealed a significant difference in accuracy between conditions [$F(2,12) = 5.51$, $MSE = 0.00019$, $P < 0.02$]. Accuracy was lower in the cue-after condition than in the other conditions [both $F(1,6) > 5.6$, $P < 0.056$], which did not differ from each other [$F(1,6) < 1.0$]. The response times were calculated relative to the first point in time at which all the information required to make a correct response had been presented. Mean response times differed across the conditions [$F(2,12) = 13.39$, $MSE = 80.371$, $P < 0.001$]. Mean response time was longer in the simultaneous condition than in the other two conditions [both $F(1,6) > 11$, $P < 0.02$]. These latter two were not significantly different from each other [$F(1,6) = 1.55$, $MSE = 85.382$, $P > 0.24$].

Electrophysiology

The two simultaneous conditions (100 and 200 ms of total presentation) were first analysed separately. The amplitude of the N2pc (measured as the mean amplitude in the 225–275 ms time window) was significantly larger in the 200-ms duration condition than in the 100-ms condition [$F(1,6) = 9.566$, $MSE = 0.109$, $P < 0.03$]. The jackknife analysis, however, revealed no difference in the onset or the offset [both $F_s(1,6) < 1.0$] of the N2pc across these conditions. The latency of the N2pc was calculated as the first time point at which half of the maximal amplitude of the N2pc was reached, leading to latency measures relatively insensitive to changes in overall amplitude. As all further analyses relied on the difference in the latency of the N2pc, the data from these two simultaneous conditions were combined and will be referred simply as the simultaneous condition.

The N2pc waveforms obtained for the three main experimental conditions are shown in Fig. 2. Time 0 for these curves corresponds to the onset of the selection cue. It can be seen that a negative deflection starts at about 160 ms

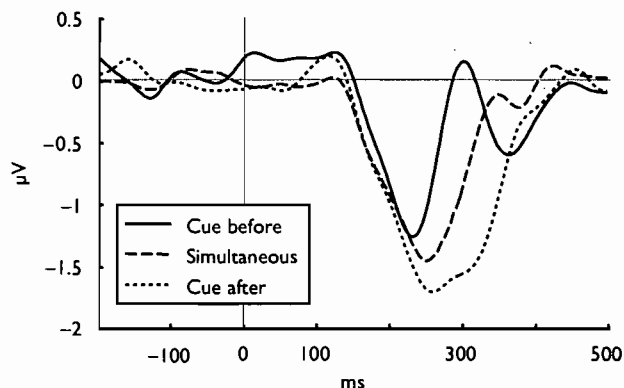


Fig. 2 N2pc waveform for the three conditions (the two simultaneous conditions were averaged, see text for details).

for every condition. A jackknife analysis revealed no significant differences in the onset of the N2pc component across conditions [$F(2,12) < 1.0$]. (The jackknives procedure was heavily tested in the context of the LRP waveform [20], which has a different topography, timing and shape than the N2pc. Consequently, this null effect needs to be interpreted with caution. The latency differences for the three conditions in this analysis are within a 12 ms window, however, indicating that even if systematic differences were present, their small magnitude makes them negligible.)

The offsets of the N2pc waveforms, however, were clearly different across conditions. The N2pc in the cue-before condition returned to the baseline first, followed by the N2pc in the simultaneous condition, and then by the N2pc in the cue-after condition. The second component (peak at about 370 ms) in the cue-before conditions was due to only one participant, and thus was not significantly different from zero and is therefore considered to be experimental noise. A jackknife analysis indicated a significant difference in the offsets of the N2pc across conditions [$F(2,12) = 18.76$, $MSE = 728$, $P < 0.0002$]. Subsequent analyses revealed significant differences between all pairs of waveforms [all $F_s(1,6) > 6$, all $P_s < 0.05$].

Visual inspection of the grand average N2pc waveforms suggests that the amplitude of the N2pc also varied across conditions. A statistical analysis, however, did not corroborate this impression. We identified the peak of the N2pc for each condition for each participant. We then used a 20 ms window (10 ms before the peak to 10 ms after the peak) and measured the mean amplitude in this window. No significant difference in amplitude was found across the three conditions [$F(2,12) = 2.25$, $MSE = 0.223$, $P > 0.14$].

The pattern of results indicates that it is very unlikely that the amplitude of the N2pc was smaller in the cue-after condition and bigger in the cue-before condition. Thus, the delay in the offset of the N2pc could not be explained by smearing of the component owing to latency jitter in the onset of the component.

Discussion

The goal of the study was to examine the effects of variations in the temporal relationship between the presentation of a spatial selection cue and the presentation of

target and distractor information (i.e. cue–target asynchrony). The electrophysiological results were very clear. As can be seen in Fig. 2, all conditions caused a well behaved N2pc component that was time-locked to the onset of the colour selection cue. No effect of the cue–target asynchrony on the onset of the N2pc was observed. In contrast, the duration (and offset latency) of the N2pc was affected by the cue–target asynchrony. Taking the simultaneous condition as a baseline, the N2pc had a longer duration when the cue was presented after the digits, whereas the N2pc had a shorter duration when the cue was presented before the digits.

The common onset time of the N2pc in all conditions suggests that the N2pc must at least reflect the initial deployment of attention, independently of target processing. The differences in the offset latency of the N2pc, however, indicate that the N2pc likely reflects more than the movement of attention per se. What information is presented, and when, also influences the N2pc. We interpret these results as reflecting different degrees of interference from the distractor, with more interference when the digits appeared before the selection cue. More interference should occur in this case than in the simultaneous condition in which attention can be directed to the correct digit earlier, because there is a greater probability that the distractor digit will be processed to some degree. Less interference should be observed when the cue occurs before the digits (relative to the simultaneous condition) because this latter condition should minimize the amount of distractor processing and give target processing a head start.

Conclusion

The onset of the N2pc was tightly time-locked to the onset of the information required to select a visual target, regardless of when the target was actually presented (within a ± 100 ms window). The duration of the N2pc, however, was shorter when the interference from the distractor was reduced, and was longer when the interference from the distractor increased. What is clear is that the state of the information to be processed (target/distractor) influenced the duration of the N2pc, and this in turn suggests that the N2pc must reflect the process that takes place beyond the initial shift of visual–spatial attention. Although we are arguing that greater interference from the distractor leads to a longer N2pc, we are not arguing that the N2pc necessarily reflects a process of distractor suppression. It is also possible to overcome distractor interference by a process of target enhancement.

Acknowledgements

We thank Manon Robert, Nathalie Bouloute, Émilie Leblanc, Catherine Ouimet, Émilie-Maude Chantelois and Alexia Pitto for technical assistance.

References

1. Luck SJ, Hillyard SA. Spatial filtering during visual search: evidence from human electrophysiology. *J Exp Psychol Hum Percept Perform* 1994; **20**:1000–1014.
2. Hopf JM, Luck SJ, Girelli M, Hagner T, Mangun GR, Scheich H, et al. Neural sources of focused attention in visual search. *Cereb Cortex* 2000; **10**:1233–1241.
3. Hopf JM, Boelmans K, Schoenfeld AM, Heinze HJ, Luck SJ. How does attention attenuate target–distractor interference in vision? Evidence from magnetoencephalographic recordings. *Brain Res Cogn Brain Res* 2002; **15**:17–29.
4. Woodman GF, Luck SJ. Electrophysiological measurement of rapid shifts of attention during visual search. *Nature* 1999; **400**:867–869.
5. Woodman GF, Luck SJ. Serial deployment of attention during visual search. *J Exp Psychol Hum Percept Perform* 2003; **29**:121–138.
6. Eimer M. The N2pc component as an indicator of attentional selectivity. *Electroencephalogr Clin Neurophysiol* 1996; **99**:225–234.
7. Jolicoeur P, Sessa P, Dell'acqua R, Robitaille N. On the control of visual spatial attention: evidence from human electrophysiology. *Psychol Res* [Epub ahead of print 24 September 2005].
8. Jolicoeur P, Sessa P, Dell'acqua R, Robitaille N. Attentional control and capture in the attentional blink paradigm: evidence from human electrophysiology. *Eur J Cogn Psychol* 2006; **18**:560–578.
9. West R, Wymbs N. Is detecting prospective cues the same as selecting targets? An ERP study. *Cogn Affect Behav Neurosci* 2004; **4**:354–363.
10. Girelli M, Luck S. Are the same attentional mechanisms used to detect visual search targets defined by color, orientation, and motion? *J Cogn Neurosci* 1997; **9**:238–253.
11. Posner MI. Orienting of attention. *Q J Exp Psychol* 1980; **32**:3–25.
12. Shiu L, Pashler H. Negligible effect of spatial precuing on identification of single digits. *J Exp Psychol Hum Percept Perform* 1994; **20**:1037–1054.
13. Luck SJ, Girelli M, McDermott MT, Ford MA. Bridging the gap between monkey neurophysiology and human perception: an ambiguity resolution theory of visual selective attention. *Cogn Psychol* 1997; **33**:64–87.
14. Yantis S, Johnston JC. On the locus of visual selection: evidence from focused attention tasks. *J Exp Psychol Hum Percept Perform* 1990; **16**:135–149.
15. Eriksen BA, Eriksen CW. Effects of noise letters upon the identification of a target letter in a nonsearch task. *Percept Psychophys* 1974; **40**:225–240.
16. Eriksen CW. The flankers task and response competition: a useful tool for investigating a variety of cognitive problems. *Vis Cogn* 1995; **2**:101–118.
17. Feintuch U, Cohen A. Visual attention and coactivation of response decisions for features from different dimensions. *Psychol Sci* 2002; **13**:361–369.
18. Schneider W. Micro experimental laboratory: an integrated system for IBM – PC compatibles. *Behav Res Methods Instrum Comput* 1988; **20**:206–217.
19. Robitaille N, Jolicoeur P. Fundamental properties of the N2pc as an index of spatial attention: effects of masking. *Can J Exp Psychol* 2006; **60**:79–89.
20. Ulrich R, Miller JP. Using the jackknife-based scoring method for measuring LRP onset effects in factorial designs. *Psychophysiology* 2001; **38**:816–827.



ELSEVIER

available at www.sciencedirect.com
www.elsevier.com/locate/brainres

**BRAIN
RESEARCH**

Research Report

Short-term consolidation of visual patterns interferes with visuo-spatial attention: Converging evidence from human electrophysiology

Nicolas Robitaille^{a,*}, Pierre Jolicœur^a, Roberto Dell'Acqua^b, Paola Sessa^b^aCentre de Recherche en Neuropsychologie et Cognition, Département de Psychologie, Université de Montréal, Montréal, Québec, Canada^bCognition and Language Laboratory, Department of Developmental Psychology, University of Padova, Padova, Italy

ARTICLE INFO

Article history:

Accepted 4 September 2007

Available online 14 September 2007

Keywords:

Spatial attention

N2pc

P3

Attentional blink

ABSTRACT

In order to investigate the interplay between visuo-spatial attention and central attention, we varied the relative probability (25% vs. 75%) of the responses to lateralized targets in an attentional blink paradigm. When the first target was associated with a less probable response, we observed a larger attentional blink, that is, a general reduction in accuracy for the second target. The efficiency of deployment of spatial attention to the second target was also reduced as a function of the response frequency for the first target. Both the N2pc, an event-related potential (ERP) associated with the deployment of attention in visual space, and the SPCN (sustained posterior contralateral negativity), an ERP associated with the maintenance of information in visual short-term memory, time-locked to T2 were significantly reduced when the first target was associated with a less frequent response. Furthermore, the P3 ERP to T2 was abolished when the response to T1 was rare but not when it was frequent. The results show that the association of T1 to either a rare or frequent response causes significant interference with the deployment of visual spatial attention to T2; and with the short-term consolidation of T2 into visual short-term memory.

© 2007 Elsevier B.V. All rights reserved.


1. General introduction

The attentional blink (AB) is a phenomenon typically observed when two briefly presented and masked visual targets, each requiring some form of delayed response, are presented at short stimulus-onset asynchronies (SOAs). The AB consists in a lower probability of correct report of the second target (T2) while the first target (T1) is generally reported successfully (Raymond et al., 1992). A generally accepted view by researchers in this domain is that the AB arises from limitations at a post-perceptual stage of processing of T2. Such limitations would prevent a modality-dependent, perceptual representa-

tion of T2 from being consolidated in visual short-term memory (VSTM; Chun and Potter, 1995; Jolicœur, 1998; Shapiro et al., 1994; Vogel et al., 1998).

The idea of a post-perceptual locus of the AB has received solid support in studies using the event-related potential (ERP) technique. Vogel et al. (1998), for instance, used ERPs to monitor various aspects of the processing of T2 during the AB interval. In a series of rapid serial visual presentation (RSVP) designs, several factors tapping distinct stages of T2 processing were examined as potential causes of the AB. The results documented the preservation of the T2-locked ERP components up to and including the N400 (e.g., P1 and N1 components) at short SOAs,

* Corresponding author. Psychology Department, University of Montreal, Pavillon Marie-Victorin, 90, Vincent d'Indy, Local D-418, Montréal, Québec, Canada H2V 2S9. Fax: +1 514 343 5787.

E-mail address 

suggesting that the AB did not interfere with stages of T2 processing that included the generation of a semantic code for T2 (see also Potter et al., 2005; Rolke et al., 2001; Visser et al., 2005). In contrast, Vogel et al. (1998) found that the amplitude of the T2-locked P3 component was markedly reduced at short SOAs (during the AB), with the P3 component returning to a normal amplitude when T2 was displayed outside the AB (see also Dell'Acqua et al., 2003a,b; Krancioch et al., 2003), or when T1 could be ignored (Sessa et al., 2007).

The nature of the functional processes reflected in the P3 component is not clear as of yet. Several researchers tend to regard the P3 as related to the decision on how to classify and respond to an eliciting stimulus (e.g., Squires et al., 1973, 1977; Verleger et al., 2005). Others maintain that the P3 reflects access of the eliciting stimulus to global mental workspace, with this access making the event conscious and therefore reportable (Dehaene et al., 2003; Koivisto and Revonsuo, 2003; Sergent et al., 2005). Probably the most influential and popular line of thinking is that linking the P3 to updating of working memory (Donchin and Coles, 1988; Johnson, 1993; Polich and Criado, 2006). Suppression of P3 in the AB would be interpreted by the first view as mere reflection of the fact that no decision could be reached about T2, by the second view as reflecting the failure of T2 to enter global mental workspace, and by the third view as reflecting the failure of T2 to be encoded in visual working memory. For the present purposes, it is important to note that all notions mentioned above are convergent with the idea that the P3 is a direct reflection of functional activity occurring once a visual stimulus has already been processed at a sensory/perceptual stage. In this particular perspective, the notions about the P3 are also convergent with AB models positing a post-perceptual 'bottleneck' along the flow of processing leading to encode T2 in VSTM (Chun and Potter, 1995; Jolicoeur and Dell'Acqua, 1998). There are, however, slight differences among the P3 models as to what exactly would be the cause of the P3 modulation observed during the AB. While indeed the former two notions imply that P3 suppression reflects the consequences of such bottleneck, the memory-updating notion implies that P3 suppression reflects just this bottleneck. Specifically, when the consolidation stage hypothesized to transfer target information in VSTM is occupied with processing T1, consolidation of T2 is postponed, and T2 remains temporarily in a stand-by state during which it is vulnerable to corruption by items trailing T2 in the RSVP stream (Chun and Potter, 1995; Dell'Acqua et al., 2003a,b; Giesbrecht and Di Lollo, 1998; Jolicoeur, 1999a).

A further important application of the ERP technique in the AB context has been useful to illuminate the impact of the AB on the efficiency of the control of visual spatial attention. The logic behind these studies was that of presenting a lateralized T2 during the AB, and tracking the displacement of spatial attention to T2 through the monitoring of a component of the ERP to T2 labeled N2pc. The N2pc consists in a greater negativity, starting about 180 ms after the onset of a visual display, over the posterior hemisphere contralateral to an attended visual target, relative to analogous regions of the hemisphere ipsilateral to the target (Eimer, 1996; Luck and Hillyard, 1994; Woodman and Luck, 2003). In general, a reduction in the amplitude of the N2pc indicates either an absolute reduction in attention allocation, or a reduction in the differential alloca-

tion of visual spatial attention to a target (relative to attention allocated to the opposite visual field), or both.

Jolicoeur et al. (2006a,b) used two distinct experimental manipulations in order to measure the N2pc to a T2 that was subject to the AB influence. The authors varied the SOA between a centrally displayed T1 and a lateralized T2. At an SOA of 200 ms, a reduction of the amplitude of the N2pc was observed relative to a control condition in which T2 was presented at an SOA of 800 ms. A second manipulation involved the task performed on a centrally displayed T1 under conditions in which the SOA between T1 and the lateralized T2 was fixed at 200 ms. On half of the trials, the subjects had to encode T1 for delayed report, whereas T1 could be ignored in the remaining trials. This was achieved by dividing the experiment into two blocks, one during which the subject was instructed to report both targets, the other in which the subject was instructed to report only the last target. When T1 had to be reported, a reduction of the amplitude of the N2pc was observed relative to a control condition in which T1 could be ignored. Based on these results, Jolicoeur et al. (2006a,b) concluded that the consolidation of T1 was likely to interfere with the deployment of spatial attention to the position occupied by T2, with the consequent difficulty to encode T2 in VSTM.

The conclusions of Jolicoeur et al. (2006a,b) could, however, be questioned based on details of the design that allowed for different interpretations of the results. Specifically, T1 was presented centrally, whereas T2 was lateralized. One could argue that processing of T1 demanded an initial state of attention focused at the center of the screen, where T1 was displayed throughout the experiment. If this were so, it is reasonable to assume that allocating attention to a lateralized T2 required a disengagement of visual spatial attention from the center of the screen and a shift to the location of T2. In this optic, the N2pc was reduced during the AB because there was less time, at the short SOA, to allow spatial attention to disengage from the position occupied by T1 and shift to the lateralized T2 relative to a condition with a long delay between T1 and T2.

An alternative explanation can also be raised for the second control condition used by Jolicoeur et al. (2006a,b). It is of note that trials in which T1 was to be encoded and trials in which T1 could be ignored were blocked. The criticism in this case would be that in blocks of trials where the subject knew in advance that T1 could be ignored, subjects were likely not to engage at all their visual spatial attention on the centrally displayed T1, in contrast with the blocks of trials where T1 had to be reported.

An attempt to solve these problems was made by Dell'Acqua et al. (2006) by using two synchronized RSVP streams of letters, one on each side of a central fixation point. In the condition of most interest in the present context, T1 consisted of a pair of simultaneously presented digits, each embedded in one of the lateralized RSVP streams. The task was to determine if the digits were the same or different. T1 could also consist of a pair of "=" signs. In those trials, subjects were instructed to ignore T1. This condition was designed to address one of the concerns mentioned previously, namely the potential discrepancy in attentional state demanded by processing T1 and T2. The subjects did not know in advance if T1 was to be processed deeply (digits) or not ("=" signs), so they presumably expanded their spatial attention so as to cover

both positions occupied by the two lateralized RSVP streams on every trial. T2, which was displayed at an SOA fixed at 250 ms, consisted of a pair of squares that each had a small gap on one of the sides. These squares were followed by masking patterns. The squares were displayed one in green and one in red, and subjects were instructed to attend selectively to only one of the squares based on a specific color in order to be able to locate the gap position (responding 'top, bottom, left or right' with no speed pressure at the end of the trial). Consistent with the results obtained by Jolicoeur et al. (2006a,b), the results of Dell'Acqua et al. (2006) showed a marked reduction both in accuracy of T2 report and in the amplitude of the N2pc to T2 in trials in which the T1 digits had to be encoded relative to trials in which the T1 "=" signs could be ignored.

Although the results of Dell'Acqua et al. (2006) helped to rule out a different initial attentional state in the processing of T1 and T2 as a potential explanation of the reduction in the N2pc amplitude found when the post-perceptual processing load was increased (i.e., under AB conditions), their interpretation is, however, not devoid of problems. The pair of "=" signs had some critical differences with the digit pairs used for T1. These stimuli were neither letters nor digits, so they were presumably easier to identify based on low-level features. The "=" signs were present on half of the trials, so they were more likely to appear than any of the digits in the context of the experiment. Furthermore, a T1 made of "=" signs was consistently composed of two identical stimuli whereas a T1 composed of digits was only an identical pair on half of the T1-digit trials. In this vein, a potential criticism might be that the ERP effects described by Dell'Acqua et al. (2006) could not be interpreted solely as reflections of a limit at post-perceptual stage of processing, because the critical task differences for T1 were confounded with variations at a sensory/perceptual stage of processing T1. To complicate further the interpretation of Dell'Acqua et al.'s (2006) results, it must be noted that the task on T1 and the task on T2 were substantially different, namely, T1 was a go/no-go task based on alphanumeric visual stimuli that had to be classified as same or different on some trials and the task on T2 was a gap localization task performed on simple geometric shapes. An additional doubt may thus arise as to the influence of task switching effects that some researchers view as different from AB effects proper (e.g., Potter et al., 1998).

The present work avoided these difficulties by counterbalancing the same physical stimuli across all experimental conditions and by using the same task for Task1 and Task2. The key manipulation was the relative probability of the response associated with different (but highly similar) T1 and T2 stimuli, and this was done based on two basic considerations. Firstly, we capitalized on the earlier work of Crebolder et al. (2002), who showed that the AB is exacerbated (lower probability of report of T2) when T1 is less likely to occur relative to the AB observed for more frequent T1 stimuli. By using equivalent stimuli in all conditions (squares with a gap, differing only in the location of the gap), we ensured that different T1 stimuli required the same degree of visual processing. We used a single SOA in all conditions so the time between the disengagement of spatial attention on T1 and the appearance of T2 was always the same. Secondly, we made use of a well-established property of the P3, namely that the amplitude of the P3 is increased for stimuli associated with

less probable classifications. Monitoring of the P3 in the present empirical context was used purposely to provide electrophysiological evidence that the frequency manipulation implemented in the present design influenced post-perceptual processing mechanisms.

We used a two-event AB paradigm in which T1 and T2 were each followed by masks, but in which there were no other stimuli, as in the work of Duncan et al. (1994). In order to remove the possibility of any task-switching between T1 and T2, we used the same stimuli for T1 and T2, and the task associated with T1 and T2 was the same. Targets were empty squares with a gap on one side, followed by a mask. Four gap locations (top, bottom, left, and right) were used, each having 25% probability of occurrence. The subject had to report the location of the gap in the square. As is typical in experiments using the AB paradigm, the response was not speeded and it was performed at the end of the trials. Two response keys were used, one for one of the gap positions (e.g., top) and the other for the remaining three gap positions (i.e., not top). Consequently, each visual stimulus had the same probability of occurrence, but they were categorized in two response categories, one with 25% probability and the others with 75% of probability. This allowed us to isolate T1-locked and T2-locked P3 activity purely related to the frequency manipulation, by subtracting the ERP time-locked to a stimulus associated with a frequent response from the ERP time-locked to the stimulus associated with an infrequent response (see Dell'Acqua et al., 2003a,b, 2005; Vogel et al., 1998).

We first conducted a behavioral AB experiment that included a manipulation of SOA, to replicate the results of Crebolder et al. (2002), namely a larger AB when T1 is assigned to a lower probability category, in a design appropriate to elicit an N2pc. We will then use a single SOA in Experiment 2, which included ERP recordings and measured the N2pc, SPCN, and P3.

2. Results of Experiment 1

The proportion of correct responses to T1 and T2 were first submitted to a four-way ANOVA (Block order of the orientation of the first squares \times SOA \times Frequency of T1 \times Frequency of T2). The block order of the orientation of the first squares had neither a main effect nor interaction with any of the others variables. Consequently, the data were collapsed across this variable. The staircase procedure successfully maintained the accuracy of response for T2 for the long SOA between the prescribed boundaries (the average accuracy for T2 was 76.3%). The average duration of T2 was 134.4 ms.

2.1. Accuracy for T1

The mean accuracy for T1 is listed in Table 1. Mean accuracy was higher at the long SOA (76.54%) than at the short SOA (69.4%), $F(1,15)=28.924$, $MSE=.0056$, $p<.0001$. At the short SOA, the accuracy of T1 was lower when T1 was rare (reduction of 5.1% from T1 frequent to T1 rare), $F(1,15)=7.420$, $MSE=.0057$, $p<.02$, which was not the case at the long SOA (augmentation of 1% from T1 frequent to T1 rare), $F(1,15)=.336$, $MSE=.0047$, $p>.5$. This led to a significant T1 frequency \times SOA interaction, $F(1,15)=4.874$, $MSE=.0062$, $p<.04$.

Table 1 – Success rate (%) for T1, for Experiments 1 and 2, for each experimental condition

Exp.	SOA	T1F		T1R	
		T2F	T2R	T2F	T2R
1	250	80.3	63.6	80.1	53.5
1	850	81.9	70.2	82.3	71.8
2	350	97.9	96.2	90.0	92.3

Note. T1F means T1 frequent, T1R means T1 rare; T2F means T2 frequent, T2R means T2 rare.

Furthermore, when T2 was rare, the accuracy for T1 was reduced (from 81.1% when T2 was frequent to 64.7% when T2 was rare), $F(1,15)=11.035$, $MSE=.0777$, $p<.005$. The accuracy of T1 at the short SOA was reduced when T2 was rare (reduction of 21.7% from T2 frequent to T2 rare), $F(1,15)=16.257$, $MSE=.0461$, $p<.001$, and at the long SOA (reduction of 11.1%) from T2 frequent to T2 rare), $F(1,15)=4.886$, $MSE=.0403$, $p<.05$. The effect was stronger at short SOA than at long SOA, which lead to a significant $SOA \times T2$ frequency interaction, $F(1,15)=10.238$, $MSE=.0087$, $p<.006$. Clearly, both the temporal distance between T1 and T2 and the frequency of the response associated to T2 influenced the accuracy of T1.

2.2. Accuracy for T2

The accuracy rate for T2 is shown in Fig. 1. Only the trials with a correct response for T1 were considered here. Generally, the accuracy for rare T2 was lower than the accuracy for frequent T2, $F(1,15)=12.10$, $MSE=.077$, $p<.004$. This difference was larger when T1 was rare than when T1 was frequent, $F(1,15)=4.78$, $MSE=.0648$, $p<.045$. Furthermore, this interaction (frequency of T1 \times frequency of T2) was larger at short SOA than at long SOA, $F(1,15)=8.08$, $MSE=.0111$, $p<.02$. Further analysis indicated that this interaction (frequency of T1 \times frequency of T2) was significant at short SOA $F(1,15)=8.87$, $MSE=.041$, $p<.009$, but not at long SOA $F(1,15)=.95$, $MSE=.03$, $p>.34$. Note that T2 accuracy was lowest for rare T2s when T1 was rare and the SOA was short, and accuracy for frequent T2s was highest when T1 was rare and SOA was short.

2.3. Effect of the repetition of the stimulus

It could be argued that the AB effect in these data is confounded with a repetition-suppression (or repetition blindness) effect. Indeed, when both targets are rare, both

targets are also identical. This is not the case for the frequent target, where there are three possible stimuli. In order to verify if a repetition-blindness effect was occurring here, we ran an analysis using only the trials where the two targets were of the frequent category. The repetition or the non-repetition of the target had no effect on the accuracy of either T1, $F(1,15)=3.003$, $MSE=.0021$, $p>.1$, or T2 $F(1,15)=.0523$, $MSE=.0013$, $p>.8$.

3. Discussion of Experiment 1

The higher accuracy for frequent T2s at short SOA when T1 was rare may appear counterintuitive, at first glance. However, this was the expected result if processing a rare T1 increases the AB. In absence of knowledge of the correct response, the subjects were more likely to guess using the frequent response rather than the rare response. This strategy would decrease accuracy for infrequent T2s but increase accuracy for frequent T2s. This is exactly what we observed, particularly when the T1-T2 SOA was short, indicating that decreasing SOA increased the probability of guessing (that is, increased the AB). We conclude that our experimental design was successful in creating an AB that was modulated by the probability of the categorization assigned to T1.

The accuracy for T1 was reduced when T2 was rare, and this effect was stronger when the SOA was short. Furthermore, the accuracy of T1 was reduced at short SOA (when T1 was rare). These results indicated that the processing of T1 was influenced by the processing of T2. This result could be explained by a central capacity sharing model (Navon and Miller, 2002; Tombu and Jolicoeur, 2003; Shapiro et al., 2006), if we assume that when the difficulty of T2 processing was increased (rare T2), more capacity would be dedicated to T2 than when T2 processing was easier (frequent T2). Consequently, less capacity would be available for T1 processing, leading to errors in the report of T1.

4. Introduction to Experiment 2

We modified the experimental design developed in Experiment 1 so we could measure the N2pc in the ERP to T2 during the task, and the frequency-related P3 differential response in the ERP to each target. This enabled us to explore the effects of a central load created by processing T1 on the deployment of

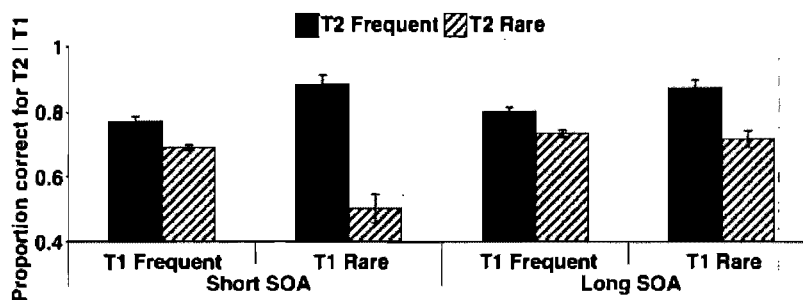


Fig. 1 – Success rate in the report of T2 in Experiment 1, for the trials where T1 was successfully reported. The error bars represent one standard deviation.

visual spatial attention to T2, and to monitor concurrently whether the frequency manipulation had the desired effect at a central stage of processing or at different stages. The results of Experiment 1 showed that the same patterns of results were obtained regardless of the order of presentation of T1 and T2 along the vertical and horizontal midlines (i.e., vertical-horizontal vs. horizontal-vertical). Given that order did not matter, we fixed the orientation of T1 to the vertical midline and of T2 to the horizontal midline, in order to evoke an N2pc to T2 in every trial. Stimuli presented on the vertical midline cannot produce an N2pc. The N2pc requires that attention be deployed to the left or to the right visual field, which, in turn, produces a left–right lateralized interhemispheric ERP difference. In order to maximize our ability to detect changes in the N2pc to T2, as a function of differences in the response probability associated with T1, we presented T2 lateralized to the left or right in every trial. This required that T1 be presented on the vertical midline on every trial. As shown in Experiment 1, however, the behavioral results were equivalent for the two types of trials (T1 on the vertical midline with T2 on the horizontal midline vs. T1 on the horizontal midline with T2 on the vertical midline), and thus the AB does not depend on this difference, allowing us to concentrate on the case in which T2 was on the horizontal midline.

We also fixed the SOA at 350 ms. The use of a fixed SOA and of stimuli having identical visual characteristic and occurrence probability ensured that the visuo-spatial characteristics of T1 in the high central attention load condition (when T1 is in the rare response category) were equivalent to those in the low central attention load condition (when T1 is in the frequent response category). Consequently, any effects of T1 processing on the visuo-spatial treatment of T2 would be attributed to the difference in central attention load created by the categorization of T1. In particular, an effect of the probability manipulation for T1 on the N2pc elicited by T2 could not be due to visual capture by T1, *per se*, given that the same stimuli and SOA were used for the two T1 response probability levels. If visual spatial attention was captured for a longer time by T1 in the low-probability condition, it would have to be the result of the categorization assigned to T1 and the subsequent increase in difficulty in updating working memory for T1 associated with a rare categorization. We assume these effects reflect central attentional capacity limitations, as demonstrated by Crebolder et al. (2002) for similar ranges of probability levels. Therefore, consistently with evidence produced in prior work (Dell'Acqua et al., 2003a,b, 2005; Vogel et al., 1998), we predicted that increases in central load would be reflected in enhanced P3 activity elicited by a T1 associated with an infrequent response relative to a T1 associated with a frequent response. Furthermore, we expected that the P3 to T2 would be significantly reduced under conditions leading to a larger AB (namely, when T1 was associated with the infrequent response).

5. Results of Experiment 2

The staircase procedure for T2 converged to an average presentation time of 77.8 ms for T2. Fifteen subjects out of 16 reached the minimal T2 duration (50 ms) during the recording. Consequently, the staircase did not succeed to

keep the mean accuracy for T2 when T1 and T2 were frequent below 87% (the mean accuracy was 92.4% in this case).

5.1. Behavior

The mean accuracy for T1 in each condition is listed in Table 1. Accuracy for T1 decreased when T1 was rare (91.2%) compared to when T1 was frequent (96.7%), $F(1,15)=13.46$, $MSE=.00358$, $p<.003$. However, this difference was stronger when T2 was frequent (decrease of 7.1% between frequent T1 and rare T1) than when T2 was rare (decrease of 3.9% between frequent T1 and rare T1), $F(1,15)=6.399$, $MSE=.0006$, $p<.024$.

The accuracy for T2 is shown in Fig. 2. Generally, we found the same pattern of results as in the short SOA condition of Experiment 1. The accuracy for T2 was reduced both when T1 was rare, $F(1,15)=20.17$, $MSE=.003$, $p<.0005$, and when T2 was rare $F(1,15)=45.98$, $MSE=.02$, $p<.0001$. More importantly, the accuracy for T2 decreased more as a function of the frequency of T2 when T1 was rare than when T1 was frequent, leading to a significant interaction between those two factors, $F(1,15)=15.44$, $MSE=.008$, $p<.002$.

Subsequent analysis of the accuracy for T2 indicated that when T1 was rare, the accuracy for T2 was dramatically reduced when T2 was rare compared to when T1 was frequent, $F(1,15)=18.32$, $MSE=.0098$, $p<.0007$. However, when T1 was frequent, the accuracy for T2 was slightly increased when T2 was rare compared to when T2 was frequent, $F(1,15)=3.93$, $MSE=.0012$, $p<.066$.

5.2. T2-locked ERP: N2pc

The N2pc waveforms are shown in Fig. 3. These waveforms were computed from the following recording site, O1, O2, PO3, PO4, PO7, PO8, P5, P6, P7, and P8, by subtracting the waveform measured at the electrode over the ipsilateral hemisphere (ipsilateral to the target) from the corresponding electrode over the contralateral hemisphere (contralateral to the target), see Experimental procedures for details. The frequency manipulation led to different numbers of trials across conditions. Therefore, using a two-way ANOVA with frequency of T1 and frequency of T2 as a factor would have led to Np2c waveforms computed from only 100 trials (50 with T2 on the left and 50 with T2 on the right), before artifact rejection. This

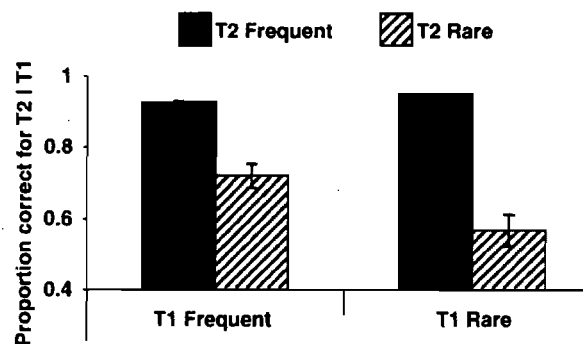


Fig. 2 – Success rate in the report of T2 in Experiment 2, for the trials where T1 was successfully reported. The error bars represent one standard deviation.

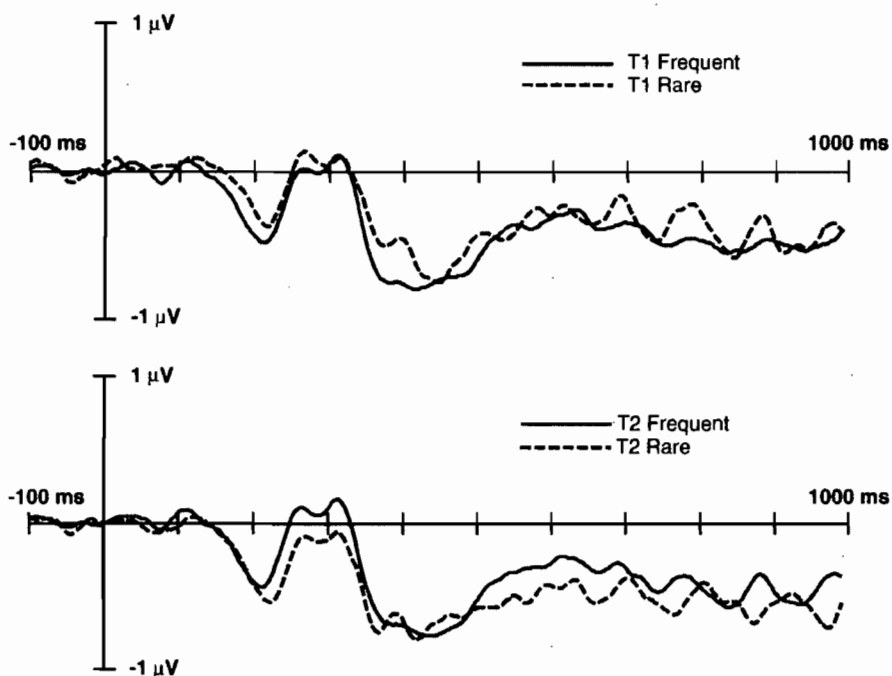


Fig. 3 – N2pc and SPCN subtraction waveforms, calculated from the pooled O1, PO3, PO7, P5, P7, and pooled O2, PO4, PO8, P6, and P8 responses. The top panel shows the N2pc and SPCN to T2 when T1 was rare and when T1 was frequent. The bottom panel shows the N2pc and SPCN to T2 when T2 was rare and when T2 was frequent.

is insufficient to give a stable N2pc. Therefore, we computed two separated one-way ANOVAs, one where the waveforms were averaged according to the frequency of T1 and one where they were averaged according to the frequency of T2. This averaging method allowed us to compute the N2pc and the SPCN with at least 400 trials (200 with T2 on the left and 200 with T2 on the right) prior to artifact rejection.

The amplitude of the N2pc component was measured by computing the mean amplitude in a 150–300 ms time window. The N2pc to T2 was reduced when T1 was rare, compared to when T1 was frequent, $F(1,15)=5.31$, $MSE=.0898$, $p<.036$. Interestingly, the frequency of T2 itself had the opposite effects on the N2pc, $F(1,15)=3.98$, $MSE=.123$, $p>.064$. Although only marginally significant, this last results indicated that the different number of trials used to calculate the T1 rare N2pc could not explain the reduction of the N2pc in this case, because the T2 rare condition (which is calculated with 400 trials) produced a larger N2pc than the T2 frequent condition (which is calculated with 1200 trials prior to artifact rejection).

There was some suggestion of latency differences across conditions. To measure the latency of the onset and of the offset of the N2pc component, we used a jackknife procedure (Miller et al., 1998). Instead of measuring the latency of the component on each of the 16 subject waveforms, 16 averages of all subjects except one (each subject is excluded once) were computed. These waveforms are more stable than the individual subject waveforms, allowing for a more stable estimate of the latency measure. The latency of each of these average waveforms was then measured by taking the point where half of the amplitude of the peak was reached. These latencies were then submitted to an ANOVA, and the F values

were corrected appropriately (see Miller et al. (1998) for the derivation of the appropriate correction). The onset of the N2pc was delayed by 16 ms in the T1-rare conditions compared to the T1-frequent conditions. This difference was marginally significant, $F(1,15)=3.15$, $p<.097$. However, the onset of the N2pc components was not delayed when T2 was rare, compared to when T2 was frequent, $F(1,15)=.56$, $p>.45$. The offset of the N2pc followed the opposite pattern. The offset of the N2pc component was not affected by the frequency of T1, $F(1,15)=.05$, $p>.8$, but it was delayed by 13 ms when T2 was rare, $F(1,15)=3.27$, $p<.091$. In brief, although the latency differences did not reach the traditional significance threshold, there was a suggestion that the N2pc ended later when the current target was rare and that it started later when the preceding target was rare.

5.3. T2-locked ERP: SPCN

The amplitude of the SPCN was measured from the same difference waveforms used to estimate the N2pc, but with a 350–600 ms time window. As for the N2pc, the amplitude of the SPCN to T2 was reduced when T1 was rare, compared to when T1 was frequent, $F(1,15)=4.52$, $MSE=.497$, $p<.05$. Furthermore, the frequency of T2 did not influence the SPCN, $F(1,15)=1.39$, $MSE=.0928$, $p>.25$.

5.4. T1-locked and T2-locked ERP: P3

The P3 waveforms at Oz, Pz, and Cz are shown in Fig. 4. Analyses were performed at several electrode sites with similar results. We report here the results for electrode Pz, which was an electrode near the peak amplitude of the P3

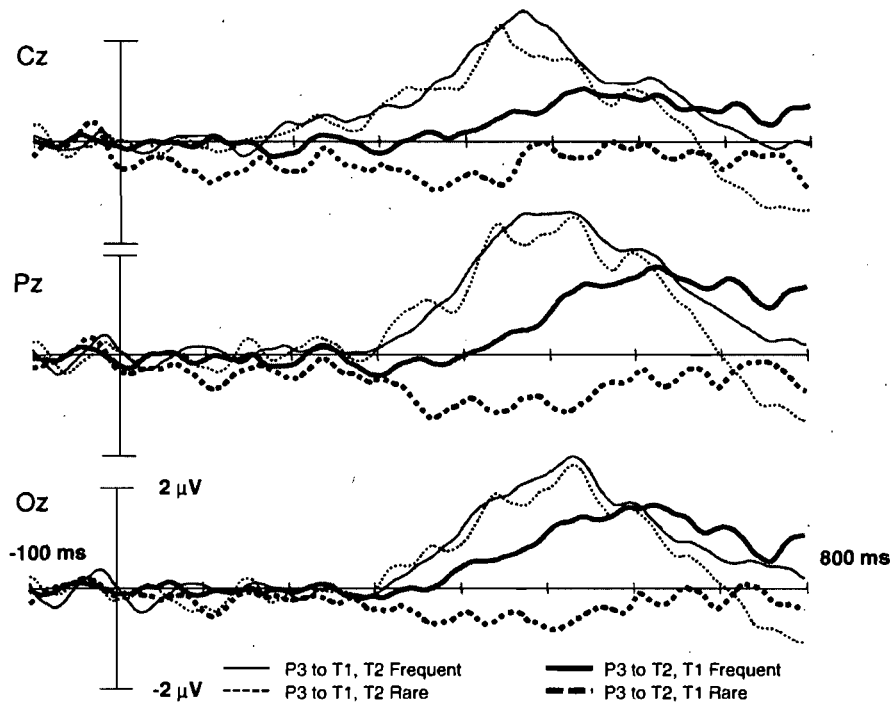


Fig. 4 – P3 subtraction waveforms (infrequent–frequent), for electrodes Cz, Pz, and Oz, for T1 (as a function of the frequency of T2) and for T2 (as a function of the frequency of T1). See text for further details.

wave. Each of these waveforms was computed by subtracting the ERP to the frequent target from the ERP to the rare target. For each target (T1, T2), two P3 waveforms were computed, averaging over the frequency of the other target. The amplitude of the P3 was measured with a 300–650 ms time window. It can be observed that the P3 to T1 was not influenced by the frequency of T2, $F(1,15)=.23$, $MSE=.589$, $p>.64$. However, the P3 to T2 was strongly reduced in amplitude when T1 was rare, $F(1,15)=28.08$, $MSE=.637$, $p<.0001$. In fact, no P3 was visible for T2 when T1 was rare, but a negativity was observed (average amplitude of $-.827 \mu V$; $t(15)=-3.678$, $p<.002$).

Furthermore, the P3 to T2, when T1 was frequent, was reduced compared to the combined P3 to T1, $F(1,15)=25.72$, $MSE=.384$, $p<.0001$. The latency of the P3 seemed also delayed in this case. We used a jackknife procedure adapted from Miller et al. (1998) to evaluate the difference in latency of the P3 to T1 and the P3 to T2. Here, the latency of the P3 components was then measured on these waveforms by measuring the point where half of the area of the P3 was reached (using a 0–1000 ms time window). Everything else was the same as the preceding latency analysis. This latency measure, also referred as fractional area measure, is very stable and resistant to noise (Luck, 2005). There was a significant latency difference between the P3 to T1 and the P3 to T2, $F(1,15)=52.14$, $p<.0001$.

6. General discussion

The goal of this study was to determine whether central capacity limitations implicated in the AB phenomenon can impair the ability to deploy visual spatial attention. We wanted to examine this issue under conditions that avoided possible

differences in visual capture by T1, differences in initial attentional state, and differences in task, across Task1 and Task2, in the various experimental conditions. To achieve these conditions, we capitalized on an earlier finding, reported by Crebolder et al. (2002), in which a larger AB was caused by processing a less frequent T1 stimulus. In Experiment 1, we extended the work of Crebolder et al. by showing that a similar probability effect on the AB can be observed with stimuli that are equiprobable (all stimuli had a probability of .25), but for which the associated categorization was either frequent (.75) or infrequent (.25). This extension of the Crebolder et al. (2002) results allowed us to use the effect of T1 frequency on the AB while nonetheless presenting stimuli that were equiprobable, and in all other ways completely equivalent. This was an important feature that enabled us to examine ERP effects, in Experiment 2, that were not compromised by stimulus confounds.

In Experiment 2, we found that the probability of the response associated with T1 both influenced accuracy of report of T2, and modulated the amplitude of the N2pc to the second target. A higher central load created by the need to process a T1 stimulus associated with a less frequent categorization reduced the amplitude of the N2pc and of the SPCN, and abolished the P3 to T2. In our view, the central processing load required to categorize T1 reduced the efficiency of the spatial selection of T2, leading to a smaller N2pc, and consequently to a weaker representation of T2 in VSTM, leading to a smaller SPCN (Dell'Acqua et al., 2006; Jolicœur et al., 2006a,b). It appears that this degraded representation was also insufficient to create a stable representation in (non-visual) working memory, resulting in the abolition of the P3, and reduced behavioral accuracy for T2.

The patterns of behavioral results for both Experiment 1 and Experiment 2 indicated that the processing of T2 was

impaired when T1 was associated with a less frequent categorization, but only at short SOA (250 ms for Experiment 1 and 350 ms for Experiment 2). In both cases, the accuracy of T2 was reduced by a higher central load, but only when T2 was rare. When T2 was frequent, accuracy was increased by the higher central load. However, it is clear that this increase in accuracy resulted from a bias to guess the frequent response when subjects had not perceived T2.

The presence of an N2pc to T2 in both T1-frequent and T1-rare conditions suggests that the subjects successfully used the selection cue (the color) to identify which of the two stimuli was the target. This was also the case in Jolicœur et al. (2006a), in a control AB experiment where the second task was to identify the side of the masked colored target in the presence of a masked colored distractor. The success rate for the localization of T2 was very high even in the conditions where an AB is usually observed for the identification of T2, indicating that the subjects were able to detect the color of the targets even when they were unable to identify the target.

The reduction of the N2pc in the T1-rare condition, however, indicated a dependency of the deployment of spatial attention on the available processing capacity of central attentional mechanisms. Previous results showed more dramatic effects of the AB on spatial attention (Dell'Acqua et al., 2006; Jolicœur et al., 2006a,b). The smaller magnitude of the reduction of the N2pc in the current paradigm could be explained in several ways. First, the effect size of the frequency of T1 in Crebolder et al. (2002) was small, especially at a ratio of 4:9, which is close to the 1:3 ratio we have here. Furthermore, the 1:3 ratio here was manipulated independently for both T1 and T2, leading to at least a rare target on 43.45% of the trials. This combined ratio could have increased the perceived frequency of the rare target and perhaps reduced the overall impact of the frequency manipulation for T1. Second, the control condition here, the T1-frequent condition, was expected to cause a central load by itself because of the short SOA between T1 and T2. This expectation was confirmed by the amplitude reduction and the delay of the P3 to T2 compared to the P3 to T1 (see Fig. 4; presumably T1 suffers very little AB interference, and so the P3 to T1 provided a measure of the P3 in the absence of AB interference). Consequently, it could be assumed that the N2pc in the T1 frequent conditions is already affected by the central load caused by a frequent T1.

The SPCN to T2 was clearly visible in both the T1-frequent and T1-rare conditions. Indeed, some visual information entered in VSTM following the presentation of T2. According to Vogel and Machizawa (2004), a greater amplitude of the SPCN signifies more items in VSTM. Robitaille and Jolicœur (2006) found evidence that the SPCN was of higher amplitude when lateralized stimuli were masked, suggesting that the mask might act as a second item in VSTM. In the present Experiment 2, the VSTM was probably loaded by a combination of items consisting of the target stimulus and the mask. The less efficient spatial selection in the T1-frequent conditions would have led to a weaker representation of T2 in VSTM, but to an equivalent representation of the mask, which would explain the small reduction of the amplitude of the SPCN.

The finding that the N2pc to T2 was increased when T2 was associated with a low-frequency response could be seen as conflicting with our initial claim that we created a design in

which the visual processing of all the targets was equivalent. Indeed, if the spatial deployment of attention to T2 was increased when T2 required the rare response, we might also assume that the spatial deployment of attention to T1 was affected by the frequency of T1. One could argue that the reduction of the N2pc to T2 when T1 was rare was caused by this greater deployment of attention to T1 in this case. Indeed, if spatial attention was more engaged or engaged for a longer period of time on a rare T1, there may have been less time to redeploy spatial attention toward T2, and thus the N2pc to T2 would be reduced in this case. However, we consider this result, the increase in the amplitude of the N2pc to a target when the response associated to it was rare, as supporting our primary hypothesis, namely that the deployment of spatial attention depends on central attention. Consider first that all four possible stimulus squares were equivalent in terms of visual features and in terms of probability of occurrence (each had a probability of .25). Furthermore, the square considered as the rare target for a specific subject was not the same for another subject—the stimulus which was the rare target was counterbalanced across subjects. These considerations suggest to us that the probability effects are very unlikely to reflect influences at sensory or perceptual levels of processing.

Interestingly, we did not find any modulation of the infrequent minus frequent difference wave (Fig. 4, used to estimate the P3) prior to 300 ms, which indicated that the early visual components (P1, N1, N2) were equivalent for the rare-response stimulus and for the frequent-response stimuli. However, the deployment of attention toward a rare-response target (T2) produced a larger N2pc to T2. The analysis of the latency of the N2pc components suggested that spatial attention may have dwelled longer on a rare target than on a frequent target. Previous evidence suggests that the locus of frequency effects (in this range of frequencies) is at or after the bottleneck in the psychological refractory period paradigm (Crebolder et al., 2002), that is, at a post-perceptual, central, stage of processing. In Experiment 2, spatial attention may have dwelled longer on T1 when T1 was rare, which could be the cause of the reduction of the N2pc to T2. Indeed, the reduction of the N2pc to T2 when T1 was rare was accompanied by a delay in the onset of the N2pc. However, this inability to disengage earlier from T1 was caused by the central attentional load created by T1, not by the visual processing of T1, per se (because all T1 stimuli were perceptually equivalent). In sum, according to this interpretation, our results indicate that the deployment of visual spatial attention depends on central attention.

The P3 to T2 was abolished when T1 was rare compared to when T1 was frequent. This result mirrors the one obtained by Vogel et al. (1998), by Vogel and Luck (2002), and by Dell'Acqua et al. (2003a,b, 2005). The P3 has been argued to reflect a process that updates the contents of working memory (Donchin and Coles, 1988). On this view, the reduced P3 amplitude for T2 when T1 was associated with a rare response suggests that subjects had a greater difficulty to create a representation of the second target in working memory. These results provide strong converging evidence for our interpretation that a T1 stimulus associated with a less-frequent categorization produced a larger AB. The delay in the onset latency of the P3 at short SOA (for the frequent T1 condition),

compared with the onset latency of the P3 for T1 itself, provides further evidence that processing T1 causes a delay in the categorization of T2, as suggested by models of the AB that ascribe an important role to the central processing of T1 by capacity limited mechanisms (Chun and Potter, 1995; Jolicoeur, 1999a,b; Sessa et al., 2007; Vogel and Luck, 2002).

It is worth pointing out that, over and above the crucial findings concerning the inverse correlation between central load and visuo-spatial processing efficiency, the present P3 results corroborate and extend in an important way previous results obtained by monitoring the ERP and the magnetoencephalographic (MEG) reflections of both targets displayed using the RSVP technique. Kessler et al. (2005a,b), and Shapiro et al. (2006) for instance, have recently shown an increasing trade-off in the magnitude of M3 responses elicited by T1 and T2 (the MEG equivalent of the P3 ERP component observed with electrophysiological recordings) as the temporal interval between their onsets was reduced. Incidentally, the overlap of M3 peak responses was observed in regions held to be of interest for identification processes (e.g., infero-temporal regions), but not in regions more likely involved in sequencing (e.g., fronto-parietal regions). In an attempt to establish a quantitative link between the P3 to T1 and AB magnitude estimated behaviorally as the percentage of correct T2 identification, McArthur et al. (1999) found that increased P3 responses to T1 were associated with increased AB effect magnitude. One of the most extensive and recent examination of the relationship between P3 responses to targets and AB magnitude is probably that carried out by Martens et al. (2006), whose focus was on the difference at the individual level between blinkers (i.e., people particularly prone to 'blink' under RSVP condition) and non-blinkers (i.e., people with small or no AB effect). The ERP recording technique in the work of Martens and colleagues included online monitoring of the ERP response during the entire RSVP stream presentation, so as to capture the ERP reflection of T1 and T2 across the different time intervals separating their onsets. The results of interest for the present discussion were those mirroring the MEG results of Kessler and colleagues. That is, the results revealed the tendency of P3 responses to T2 to be partially suppressed and postponed in blinkers relative to non-blinkers, thus providing the ERP equivalent of the trade-off between P3 responses to T1 and T2 that the MEG results described above had illuminated. The extension provided by the present investigation stays in the method used to isolate P3 activity in the ERP elicited by targets under the present circumstances. Contrary to the work just described, in which this technique was not adopted, we used a subtraction method that was specifically designed to isolate P3 activity that was associated to the systematic manipulation of the frequency of the response to a target class. This method, apart from enabling a more accurate individuation of the portion of the ERP specifically responsive to the variable manipulated, allowed us to 'clean' the P3 response from the potentially spurious cumulative EEG activity that is certainly generated when more than one stimulus is displayed to subjects. Our experimental design allowed us to isolate that portion of the P3 that was specifically related to the frequency of the classification of the targets, independently of the frequency of presentation of individual stimuli, pointing to a central locus

of processing, as we have discussed at length before. With these considerations in mind, we interpret the P3 results as a parallel, independent test that the frequency manipulation adopted herein affected central processing stages, and this suggests strongly that the attenuation of the N2pc to T2 observed in the results is a relatively 'pure' reflection of engaging, in close temporal contiguity, mechanisms devoted to the control of central attention and mechanisms devoted to the control of visuo-spatial attention.

7. Experimental procedures

7.1. Experiment 1

7.1.1. Subjects

Sixteen volunteers, 14 women, aged between 19 and 26 (average 22), were paid for their voluntary participation. They reported no neurological problems, normal or corrected-to-normal vision, and normal color vision. We obtained informed consent from each subject at the beginning of the experiment.

7.1.2. Stimuli

The stimuli were presented on a 15-inch color cathode-ray tube (CRT) driven by a microcomputer running MEL 2.01 software at 60 HZ in 640×480 pixel mode. The stimuli were outline squares, subtending 1.2° of visual angle, .2° thick, shown in pink or green. Each squares contained a gap (.2° thick), in the middle of one of the sides. The squares were always presented in pairs (one in left visual field, one in right visual field), each square centered 3.6° off-center. A fixation point (.2°) was present at the center of the display. Counterbalancing (explained below) ensured that the small difference in luminance across the green and pink stimuli could not have influenced the results.

7.1.3. Procedure

The sequence of events in each trial is illustrated in Fig. 5. Each trial began with two symbols at the center of the display, indicating (in reading order) if the answers for the last trial were correct (+) or incorrect (-). The subject started each trial by pressing the space bar on a standard computer keyboard. The + or - sign was then replaced by a small fixation point. The fixation point remained alone on the screen for 500 ms. The first stimulus pair then appeared and consisted of two squares, one pink and one green, presented 3.6° from the center of the screen. For half of the experiment, the first pair of stimuli was on the vertical midline. For the second half of the experiment, the first pair of stimuli was presented on the horizontal midline. This condition was blocked, that is, all vertical first trials were presented in one a part of the experiment, and all the horizontal first trials were presented in another part of the experiment. The order of the block was counterbalanced across subject. The squares remained on the screen for 100 ms and were immediately followed by a mask. The mask consisted of a ticker square (.4°) having a gap on each four sides, presented for 33 ms.

Either 250 or 850 ms after the onset of the first display, a second display appeared. This display also contained a pink and a green square, at 3.6° from the center of the screen. The square in this display was always orthogonally located relative to the

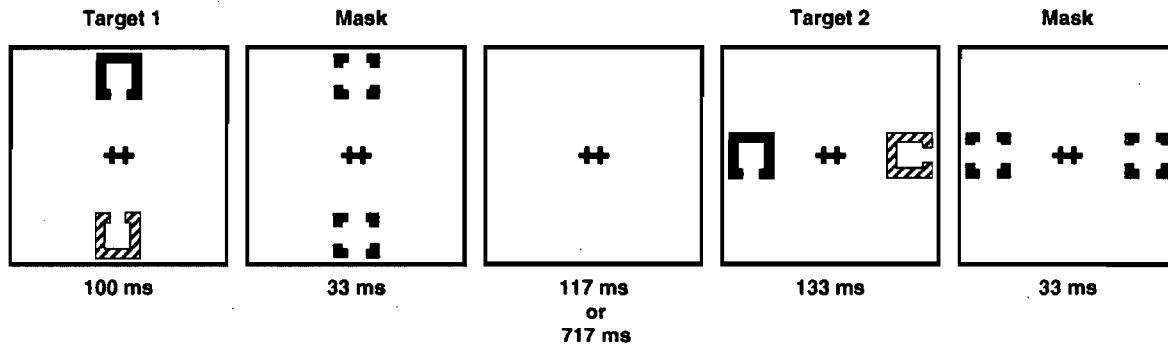


Fig. 5 – Sequence of events in each trial. The actual target and distractor were pink and green (equiluminant), followed by a grey mask.

first one, so when the first set of squares was presented on the vertical midline, the second set of squares was presented on the horizontal midline, and conversely when the first was on the horizontal, the second was on the vertical. The second display was also masked. The duration of the second target was adjusted with a staircase procedure, to ensure accuracy between 70 and 87%, for the second target, when the SOA was 850 ms. The duration of T2 was adjusted after each block (i.e., after the 32 practice trials at the beginning of each part and after the 128 trials of each of the two experimental blocks of each experiment part). At each adjustment, the number of video frames (16.7 ms each) for T2 was increased by one if the accuracy was lower than 70% and was decreased by 1 if the accuracy was higher than 87%.

For half of the subjects, the task was to report the location of the gap in the pink squares. For the other half, the task was to report the location of the gap in the green squares. Both responses had to be entered in order of target presentation at the end of the trial, using the keyboard. Subjects were aware that the reaction times were not recorded and they were instructed to focus on maximizing accuracy.

Each subject received a response-key mapping at the beginning of the experiment. The response-key mapping was identical for the first and the second response. The task was to determine the location of the gap in the target square and to respond as a function of this location (e.g., left vs. not-left). Given that each gap position was equally likely to occur, there was no frequency manipulation for the stimuli themselves, but only for the responses produced by the subject. One response was more frequent (e.g., not-left, 75% of trials) than the other (e.g., left, 25% of trials). The gap location mappings (4 different ones) were counterbalanced across subjects. Each subject executed two blocks of 256 trials (512 trials total), in which trials with different SOAs, T1 gap locations, and T2 gap locations were presented in a randomized order.

7.2. Experiment 2

7.2.1. Subjects

Of the 23 subjects who were tested, 7 were excluded from the analyses because they had an insufficient number of trials after the artifacts rejection procedures. The remaining 16 subjects (12 women) were between 18 and 26 years of age (average 20.6), had a normal or corrected to normal vision, normal color vision, and declared having no neurological disease.

7.2.2. Stimuli

The stimuli were displayed on a 17-inch computer screen located 57 cm in front of the subject. The stimuli were identical to those in the first experiment, except that their size was 13% bigger due to a larger screen. To ensure an equal initial response of the brain to the colored stimuli, the luminance of the stimuli was equated. The luminance and chromaticity were measured with a Minolta CS-100 chromameter. The luminance of the green was 19.7 cd/m² ($x=.292, y=.550$) CIE (x, y) chromaticity coordinates (Wyszecki and Stiles, 1982); that of the pink was 18.5 cd/m² ($x=.386, y=.279$), the fixation point was 30.8 cd/m² ($x=.280, y=.302$), and the background was .10 cd/m² ($x=.449, y=.442$).

7.2.3. Procedure

The procedure was almost identical to the one used in the first experiment except for the following: the duration of T1 was 133 ms, the SOA was fixed at 350 ms, and T1 was always vertical and T2 horizontal. Each subjects had 32 practice trials followed by 25 blocks of 64 trials, for a total of 1600 experimental trials. For this experiment, the staircase procedure adjusted the duration of T2 in order to achieve an accuracy between 80% and 87%, for the conditions where T1 and T2 were both frequent.

7.2.4. ERP recording and analysis

The recordings were made with a BioSemi Active-two system, with 70 active Ag–AgCl scalp electrodes, 64 of which were positioned using the extended International 10–20 system (see Pivik et al., 1993), two were at the mastoids, and 4 for the electrooculogram, in an electrically shielded and dimly lit room. The EEG was algebraically re-referenced to the average of the left and right mastoids. The electrooculogram (EOG) was recorded with active Ag–AgCl electrodes placed at the left and right canthi and above and below the left eye. HEOG was obtained by subtracting the signal at the left electrode from the signal recorded at the right electrode. VEOG was obtained by subtracting the signal at the electrode above the left eye from the signal at the electrode below the left eye. The signals were amplified, low-pass filtered with a cut-off frequency of 67 Hz, and digitized at 256 Hz during the recording. They were filtered again, during post-recording analysis, using a Butterworth zero-phase high-pass filter with a cut-off frequency of .05 Hz and then a Gaussian low-pass filter with a cut-off frequency of 30 Hz. Eye blinks and eye movements were detected using an automated function.

Trials with eye blinks and eye movement were removed during post-recording analysis. Furthermore, if an electrode contained a recording artifact during a trial, this trial was also removed from the analysis. As a further precaution to ensure that subjects did not move their eyes in the direction of the target (despite screening individual trials on the basis of the HEOG), separate average HEOG curves were computed for left-target trials and for right-target trials. Any residual tendency of the subject to move their eyes toward the target, for the trials included in the analysis, would produce systematic deviations in these average HEOG waveforms. For each subject, we averaged all the left trials and all the right trials. The maximal amplitude of the difference between the HEOG to the left trials and the HEOG to the right trials for any given subject was 2.3 μ V. This indicated that on average, the eye moved less than .15° toward the target for this subject (Lins et al., 1993).

For the N2pc and the SPCN, average waveforms were computed at each scalp electrode site for each condition with a 100 ms pre-stimulus baseline and a 1000 ms post-stimulus period relative to the onset of T2. The epochs were baseline corrected based on the mean activity during the 100 ms pre-stimulus period, for each electrode site. The average ipsilateral and contralateral waveforms were computed for all lateralized posterior electrode pairs. However, given that the results were similar across several sites, and that we are more interested in differences between conditions rather than differences between electrode sites, we pooled the O1, PO3, PO7, P5, and P7 electrodes together and O2, PO4, PO8, P6, and P8 together. We first computed an average ipsilateral waveform by averaging the waveform for the left pool of electrodes for trials in which the target was on the left with the waveform for the right pool of electrodes for trials in which the target was on the right. Similarly, we computed an average contralateral waveform by averaging the right-sided response to left targets with the left-sided response to right targets. These waveforms were then subtracted (contralateral–ipsilateral) to produce an N2pc/SPCN difference waveform for each condition.

For the P3, a 100 ms pre-stimulus baseline and an 800 ms post-stimulus window were computed. For each target, four waveforms were averaged, according to the frequency of both target response category. The data were collapsed across T2 on the left and T2 on the right trials. The P3 to T1 were calculated by subtracting the frequent T1 waveform from the rare T1 waveform. The P3 to T2 were calculated by subtracting the frequent T2 waveform from the rare T2 waveform.

REFERENCES

- Chun, M.M., Potter, M.C., 1995. A two-stage model for multiple target detection in rapid serial visual presentation. *J. Exp. Psychol. Hum. Percept. Perform.* 21, 109–127.
- Crebolder, J., Jolicœur, P., McIlwaine, J.D., 2002. Loci of signal probability effects and of the attentional blink bottleneck. *J. Exp. Psychol. Hum. Percept. Perform.* 28, 695–716.
- Dehaene, S., Sergent, C., Changeux, J.-P., 2003. A neuronal network model linking subjective reports and objective physiological data during conscious perception. *Proc. Natl. Acad. Sci. U. S. A.* 100, 8520–8525.
- Dell'Acqua, R., Jolicœur, P., Pesciarelli, F., Job, R., Palomba, D., 2003a. Electrophysiological evidence of visual encoding deficits in a cross-modal attentional blink paradigm. *Psychophysiology* 40, 629–639.
- Dell'Acqua, R., Pascali, A., Jolicœur, P., Sessa, P., 2003b. Four-dot masking produces the attentional blink. *Vis. Res.* 43, 1907–1913.
- Dell'Acqua, R., Jolicœur, P., Vespignani, F., Toffanin, P., 2005. Central processing overlap modulates P3 latency. *Exp. Brain Res.* 165, 54–68.
- Dell'Acqua, R., Sessa, P., Jolicœur, P., Robitaille, N., 2006. Spatial attention freezes during the attention blink. *Psychophysiology* 43, 394–400.
- Donchin, E., Coles, M.G.H., 1988. Is the P300 component a manifestation of context updating? *Behav. Brain Sci.* 11, 357–374.
- Duncan, J., Ward, R., Shapiro, K.L., 1994. Direct measurement of attentional dwell time in human vision. *Nature* 369, 313–315.
- Eimer, M., 1996. The N2pc component as an indicator of attentional selectivity. *Electroencephalogr. Clin. Neurophysiol.* 99, 225–234.
- Giesbrecht, B.L., Di Lollo, V., 1998. Beyond the attentional blink: visual masking by object substitution. *J. Exp. Psychol. Hum. Percept. Perform.* 24, 1454–1466.
- Johnson, R., 1993. On the neural generators of the P300 component of the event-related potential. *Psychophysiology* 30, 90–97.
- Jolicœur, P., 1998. Modulation of the attentional blink by on-line response selection: evidence from speeded and unspeeded task1 decisions. *Mem. Cogn.* 26, 1014–1032.
- Jolicœur, P., 1999a. Dual-task interference and visual encoding. *J. Exp. Psychol. Hum. Percept. Perform.* 25, 596–616.
- Jolicœur, P., 1999b. Concurrent response selection demands modulate the attentional blink. *J. Exp. Psychol. Hum. Percept. Perform.* 25, 1097–1113.
- Jolicœur, P., Dell'Acqua, R., 1998. The demonstration of short-term consolidation. *Cogn. Psychol.* 36, 138–202.
- Jolicœur, P., Sessa, P., Dell'Acqua, R., Robitaille, N., 2006a. Attentional control and capture in the attentional blink paradigm: evidence from human electrophysiology. *Eur. J. Cogn. Psychol.* 18, 560–578.
- Jolicœur, P., Sessa, P., Dell'Acqua, R., Robitaille, N., 2006b. On the control of visual spatial attention: evidence from human electrophysiology. *Psychol. Res.* 70, 414–424.
- Kessler, K., Schmitz, F., Gross, J., Hommel, B., Shapiro, K., Schnitzler, A., 2005a. Cortical mechanisms of attention in time: neural correlates of the lag-1 sparing phenomenon. *Eur. J. Neurosci.* 21, 2563–2574.
- Kessler, K., Schmitz, F., Gross, J., Hommel, B., Shapiro, K., Schnitzler, A., 2005b. Target consolidation under high temporal processing demands as revealed by MEG. *Neuroimage* 26, 1030–1041.
- Koivisto, M., Revonsuo, A., 2003. An ERP study of change detection, change blindness, and visual awareness. *Psychophysiology* 40, 423–429.
- Kranciocich, C., Debener, S., Engel, A.K., 2003. Event-related brain potential correlates of the attentional blink phenomenon. *Cogn. Brain Res.* 17, 177–187.
- Lins, O.G., Picton, T.W., Berg, P., Scherg, M., 1993. Ocular artifacts in EEG and event-related potentials: I. Scalp topography. *Brain Topogr.* 6, 51–63.
- Luck, S.J., 2005. *An Introduction to the Event-Related Potential Technique*. MIT Press, Cambridge, MA.
- Luck, S.J., Hillyard, S.A., 1994. Spatial filtering during visual search: evidence from human electrophysiology. *J. Exp. Psychol. Hum. Percept. Perform.* 20, 1000–1014.
- Martens, S., Munneke, J., Smid, H., Johnson, A., 2006. Quick minds don't blink: electrophysiological correlates of individual differences in attentional selection. *J. Cogn. Neurosci.* 18, 1423–1438.
- McArthur, G., Budd, T., Michie, P., 1999. The attentional blink and P300. *Neuroreport* 10, 3691–3695.

- Miller, J.P., Patterson, T., Ulrich, R., 1998. Jackknife-based method for measuring LRP onset latency differences. *Psychophysiology* 35, 99–115.
- Navon, D., Miller, J., 2002. Queuing or sharing? A critical evaluation of the single-bottleneck notion. *Cogn. Psychol.* 44, 193–251.
- Pivik, R.T., Broughton, R.J., Coppola, R., Davidson, R.J., Fox, N., Nuwer, M.R., 1993. Guidelines for the recording and quantitative analysis of electroencephalographic activity in research contexts. *Psychophysiology* 30, 547–558.
- Polich, J., Criado, J.R., 2006. Neuropsychology and neuropharmacology of P3a and P3b. In: Karakaş, S., Başar, E. (Eds.), *Models and Theories on Brain Function with Special Emphasis on Cognitive Processing*. *Int. J. Psychophysiol.*, 60, pp. 172–185.
- Potter, M.C., Chun, M.M., Banks, B.S., Muckenhoupt, M., 1998. Two attentional deficits in serial target search: the attentional blink and an amodal task-switch deficit. *J. Exp. Psychol. Learn. Mem. Cogn.* 24, 979–992.
- Potter, M.C., Dell'Acqua, R., Pesciarelli, F., Job, R., Peressotti, F., O'Connor, D., 2005. Bidirectional semantic priming in the attentional blink. *Psychon. Bull. Rev.* 12, 460–465.
- Raymond, J.E., Shapiro, K.L., Arnell, K.M., 1992. Temporary suppression of visual processing in an RSVP task: an attentional blink? *J. Exp. Psychol. Hum. Percept. Perform.* 18, 849–860.
- Robitaille, N., Jolicoeur, P., 2006. Fundamental properties of the N2pc as an index of spatial attention: effects of masking. *Can. J. Exp. Psychol.* 60, 101–111.
- Rolke, B., Heil, M., Streb, J., Hennighausen, E., 2001. Missed prime words within the attentional blink evoke an N400 semantic priming effect. *Psychophysiology* 38, 165–174.
- Sergent, C., Baillet, S., Dehaene, S., 2005. Timing of the brain events underlying access to consciousness during the attentional blink. *Nat. Neurosci.* 8, 1391–1400.
- Sessa, P., Luria, R., Verleger, R., Dell'Acqua, R., 2007. P3 latency shifts in the attentional blink: further evidence for second target processing postponement. *Brain Res.* 1137, 131–139.
- Shapiro, K.L., Raymond, J.E., Arnell, K.M., 1994. Attention to visual pattern information produces the attentional blink in rapid serial visual presentation. *J. Exp. Psychol. Hum. Percept. Perform.* 20, 357–371.
- Shapiro, K., Schmitz, F., Martens, S., Hommel, B., Schnitzler, A., 2006. Resource sharing in the attentional blink. *Neuroreport* 17, 163–166.
- Squires, K.C., Hillyard, S.A., Lindsay, P.H., 1973. Vertex potentials evoked during auditory signal detection: relation to decision criteria. *Percept. Psychophys.* 14, 265–272.
- Squires, N.K., Donchin, E., Squires, K.C., Grossberg, S., 1977. Bisensory stimulation: inferring decision-related processes from the P300 component. *J. Exp. Psychol. Hum. Percept. Perform.* 3, 299–315.
- Tombu, M., Jolicoeur, P., 2003. A central capacity sharing model of dual-task performance. *J. Exp. Psychol. Hum. Percept. Perform.* 29, 3–18.
- Verleger, R., Jaśkowski, P., Wascher, E., 2005. Evidence for an integrative role of P3b in linking reaction to perception. *J. Psychophysiol.* 19, 165–181.
- Visser, T.A.W., Merikle, P.M., Di Lollo, V., 2005. Priming in the attentional blink: perception without awareness? *Vis. cogn.* 12, 1362–1372.
- Vogel, E.K., Luck, S.J., 2002. Delayed working memory consolidation during the attentional blink. *Psychon. Bull. Rev.* 9, 739–743.
- Vogel, E.K., Machizawa, M.G., 2004. Neural activity predicts individual differences in visual working memory capacity. *Nature* 428, 748–751.
- Vogel, E.K., Luck, S.J., Shapiro, K.L., 1998. Electrophysiological evidence for a postperceptual locus of suppression during the attentional blink. *J. Exp. Psychol. Hum. Percept. Perform.* 24, 1656–1674.
- Wyszecki, G., Stiles, W.S., 1982. *Color Science: Concepts and Methods, Quantitative Data and Formulae*, 2nd Ed. John Wiley and Sons, New York.
- Woodman, G.F., Luck, S.J., 2003. Serial deployment of attention during visual search. *J. Exp. Psychol. Hum. Percept. Perform.* 29, 121–138.

Annexe 2 : autorisation des co-auteurs

Annexe 3 : curriculum vitae du candidat

Curriculum Vitæ Nicolas Robitaille

Education

- 2000-2003 B.Sc. Baccalauréat en Psychologie,
Université de Montréal
- 2003-2009 Ph.D. Doctorat en psychologie, orientation neuropsychologie et
sciences cognitives
Université de Montréal

Distinction

- 2003 Canadian Psychological Association Certificate of Academic
Excellence for Honours Thesis
- 2003-09 Graduate Study Faculty scholarship (10 000\$/year)
2006-08
- 2005-09 REPRIC pilot project grant to Pierre Jolicoeur, René Marois et
2006-09 Nicolas Robitaille (10 000\$).
- 2006-05 NSERC ES-D scholarship (21 000\$/year)
2008-04
- 2007 Graduate Study Faculty Prize for best oral presentation (500\$)

Papers with review committee

- Robitaille, N., Grimault, S., Jolicoeur, P.** (in press). Bilateral parietal and contralateral responses during maintenance of unilaterally-encoded objects in visual short-term memory: Evidence from magnetoencephalography. *Psychophysiology*.
- Grimault, S., **Robitaille, N.**, Grova, C., Lina, JM., Dubarry, AS., Jolicoeur, P. (accepted with minor correction). Oscillatory activity in parietal cortex during retention in visual short-term memory: Cortically-constrained source localization of magnetoencephalographic activity. *Human Brain Mapping*.
- Perron, R., Lefebvre, C., **Robitaille, N.**, Brisson, B., Gosselin, F., Arguin M., Jolicoeur, P. (In press). Attentional and anatomical considerations for the representation of simple stimuli in visual short-term memory: Evidence from human electrophysiology. *Psychological Research*.
- Robitaille, N.,** Lepore, F., Bacon, B.A., ElleMBERG, D., Guillemot, J.P. (2008). Receptive field properties and sensitivity to edges defined by motion in the postero-lateral suprasylvian (PLLS) area of the cat. *Brain Research*, 1187, 82-94.
- Jolicoeur, P., Brisson, B., **Robitaille, N.** (2008). Dissociation of the N2pc and Sustained Posterior Contralateral Negativity in a Choice Response Task. *Brain Research*, 1215, 160-172.
- Robitaille, N.,** Jolicoeur, P., Dell'Acqua, R., Sessa, P. (2007). Short-term consolidation of visual patterns interferes with visuo-spatial attention: Converging evidence from human electrophysiology. *Brain Research*, 1185, 158-169.
- Brisson, B., **Robitaille, N.,** & Jolicoeur, P. (2007). Stimulus intensity affects the latency but not the amplitude of the N2pc. *NeuroReport*, 18, 1627-1630.

Robitaille, N. et Jolicœur, P. (2006a) Fundamental properties of the N2pc as an index of spatial attention : effect of masking. *Canadian Journal of Experimental Psychology*. 60(2), 101-111.

Robitaille, N., Jolicœur, P. (2006b). Effect of cue-target interval on the N2pc. *NeuroReport*. 17(15):1655-1658.

Jolicœur, P., Sessa, P., Dell'acqua, R. et **Robitaille, N.** (2006a). On the control of visual spatial attention : evidence from human electrophysiology. *Psychological Research*, 70(6), 414-424.

Jolicœur, P., Sessa, P., Dell'acqua, R. et **Robitaille, N.** (2006b). Attentional control and capture in the attentional blink paradigm : Evidence from human electrophysiology. *European Journal of Cognitive Psychology*, 18(4), 560-578.

Dell'Acqua, R., Sessa, P., Jolicœur, P., **Robitaille, N.** (2006). Spatial attention freezes during the attention blink. *Psychophysiology*. 43(4), 394-400.

Book Chapter

Jolicœur, P., Dell'Acqua, R., Brisson, B., **Robitaille, N.**, Sauvé, K., Leblanc, É., Prime, D., Grimault, S., Marois, R., Sessa, P., Grova, C., Lina, J.-M., & Dubarry, A.-S. (in press). Visual spatial attention and visual short-term memory : Electromagnetic exploration of mind. In V. Coltheart (Ed.), *Tutorials in visual cognition*. Hove (UK): Psychology Press.